ADDED RESOLUTION ELEMENTS IN TANDEM MASS SPECTROMETRY FOR CHEMICAL ANALYSIS

BY

DEAN DONALD FETTEROLF

A DISSERTATION PRESENTED TO THE GRADUATE COUNCIL
OF THE UNIVERSITY OF FLORIDA IN
PARTIAL FULFILLMENT OF THE REQUIREMENTS
FOR THE DEGREE OF DOCTOR OF PHILOSOPHY

UNIVERSITY OF FLORIDA
1983

ACKNOWLEDGEMENTS

I would like to extend my gratitude to Dr. Richard A. Yost for his acceptance and guidance during this research. I will always value his friendship and judgement.

I acknowledge the members of my committee, including Drs. John G. Dorsey, John R. Eyler, H. Anson Moye, and James D. Winefordner for their suggestions and guidance. I would also like to thank Dr. John Eyler for his helpful discussions on ion/molecule reactions.

This research would not have been possible without the support of and discussions with my colleagues and friends in the research group, including Ted Britton, Mary Beth Budd, Sue Hummel, Jodie Johnson, Bob Perchalski, and Mike Trehy. I would like to give special thanks to Dr. Neil Brotherton for his many helpful discussions.

I would also like to thank my many colleagues and friends in the J.G.D. and J.D.W. research groups for their support. In addition I would like to thank Jeanne Karably for her editorial assistance and typing of this dissertation.

Finally, I acknowledge the support of my family throughout my undergraduate and graduate education. Without the support of my parents, my sisters, and brother this work would not have been possible.

TABLE OF CONTENTS

PAGE

ACKNOWLEDGEMENTS ii

ABSTRACT v

CHAPTER

1 INTRODUCTION 1

The Analytical Procedure 1
Information Theory 2
Informing Power in Mass Spectrometry ... 4
Tandem Mass Spectrometry 10
Organization of the Dissertation 21

2 ADDED RESOLUTION ELEMENTS IN SAMPLE INTRODUCTION AND IONIZATION 23

Sample Introduction 24
Sample Ionization 32

3 ADDED RESOLUTION ELEMENTS IN THE COLLISIONALLY-ACTIVATED DISSOCIATION PROCESS 41

Ion Activation 42
Energy Resolution 48
Pressure Resolution 62
Reactive Collisions 74

4 APPLICATION TO STRUCTURE ELUCIDATION 86

Isomer Differentiation 87
Reactions of Hydrocarbon Ions with Acetylene 101
Ions Formed in Chemical Ionization 111
Computer-Aided Interpretation 120

5 APPLICATION TO MIXTURE ANALYSIS 127

GC/MS/MS Analysis of Priority Pollutants 128
Determination of Chlorinated Hydrocarbons in Serum and Urine 143

6 CONCLUSIONS AND FUTURE WORK 160

REFERENCES 163

BIOGRAPHICAL SKETCH 169

Abstract of Dissertation Presented to the Graduate
Council of the University of Florida in Partial
Fulfillment of the Requirements for the Degree
of Doctor of Philosophy

ADDED RESOLUTION ELEMENTS IN TANDEM MASS SPECTROMETRY FOR CHEMICAL ANALYSIS

By

Dean Donald Fetterolf

April, 1983

Chairman: R.A. Yost
Major Department: Chemistry

The concepts of information theory have been applied to tandem mass spectrometry. The roles of the added resolution elements, which increase the informing power, were investigated for chemical analysis using a triple quadrupole mass spectrometer. It has been demonstrated that the added resolution elements in sample introduction and ionization as well as in the collisionally activated dissociation (CAD) process lead to increased sensitivity and selectivity for structure elucidation and mixture analysis.

The effects of collision energy on the appearance of the daughter spectra were investigated in terms of energy-resolved breakdown curves. These curves show good agreement with theoretical curves predicted by the quasi-equilibrium theory (QET) and with those obtained by

angle-resolved mass spectrometry. The effects of energy and pressure on the efficiency of the CAD process were also investigated. These resolution elements increase our understanding of the CAD process, but also aid in the differentiation of isomeric ion structures. For example, the cyclopropane ion can be differentiated from the linear propene ion by energy-resolved breakdown curves.

The use of reaction collisions has been demonstrated to be a powerful new method for differentiating isomeric ion structures. The cyclopentadiene and the linear 1-propene-3-yne molecular ions can be readily distinguished by reactive collisions with isobutane. These reactive collisions are also helpful in determining the mechanisms for the formation of adduct ions in chemical ionization, as well as those occurring in the reactions of hydrocarbon ions with acetylene.

The careful selection and optimization of these added resolution elements in mixture analysis have lead to the development of a method for the rapid screening (100 samples/hr) of chlorinated compounds in serum and urine at the sub-ppb level. Limits of detection of 0.05 ppb and 0.250 ppb for hexachlorobenzene and trichlorophenol, respectively, were obtained for a 1 μl injection of an unconcentrated extract of serum or urine.

Combined chromatography and tandem mass spectrometry has been demonstrated for the separation of isomers and the identification of classes of compounds in complex environmental samples through the use of the various operating modes in MS/MS.

CHAPTER 1
INTRODUCTION

The Analytical Procedure

Chemical analyses are essentially information processes with the goal of obtaining knowledge about the composition of a sample. The analyses to be performed cover a wide range of applications in a wide variety of fields. The knowledge in all analyses is gained through a series of planning, measuring, and interpretation steps. This series of steps forms an analytical procedure, which is characterized by figures of merit. These figures of merit, including sensitivity, selectivity, specificity, accuracy, precision and limit of detection, permit the analyst to critically evaluate the results of an analytical procedure.

One often overlooked figure of merit, the informing power, can provide the analyst with a means of evaluating the amount of information available in a given procedure. Since the chemical content of a sample cannot be directly measured, the results are derived from the measurement of other physical quantities such as mass or absorbance. These measurements can be made at a fixed or scanned parameter. Absorbance, for example, can be measured at a given wavelength or over a range of wavelengths to produce an absorption spectrum. Many modern analytical techniques have several experimental parameters which can be varied. The information in this measurement is transferred in signals such as current or voltage. The signals can then be displayed with an output device such as a digital volt meter or a strip chart recorder. The interpretation of this information by the analyst results in chemical knowledge about the sample.

Since the range of the varied experimental parameters, as well as the intensity level of the signal, is limited in time, space and magnitude, they can be represented by a finite numerical value known as the informing power. The informing power tells us how much information is available but nothing about the value of that information.

Information Theory

The informing power, P_{inf}, of an analytical procedure may be expressed in terms of "binary digits" or bits. As defined by Kaiser (1), the informing power may be expressed as

$$P_{inf} = \sum_{i=1}^{n} \log_2 S_i \quad . \qquad (1)$$

where n is the number of different quantities to be determined and S_i is the number of measurable steps for a given quantity. These n different measurements may belong to different parameters, such as wavelength or mass number.

If x is the variable parameter and δx is the smallest distinguishable difference in x, then the number of steps of x is given by $x/\delta x$. Note that this is the definition of resolution, R(x).

$$R(x) = \frac{x}{\delta x} \tag{2}$$

By substituting into Equation (1) and allowing for the variation in the parameter x, the summation can be replaced with an integral evaluated from x_a to x_b:

$$P_{inf} = \int_{x_a}^{x_b} R(x) \log_2 S(x) \frac{dx}{x} \quad . \tag{3}$$

If, for example, the resolution R(x) is constant and S(x) is fixed by the detection system, then the expression may be simplified:

$$P_{inf} = R(x) \log_2 S(x) \ln \left(\frac{x_b}{x_a}\right) \quad . \tag{4}$$

This informing power is a figure of merit for the instrument and is independent of the chemical system to be measured. It may be increased by improving any of the three terms in Equation (4). An increase in P_{inf} is desirable because the analytical usefulness of the technique will increase. This increase in P_{inf} may be achieved by the addition of other resolution elements.

Many modern analytical techniques such as time-resolved phosphorimetry, gas chromatography/mass spectrometry (GC/MS) or mass spectrometry/mass spectrometry (MS/MS) have more than one resolvable parameter. These added parameters or resolution elements can greatly increase the informing power of the analytical technique. The only requirement for the addition of another resolution element is that the physical property of the analyte show some differentiation with respect to that parameter. In time-resolved phosphorimetry, for instance, a second monochromator and time-resolution add to the informing power. In tandem mass spectrometry, a second mass analyzer enters as a resolvable parameter. Following the derivation of Equation (3), Fitzgerald and Winefordner (2) have shown that for 2 resolvable parameters

$$P_{inf} = \int_{y_1}^{y_2} \int_{x_1}^{x_2} R(x)\ R(y)\ \log_2 S(x,y)\ \frac{dx}{x}\ \frac{dy}{y}\ \text{bits.} \quad (5)$$

Similarly, the addition of other resolvable parameters (such as energy resolution in MS/MS) can further increase the informing power.

Informing Power in Mass Spectrometry

From the definition of informing power [Equation (3)] it is obvious that increased resolution is important for high informing power in spectral methods. If the spectral resolution R(x) is constant, as in a magnetic sector mass spectrometer, and if $S(x)$ is fixed by the detection system, then both terms can be taken out of the integral:

$$P_{inf} = R(x) \log_2 S(x) \ln \left(\frac{x_b}{x_a}\right) \quad . \tag{6}$$

The higher the mass resolution the greater the informing power of mass spectrometry.

However, in the case of quadrupole mass filters, the minimum resolution element, δx, is constant rather than the resolution $R(x)$. For unit mass resolution, $\delta x = 1$. The informing power can therefore be expressed as

$$P_{inf} = \frac{1}{\delta x} \log_2 S(x) \int_{x_a}^{x_b} dx \tag{7}$$

$$= 1 \cdot \log_2 S(x) \cdot (x_b - x_a) \text{ bits.} \tag{8}$$

For a single quadrupole mass spectrometer with a mass range of 1000 amu, and an ion intensity range of 2^{12} bits, $P_{inf} = 1.2 \times 10^4$ bits.

One way to increase the informing power of mass spectrometry is by the addition of other resolution elements. The most commonly used added resolution element in mass spectrometry is the separation of compounds by gas chromatography (GC/MS). Recalling Equation (5) and assuming that the resolution for a capillary GC column with 1.0 x 10^5 theoretical plates and a one hour analysis time is constant (i.e., $R(y) = \frac{t_r}{t_w} = (N/5.54)^{\frac{1}{2}}$), then

$$P_{inf} = \frac{1}{\delta x} \log_2 S(x) \int_{x_1}^{x_2} dx \cdot R(y) \int_{y_1}^{y_2} \frac{dy}{y} \qquad (9)$$

$$= 1.2 \times 10^4 \cdot (\frac{10^5}{5.54})^{\frac{1}{2}} \cdot \ln(\frac{3600}{60})$$

$$= 6.6 \times 10^6 \text{ bits.}$$

An alternative to combining gas chromatography with mass spectrometry is combining mass spectrometry with mass spectrometry. The addition of a second mass analysis in MS/MS is analogous to the addition of a second monochromator in molecular fluorescence. For a quadrupole MS/MS instrument the informing power is simply the product of the informing power of a single mass spectrometer and that of a second mass analyzer. Therefore, $P_{inf} = 1.2 \times 10^4 \cdot 10^3 = 1.2 \times 10^7$ bits. Note that for the best commercially available high resolution sector mass spectrometer (with an equivalent mass range, detection system, and a mass resolution of 25,000) the informing power is only 1.4 x 10^6 bits, approximately 10 times less than that for a quadrupole MS/MS instrument.

In MS/MS, the experimental variables associated with the collisionally activated dissociation (CAD) (sometimes called collision-induced dissociation (CID)) process, pressure and energy, are other potential resolution elements. The pressure in the triple quadrupole MS/MS used here can be varied from 0 to 10 x 10^{-3} torr with a practical resolution of 0.5 x 10^{-3} torr. The collision energy can be varied from 0 to 30 eV with a practical resolution of 2 eV. Table 1 summarizes the informing power for various combinations of these added resolution elements in mass spectrometry.

At this point, it is important to briefly discuss the limitations of these calculations of informing power. Often the practical resolving power of a parameter is less than that calculated. In molecular absorption spectrophotometry, for example, the practical resolution R(x) is determined not by the bandpass of the monochromator but by the width of the absorption bands. Due to the interdependence of parameters in MS/MS, only one half of the informing power is commonly used. The fragment ions must have a mass less than the parent ion; therefore only one half of the resolvable elements are present. The use of reactive collisions in the center quadrupole makes it possible to form a reaction complex with a mass greater than the parent ion, thereby increasing the informing power.

In addition to these measurable experimental parameters other variables can be used to increase the informing power of MS/MS. These variables, which are procedural in nature, include the choice of chemical ionization or

Table 1. Informing Power of Mass Spectrometric Techniques

Technique	P_{inf}	Increase in P_{inf} Compared to MS
MS[a]	1.2×10^4	--
Packed-GC/MS[b]	7.8×10^5	65
Capillary-GC/MS[c]	6.6×10^6	550
MS/MS	1.2×10^7	1000
		Increase in P_{inf} Compared to MS/MS
Energy resolved/MS/MS[d]	1.8×10^8	15
Pressure resolved/MS/MS[e]	2.4×10^8	20
Packed-GC/MS/MS	7.8×10^8	65
Energy and pressure resolved MS/MS	3.6×10^9	300
Capillary-GC/MS/MS	6.6×10^9	550

[a] MS: 1000 amu; unit resolution; intensity range, $S_A = 2^{12}$

[b] Packed-GC: 2.0×10^3 theoretical plates; 0.5 hour analysis

[c] Capillary-GC: 1.0×10^5 theoretical plates; 1 hour analysis

[d] Energy resolution: 0-30 eV; 2 V steps

[e] Pressure resolution: 0-10 millitorr; 0.5 millitorr steps

electron impact, selection of positive or negative ions or the choice of reactive collisions. The analytical utility of these added resolution elements is demonstrated in the following chapters. Because of the difficulty in continuously "scanning" these variables, it is difficult to express their effects on informing power.

A comparison between the amount of information needed to solve a given analytical problem and the informing power of the chosen technique is useful. Consider, for example, the identification of a pure compound by mass spectrometry. If it is assumed to be one of the 5 million compounds indexed by Chemical Abstracts, then an informing power of at least $\log_2 (5 \times 10^6)$ or 23 bits would be required. If the analytical problem is to determine how many of those 5 million compounds are present in a sample, a minimum of 5×10^6 bits are required.

In theory, any technique with an informing power greater than 5×10^6 bits (such as MS/MS, with an informing power of 1.2×10^7 bits) would be capable of solving this problem. In practice, significantly greater informing power than this would be required. In order for the minimum informing power to be adequate to answer a given problem, all the bits of the information must be independant (i.e., not redundant), a condition not generally achieved. Real analytical systems are also subject to noise and interference, thereby reducing the informing power. An excess of informing power is not wasted information therefore, but is necessary to increase the reliability and precision of the analysis.

Tandem Mass Spectrometry

One of the most powerful resolution elements which can be used in mass spectrometry is the addition of a second stage of mass analysis.

Tandem mass spectrometry (MS/MS) is a rapidly developing field of mass spectrometry based upon a new generation of instruments in which two or more mass analyzers are used in sequence for both the separation and identification of compounds. The applications of these instruments include complex mixture analysis, structure elucidation and fundamental mechanistic and energetic studies.

MS/MS is the subject of a timely new book edited by McLafferty (3) and reviewed for a broad audience recently in Science (4) and Chemical and Engineering News (5). Its development has also been critically assessed in the most recent biannual review of mass spectrometry in Analytical Chemistry (6). Instrumentation for tandem mass spectrometry has been reviewed by Yost and Fetterolf (7).

Evolution of MS/MS Instruments

Despite the fact that the early commercialization of mass spectrometry in the 1940s was spurred by interest in quantitative mixture analysis by the petroleum industry, the single MS is not well suited to mixture analysis. The coupling of a gas chromatograph for separation with the mass spectrometer for identification in the late 1950's made possible the sensitive, selective analysis of mixtures.

Although MS/MS is most commonly thought of today as a mixture analysis technique, it has its roots in the use of so-called "metastable" ions to aid in structural elucidation (8). Decoupling of the sectors in a normal geometry (electric sector before magnetic sector) instrument made it possible to observe these metastable ions without interference from the normal "stable" ions (9). A more versatile instrument for metastable studies was realized by reversing the double-focussing geometry (magnetic sector first), providing for "Mass-Analyzed Ion Kinetic Energy Spectrometry" or MIKES (10). A scan of all metastables arising from a given parent ion (selected by the magnetic sector) was obtained simply by scanning the electric sector voltage. A significant increase in the variety and intensity of fragment ions was obtained by collisionally activated dissociation (CAD) (11). The extension of these techniques into mixture analysis opened the way for the widespread use of MS/MS (12). During this same period, there were a great variety of tandem mass spectrometers developed for fundamental studies of ion-molecule reactions (13).

As the analytical applications of MS/MS for mixture analysis have been demonstrated, new tandem instruments specifically designed for rapid, sensitive, and selective analysis have been developed. These have included multiple quadrupole (14,15) and multiple sector (16,17) MS/MS instruments. These and other high performance tandem mass spectrometers, most with sophisticated data systems, are now available from a number of sources (18-23).

The use of quadrupoles for both stages of mass analysis in MS/MS leads to several important features. Mass analysis in quadrupoles requires that the ions have relatively low kinetic energies, in the range of 2-20 eV if good resolution is to be maintained. The CAD process is extremely efficient at these low energies, particularly if an RF-only quadrupole is employed as a collision chamber to focus the ions scattered by the collision process. Many of the features of quadrupoles which have led to their widespread use in GC/MS are equally important in MS/MS. These include small size, simplicity and low cost, rapid scanning, ease of computer control, absence of artifact peaks and tolerence of high pressures.

The earliest tandem quadrupole instruments were designed for studies of ion/molecule reactions. A tandem quadrupole instrument was reported in 1972 (24) which employed a field-free collision cell between two homemade quadrupole mass filters with unit mass resolution up to mass 200. The second quadrupole could also be mounted after the collision cell at right angles to detect ions scattered at 90°. A similar system was reported for investigation of the angular distribution of ion/molecule reaction products (25). The selected ion flow tube (SIFT) system described recently (26) employs tandem quadrupoles with a 1 m long drift tube in between for the study of these reactions.

The concept of employing an RF-only quadrupole as a fragmentation chamber between two quadrupole mass filters was developed independently in the early 1970's by McGilvery and Morrison at Latrobe University (27) and by Vestal and Futrell at the University of Utah (28). Both groups designed triple quadrupole instruments to study the photodissociation of ions. Even at pressure down to 10^{-8} torr in the center quadrupole, ions from CAD greatly exceeded those from photodissociation. These early instruments proved to be extremely useful for studies of ion/photon interactions, but the CAD "interference" was not recognized as analytically useful.

The concept of a computer-controlled tandem quadrupole instrument using CAD for mixture analysis was developed in 1975 by Yost and Enke at Michigan State University. Their early studies were performed on the LaTrobe instrument, modified for CAD (29,30). The use of Michigan State's triple quadrupole instrument for mixture analysis and structure elucidation was then demonstrated (14,31). Shortly thereafter, Hunt and coworkers assembled a triple quadrupole instrument and applied it to mixture analysis (32). Zackett and coworkers subsequently assembled a double quadrupole instrument, with a field-free collision cell (33).

In the past few years, three companies (Finnigan MAT, Sciex and Extranuclear) have developed computerized triple quadrupole MS/MS systems.

Instrumentation

The mass spectrometer used in this research was a Finnigan Triple Stage Quadrupole (TSQ) (15). Figure 1 is a cutaway view of the components of the instrument. It consists of, in series, a dual electron impact (EI)/ chemical ionization (CI) source, a quadrupole mass filter, an RF-only center quadrupole collision region, a second mass filter and a channeltron electron multiplier.

Ions formed in the source are accelerated and focussed through a lens stack into the mass analyzer section. Quadrupoles 1 and 3 act as conventional mass filters when the appropriate RF and DC voltages are applied or alternatively may be employed simply as an RF-only focussing device (allowing all ions to pass). The gas tight center quadrupole collision cell is operated in the RF-only mode to focus daughter ions produced by CAD. The collision cell may be pressurized with an inert gas (e.g., N_2 or Ar) at pressures up to 1×10^{-2} Torr. In addition, a 0-30 volt DC potential can be applied to the collision cell in order to determine the ion kinetic energy. The continuous dynode multiplier with conversion dynodes located after quad 3 is capable of detecting positive and negative ions. Using analog switching circuitry it is possible to alternate rapidly between positive and negative ion operation.

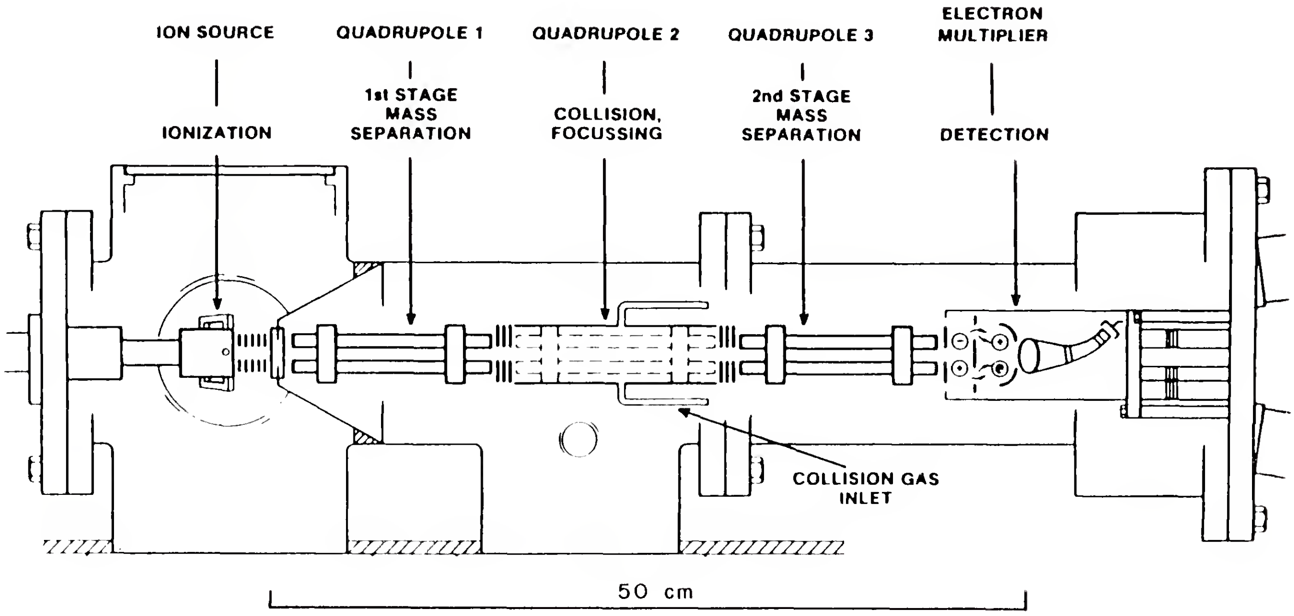

Figure 1: Cutaway view of the Finnigan triple quadrupole mass spectrometer.

The instrument is also equipped with a Data General Nova 3/12 minicomputer and a 32 Mbyte CDC disk drive which provides convenient, interactive control of all instrument configurations and scan modes during real time data acquisition. The data system also senses analog inputs (e.g., collision gas pressure, ion kinetic energy or GC temperature) and provides temperature programming of the gas chromatograph and solids probe. The unit mass resolution provided in both stages of mass analysis also permits the use of some conventional GC/MS software to process the data, such as data output, library searching and quantitation.

Operational Modes

There are three modes of operation for quads 1 and 3: 1) scanning over a selected mass range; 2) selecting a single ion to pass (single ion monitoring); and 3) RF-only, in order to pass all ions. These modes can be varied independently or in combination to provide a variety of operational modes. The five operational modes are normal mass spectrum, daughter spectrum, parent spectrum, neutral loss spectrum and single reaction monitoring.

A normal mass spectrum is obtained by placing either quad 1 or 3 in the RF-only mode and scanning the other. The use of this mode is compared to both parent and neutral loss modes in Chapter 5 for the analysis of priority pollutants.

A daughter scan produces the spectrum of all the fragment or daughter ions from a selected experiment. Quad 1 is operated in the single ion mode (selects the parent ion). The daughter ions formed in quad 2 are mass analyzed by scanning quad 3. A daughter spectrum is particularly useful in mixture analysis since it gives the mass spectrum of the selected component. The use of daughter scans for structure elucidation and mixture analysis is discussed in Chapters 4 and 5, respectively.

A parent scan yields a spectrum of all the parent ions which produce the selected daughter ions. In this mode quad 1 is scanned while quad 3 selects the daughter ion of interest. Parent spectra are useful in determining all the compounds which fragment to give a characteristic fragment ion. The use of parent spectrum is discussed in Chapter 5 for the determination of phthalates in the GC/MS/MS analysis of priority pollutants.

A neutral loss scan shows all the parent ions which lose a selected mass upon fragmentation. In a neutral loss scan quads 1 and 3 are scanned simultaneously with a fixed mass difference. The neutral loss mode is particularly useful in screening complex mixtures for classes of compounds. The use of the neutral loss mode for the analysis of chlorinated compounds is also presented in Chapter 5.

The fifth operating mode is selected reaction monitoring (SRM), in which the two mass analyzers are set to monitor specific parent/daughter pairs, analagous to selected ion monitoring in GC/MS. This is useful in the quantitative analysis of selected compounds at maximum sensitivity. The use of SRM in the determination of chlorinated compounds in serum and urine at the sub-ppb level at a rate of 100 injections/hour is discussed in Chapter 5. The careful selection and use of these various operating modes permit new analytical procedures to be developed to carry out analyses otherwise difficult or impossible.

In conventional mass spectrometry a given scan is repeated several times. In MS/MS it is desirable to vary the sequence of operating modes. To meet these complexities of MS/MS instrument control and data acquisition, computer automation is essential. The Finnigan TSQ is equipped with a Data General Nova 3/12 minicomputer and a 32 Mbyte CDC disk drive. This computer automation provides convenient, interactive control of all instrument configurations and scan modes during real time operation. This permits the analytical chemist to define a predetermined sequence of events that will cycle automatically during data acquisition. For some applications it is desirable to use continuous feedback from the data in order for the data system to intelligently select the best instrument configuration for acquiring the next set of data. In order to obtain a complete 3-dimensional fragmentation map of a molecule, a daughter spectrum at every m/z could be obtained. Molecules rarely, if ever, fragment to give an ion at every m/z. Using feedback control, the data from an electron impact mass spectrum can be used to select the parent ions, thereby reducing the amount of data collected.

Applicability

The tandem mass spectrometer has a wide range of applicability to analytical as well as fundamental studies. It has been pointed out that the modern MS/MS instrument is a complete chemical laboratory with capabilities for synthesis, separation, reaction, and analysis all in sequence (34).

For mixture analysis, MS/MS offers a wide range of applicability and compliments GC/MS, by providing more rapid and often more selective and sensitive analysis of targeted compounds. Thermally labile and low volatility samples may be analyzed directly. Mixtures can often be analyzed for trace components with little or no sample preparation due to the elimination of "chemical noise." This feature, combined with the essentially simultaneous access to mixture components, makes for extremely rapid analysis, especially for targeted compounds. For example, the detection of chlorinated compounds in human serum and urine at the 100 parts per trillion level at the rate of 100 samples/hour is discussed in Chapter 5.

For the elucidation of the structures of gas phase ions and ultimately entire compounds, MS/MS offers an entirely new dimension of information. A major limitation of a conventional mass spectrum is that it does not indicate the genetic relationship between the ions in the spectrum. The consequences of this missing information are far reaching. The interpretation of a mass spectrum is often a difficult and time consuming process based on the intuition and catalogued fragmentation reactions gained through experience. The only information on each piece of the puzzle (a fragment ion) is its mass and intensity. MS/MS provides a great deal more information about each piece and its neighbors: where it came from (its precursors) and where it goes (its fragments). The potential of the MS/MS technique for structural elucidation has been explored (31,35,36). Computerized interpretation of MS/MS data for the elucidation of structure shows promise (4,37) and is discussed in Chapter 4.

Fundamental studies of ion molecule reactions, the earliest application of tandem mass spectrometry, are increasingly important because of the widespread analytical use of MS/MS. They not only increase our understanding of the processes involved, but also illuminate new approaches for analysis such as the use of reactive collisions as described in Chapter 3. These fundamental studies will benefit from the commercial availability of sophisticated new computer controlled MS/MS instruments.

Organization of the Dissertation

This dissertation is divided into six chapters. This first chapter introduced the concepts of the analytical procedure and information theory and its application to mass spectrometry. In addition this chapter presented a review of the development, instrumentation, operating modes and application of tandem mass spectrometry.

Chapter 2 describes the added resolution elements in sample introduction and ionization methods. The roles of these added resolution elements in mixture analysis and structure elucidation are discussed.

The third chapter provides a detailed investigation of energy resolution in the low energy CAD process in triple quadrupole mass spectrometry. A comparison between energy-resolved breakdown curves and the quasi-equilibrium theory of mass spectrometry is presented. In addition reactive collisions are used to investigate the low-energy collision process and to provide an added resolution element in MS/MS.

Chapter 4 discusses the application of all these additional resolution elements to structure elucidation. Energy resolution and reactive collisions are used to differentiate isomeric species and investigate the reactions of the ions found in flames. MS/MS permits the structure of ions formed in chemical ionization to be determined. Finally, the use of computer-aided interpretation of MS/MS data is presented.

Chapter 5 discusses the application of combined chromatography and tandem mass spectrometry to the analysis of priority pollutants. In addition, the determination of chlorinated compounds in serum and urine at the sub-part per billion level at the rate of 100 samples/hour is presented.

The final chapter presents a summary of this work and discusses future research.

CHAPTER 2
ADDED RESOLUTION ELEMENTS IN SAMPLE INTRODUCTION AND IONIZATION

In MS/MS the modes of sample introduction and ionization can be effective resolution elements. The use of these added resolution elements in MS/MS not only increases the informing power but also aids in the optimization of the analytical procedure by providing an added dimension of information. As in any analysis, the sample and the type of information desired determine the analytical method to be used. Following the choice of a suitable method, the conditions under which the analyses are to be carried out must be determined.

In an analytical procedure with several variables, it is generally not necessary to scan each variable over its entire range during the analysis; rather, one variable is commonly scanned while the others are fixed. Optimization of these added dimensions can increase the informing power of the technique, even though the parameters are fixed. In MS/MS the sample introduction and ionization methods are fixed depending upon the sample and the analytical problem to be solved.

The choice of these conditions is aided by preinformation. For example, consider the trace analysis of a specific isomer of tetrachlorodibenzo-p-dioxin (TCDD), such as 2,3,7,8-TCDD. There is a good probability that some of the other 21 TCDD isomers, as well as other isobaric polychlorinated compounds, such as polychlorinated biphenyls (PCBs) will be present. In this case, the use of a chromatographic step prior to mass analysis is required. In addition, negative ion CI would be the best ionization method because of its greater sensitivity and selectivity for electronegative compounds than positive CI or electron impact. The role of sample introduction and ionization in MS/MS is discussed below.

Sample Introduction

In MS/MS, as in conventional mass spectrometry, the type of sample and the information desired dictate the method of sample introduction. The sample can be introduced directly into the instrument or separated into its components. For mixture analysis by MS/MS, for instance, the direct insertion probe is widely used because it permits the rapid introduction of samples with little or no sample preparation. Samples as complex as coal liquids (38), blood serum (39) and industrial sludge (32) have been introduced with the probe without sample cleanup. Rapid derivitization on the probe of polynuclear aromatic hydrocarbons to nitro-polynuclear aromatic hydrocarbons with N_2O_4, for example, has been performed prior to analyzing the sample (40). As the sample is heated slowly spectra can be obtained as components of different volatility are evaporated from the probe. This "microdistillation" can provide limited separation of a mixture.

Consider, for example, the analysis of a targeted compound (camphor, mw = 152) in a sample as complex as bark from the Cinnamomum camphora tree. Figure 2a shows the total ion current and the reconstructed ion current (RIC) for m/z 153 as a 1 mg sample of bark is heated ballistically from 20 to 350°C in approximately 1.5 minutes. The normal CI mass spectrum (Figure 2b) of the sample shows, in addition to the 153^+ protonated molecular ion of camphor, an intense hydrocarbon background (peaks every 14 amu) with an ion at essentially every mass. The time resolution provided by the microdistillation might help in confirming the presence of camphor in the sample. Relying soley upon the 153^+ ion, however, does not rule out other compounds which produce an ion at m/z 153. A much more selective and informative approach would be MS/MS, in which the first mass analyzer can separate m/z 153 from the other ions, and the second mass analyzer can be scanned to obtain its daughter spectrum. The daughter spectrum of m/z 153 from the sample and that of pure camphor are compared in Figure 3, providing positive identification of the compound at m/z 153.

A modified direct insertion probe is also used for introduction of labile or involatile samples in combination with ionization techniques such as desorption chemical ionization (DCI), secondary ion mass spectrometry (SIMS), and fast atom bombardment (FAB). Since these

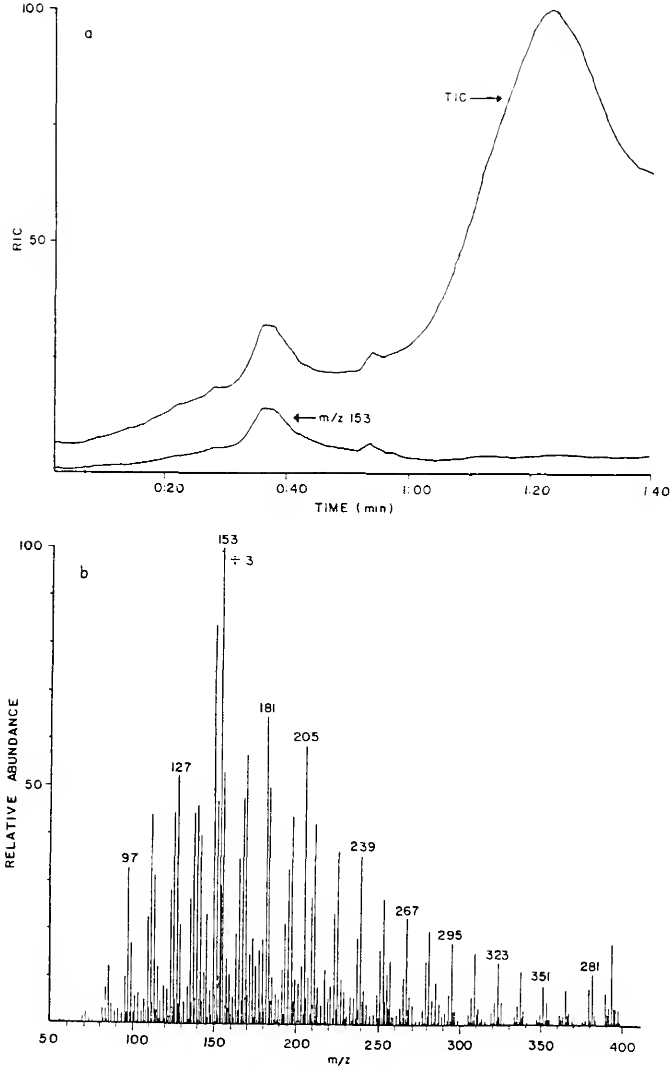

Figure 2. Analysis of tree bark (Cinnamomum camphora). (a) Reconstructed ion current (RIC) for m/z 153 and total ion current (TIC); (b) CI mass spectrum.

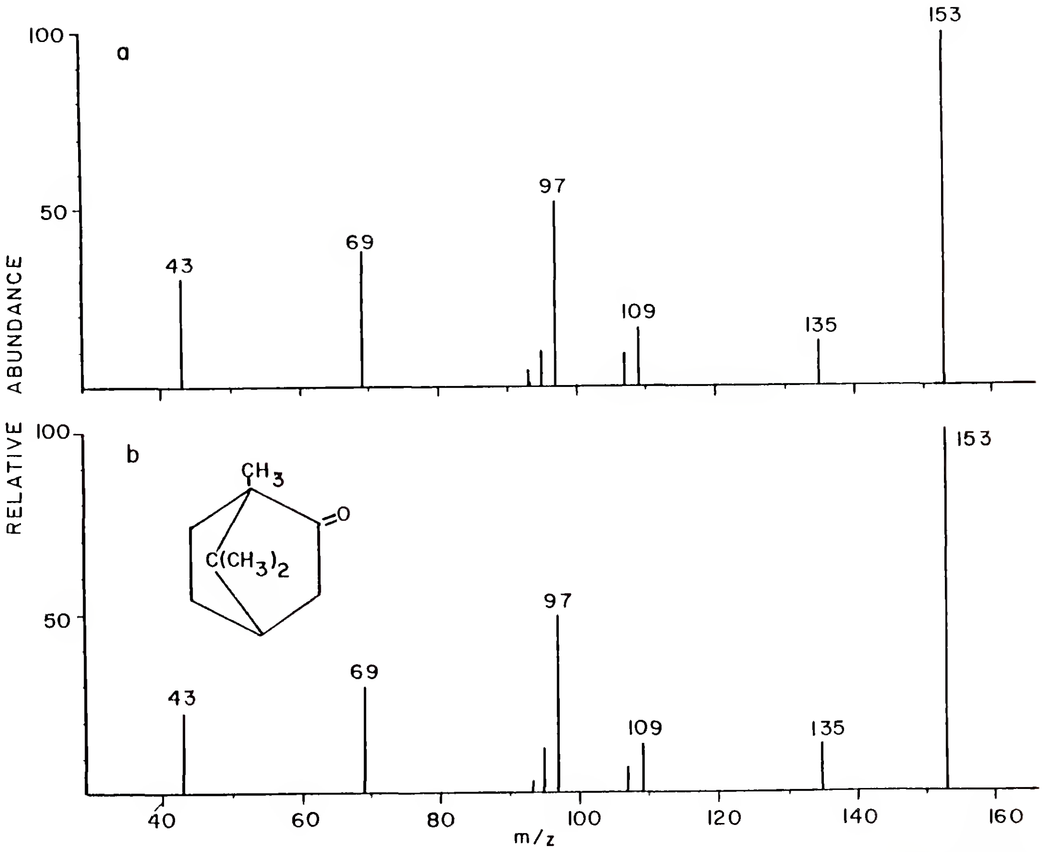

Figure 3. Daughter spectra of m/z 153 from (a) tree bark (Cinnamomum camphora); (b) pure camphor.

techniques often provide only molecular weight information, MS/MS offers the advantage of obtaining structural information by fragmentation of the molecular ion.

In terms of informing power, an extremely powerful resolution element in mass spectrometry is the addition of a chromatographic step for the separation of mixture components. Chromatographic separation, for instance, can separate isomers, which, because of their identical molecular weight, cannot be separated mass spectrometrically. Figure 4 shows the separation of ethylbenzene (C_8H_{10}; mw = 106) and m-xylene (C_8H_{10}; mw = 106) on a 20 m SE-54 capillary column (inset) and the daughter spectra for the protonated molecular ions $(M+H)^+$ formed by methane CI. The daughter spectrum of ethylbenzene shows a base peak at m/z 79 corresponding to the loss of ethylene (C_2H_4). It also indicates that protonation takes place on the benzene ring rather than the ethyl group. On the other hand, a base peak at m/z 91 from m-xylene indicates protonation on a methyl group followed by the loss of methane.

Besides providing a daughter spectrum for each chromatographic peak, MS/MS can be employed in other ways to enhance GC/MS. For instance, MS/MS can provide a molecular weight profile for all compounds with a specific functional group through the use of neutral loss and parent scans. This makes the MS/MS a versatile "selective" GC detector. By selection of the operating mode, the

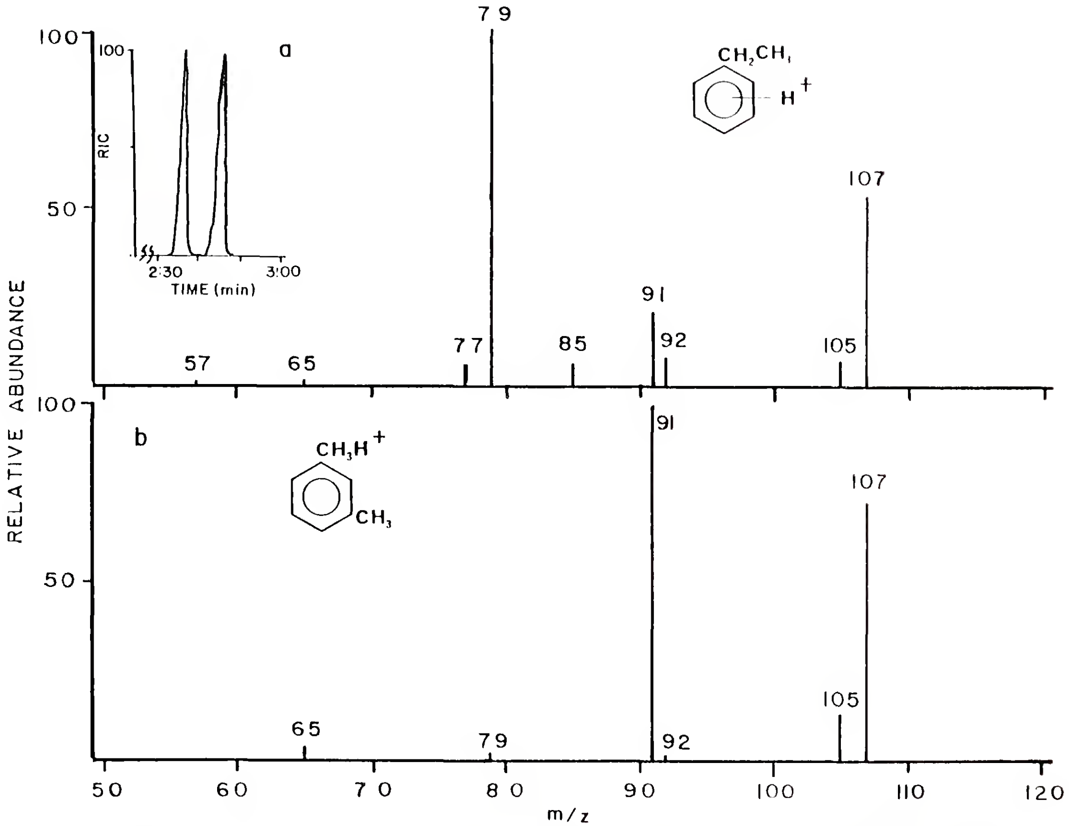

Figure 4. Daughter spectra of (a) ethylbenzene $(M+H)^+$; (b) m-xylene $(M+H)^+$. Inset shows the chromatogram for their separation.

MS/MS can identify the molecular ion for each GC peak. The MS/MS can therefore become a selective detector for phthalates (parent scan for 149^+ or 148^-), halogenated compounds (parent spectrum for X^- or neutral loss of X or HX), or carboxylic acids (neutral loss of COOH), to name but a few. The use of MS/MS as a selective GC detector is demonstrated in Chapter 5.

Combining chromatography, particularly capillary GC, with MS/MS requires rapid scanning if complete MS/MS information is to be acquired for each chromatographic peak. Monitoring only one or two parent/daughter pairs in GC/MS/MS (selected reaction monitoring or SRM) provides much greater sensitivity, albeit at the expense of selectivity. SRM is still more selective than the analogous single ion monitoring (SIM) in normal GC/MS, since the selected parent ion must fragment to form the selected daughter ion in order to be detected. GC/MS/MS (with SRM) may offer better limits of detection than GC/MS (with SIM) due to the enhanced selectivity. This reduction in chemical noise is particularly important in GC/MS/MS, since column bleed is often the major limitation on GC/MS detection limits (41). For example, a detection limit of 100 pg/mL was obtained for deacetylmetipranolol in serum by capillarly GC/MS/MS, using SRM and an isotopically labeled internal standard (15).

For the analysis of a few components in a complex mixture, a short (50 cm) packed-GC column coupled directly to the ion source provides an extremely rapid (up to 100 injections/hour) method for the introduction of volatile samples. Limited chromatographic separation of the mixture components is achieved with this short column. The separation of the components is performed by the first mass analyzer while monitoring specific daughter ions with the second mass analyzer. The analysis of chlorinated compounds in serum and urine using this method of sample introduction is described in Chapter 5.

For the analysis of samples with low volatility or thermally labile functional groups, high pressure liquid chromatography (HPLC) is preferable to GC for the separation of mixtures. MS/MS offers the ability to overcome two major drawbacks of the common direct liquid introduction (DLI) method of LC/MS. In the DLI approach, the solvent acts as the reagent gas for chemical ionization. The intense reagent ions create chemical noise that precludes scanning below approximately 100 daltons. The CI spectra also lack the structural information needed for peak identification. In LC/MS/MS, however, fragmentation of the molecular ion by CAD permits identification. The LC/MS/MS analyses of aromatic acids (42) and sulfa drugs (43) have been carried out using a DLI split interface with triple quadrupole systems. A triple quadrupole system employing a moving belt LC interface has also been described (44). The use of micro-LC techniques for LC/MS/MS and the development of an improved interface are currently underway in our laboratory.

Combining these various methods of sample introduction with MS/MS offers increased informing power and increases the applicability of MS/MS by extending the range of samples which can be analyzed.

Sample Ionization

In addition to the added resolution elements in sample introduction the choice of the ionization method can increase the sensitivity or specificity in the analysis of targeted compounds by MS/MS. The best method of ionization in MS/MS depends upon the application and type of sample. For structural elucidation of pure compounds, ionization by electron impact is the method of choice. Each ion produced in the ion source can then be mass selected and fragmented by CAD. This generates a complete three-dimensional structural map (14) or a fragmentation tree (Chapter 4) of the compound. For mixture analysis, however, it is desirable to form only one ion for each component, characteristic of its molecular weight. Chemical ionization is typically the method of choice. An added dimension in chemical ionization is the ability to enhance the ionization of the compounds of interest with respect to the sample matrix by selection of positive or negative ions and the choice of an appropriate reagent gas.

For maximum sensitivity in mixture analysis, fragmentation of the molecular ion ideally should produce only one intense, characteristic daughter ion. For qualitative analysis, such as in the determination of camphor in tree bark (Figure 3), however, multiple fragment ions are desirable.

Because of its widespread use for MS/MS mixture analysis the added resolution elements in chemical ionization merit further attention. Since its introduction by Munson and Field in 1966 (45), a wide variety of CI methods have been developed. Most commonly these involve the use of gas phase Brönsted acids such as CH_5^+, $C_4H_9^+$, and NH_4^+ to convert the sample molecules to positively charged even-electron ions $(M+H)^+$ or $(M-H)^+$. These reagent ions are produced by bombarding methane, isobutane, or ammonia, respectively, at pressures of approximately 1 torr with high energy electrons (100-400 eV). If non-selective ionization is desired, CH_5^+ (with its low proton affinity) will produce even-electron ions for most compounds. Ionization by NH_4^+ (with a higher proton affinity) is more selective. It will protonate nitrogen containing compounds and form $(M+NH_4)^+$ adduct ions with oxygen-containing compounds (46). This added selectivity could be used in MS/MS, for example, for the analysis of nitrogen compounds in coal liquids. The nucleophilic addition of $NO^{+\cdot}$ to organosulfur compounds has been investigated for the analysis of crude oils by triple quadrupole MS/MS (47). The $(M+NO)^+$ adduct ions formed in the ion source can be detected by a neutral loss scan for NO (30 amu).

Negative ion chemical ionization is very selective and sensitive for electronegative compounds such as those containing halogenated, nitro or carboxyl groups. This added selectivity helps reduce background interference from the sample matrix, making possible the analysis of pollutants in untreated sample matrices at the part-per-billion level by MS/MS (32). The use of negative CI and single-reaction monitoring is described in Chapter 5 for the determination of chlorinated compounds in serum and urine. Although the ionization efficiency of negative ion CI can be significantly greater than that of positive ion CI, the greater stability of negative ions often results in a lower fragmentation efficiency and fewer daughter ions. The selection of the optimum ionization technique for trace analysis by MS/MS must therefore include consideration of ionization and fragmentation efficiencies, as well as the level of background "chemical noise" from the sample matrix. The ability to rapidly alternate the acquisition of positive and negative ion data with quadrupole instruments is a particularly powerful tool for mixture analysis by MS/MS.

A particularly useful ionization technique for mixture analysis by MS/MS is atmospheric pressure chemical ionization (APCI) (48). It can provide extremely selective and sensitive analysis for targeted compounds in a variety of samples (49).

The ionization techniques discussed above are generally applicable to volatile and thermally stable samples. The analysis of compounds with thermally labile, polar functional groups (OH, COOH, and NH_2) or of high molecular weight requires the use of specialized ionization techniques. These ionization techniques often produce only a molecular or pseudo-molecular ion such as $(M+H)^+$ or $(M+Na)^+$. Combining these techniques with MS/MS permits structural information to be obtained by fragmentation of these ions. These ionization techniques extend the range of applications to samples otherwise not amenable to analysis by mass spectrometry.

The simplest of these methods, desorption chemical ionization (DCI) (50), involves placing a small amount of the sample on a copper probe tip or a desorption emitter extending into the ion source and rapidly heating the sample under chemical ionization conditions. Figure 5a shows the DCI spectrum of bilirubin ($C_{33}H_{36}N_4O_6$; MW = 584), a component of blood and a bile pigment, using NH_3 as the reagent gas. The protonated molecular ion at m/z 585 as well as a large number of low mass fragments is

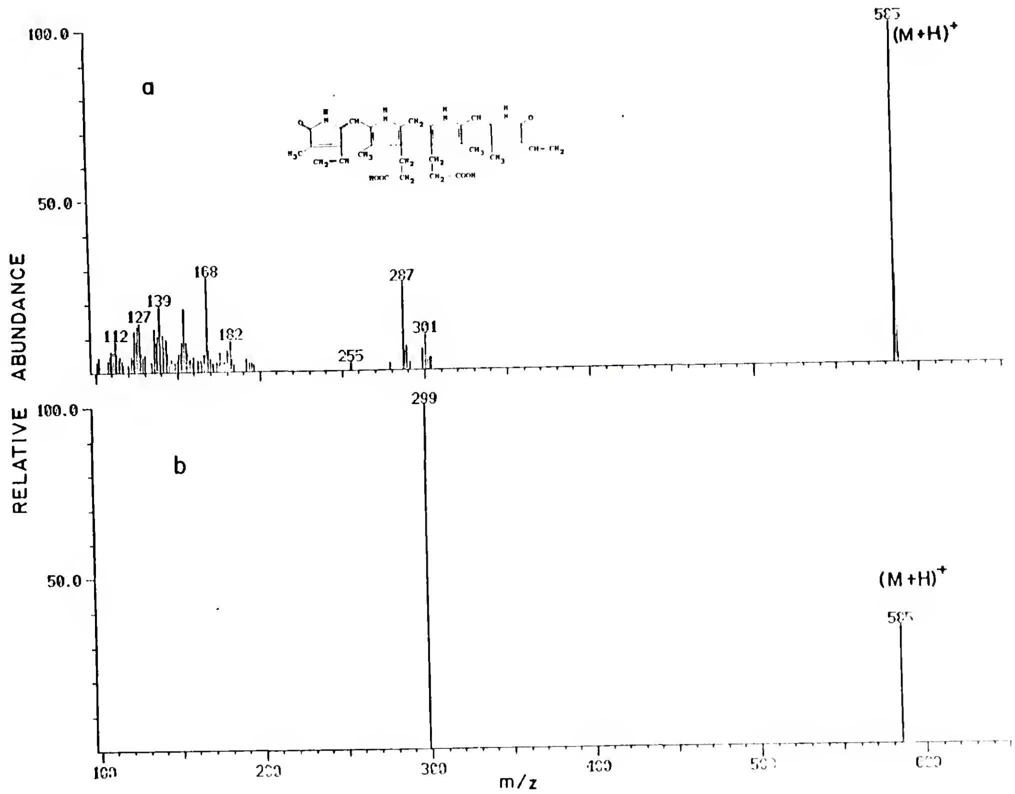

Figure 5. Mass spectra of Bilirubin (a) Desorption NH_3/CI mass spectrum; (b) Daughter spectrum of $(M+H)^+$.

observed. The daughter spectrum (Figure 5b) of m/z 585 shows only 1 fragment (m/z 299) which corresponds to fragmentation of the molecule at the CH_2 bridge.

Other "soft" ionization techniques can be employed in MS/MS. Field desorption (FD) has been combined with sector MS/MS instruments for several biomedical applications, including peptide sequencing (51) and the study of the covalent binding of benzo-a-pyrene with DNA (52). The combination of secondary ion mass spectrometry (SIMS) with MS/MS has been shown to be well suited for the analysis of complex solid samples (53). Fast atom bombardment (FAB) has recently emerged as an alternate method for the ionization of involatile samples, in which a beam of atoms replaces the ion beam in SIMS (54).

The Discharge Ionization/Secondary Ion Mass Spectrometry (DISIMS) accessory on the triple quadrupole offers the same characteristics as FAB. Using the DISIMS technique, the sample is introduced on an extended probe and its surface bombarded with 5 KeV Xe atoms. This bombardment yields secondary ions which are then mass analyzed. The unique feature of FAB is the use of a viscous liquid matrix (usually glycerol) for sample support. This glycerol matrix minimizes damage to the analyte caused by the high energy neutrals and facilitates diffusion of fresh sample to the surface.

This matrix produces a background of ions at almost every mass, with particularly intense ions due to glycerol and proton-bound polymers of glycerol. DISIMS or FAB spectra tend to exhibit an intense protonated molecular ion. The DCI and DISIMS spectra of 1 nanomole of the pentapeptide leu-enkephalin (TRY-GLY-GLY-PHE-LEU) are compared in Figure 6. The DCI spectrum shows a very weak molecular ion at m/z 555 and extensive fragmentation which make interpretation rather difficult. On the other hand, the DISIMS spectrum shows an intense protonated molecular ion at m/z 556 and several structurally significant fragments which permit the sequence of the peptide to be determined. The isotopic cluster centered at m/z 262 is due to diatomic xenon ions (Xe_2^+) produced in the discharge. Recently, Hunt and coworkers have combined FAB with MS/MS for the sequencing of underivatized peptides (55).

The use of the FAB technique has several drawbacks. A major drawback is the requirement that the compound of interest be soluble in glycerol. In addition, the intense ions at every mass due to the glycerol matrix and intense ions from the Xe discharge (Xe^+, Xe^{2+}, Xe_2^+) obscure weak ion signals. It is also possible for some of the fast atoms to travel through the quadrupoles to the detector producing an increased background. Despite drawbacks, these techniques are invaluable, since they extend the range of MS/MS to involatile and thermally labile samples.

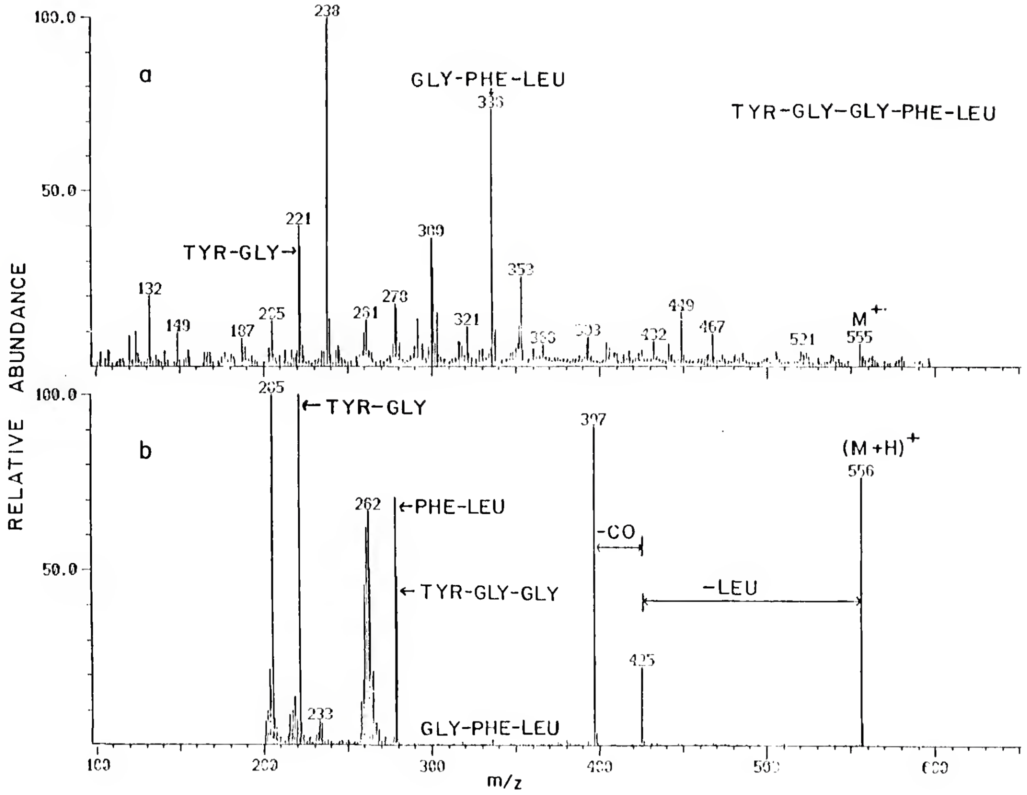

Figure 6. Mass spectra of Leu-Enkephalin (a) Desorption NH_3/CI spectrum; (b) DISIMS spectrum.

A final consideration in sample introduction and ionization for MS/MS is ion source cleanliness. Contaminants that would normally be separated from the sample during extraction or by the chromatography step in GC/MS are often introduced into the ion source on a direct insertion probe. Repeated introduction of "dirty" samples such as blood serum or oil directly into the ion source can rapidly lead to increased background and decreased sensitivity. A partial solution to this problem is provided by the ion source in our instrument, in which changing ion volumes is as rapid as changing samples on the probe.

The choice of ionization methods (EI or CI) provides an added dimension of information in MS/MS. The extensive fragmentation in electron impact is valuable in structure elucidation. In chemical ionization, the selection of ion polarity and the reagent gas are effective resolution elements which increase the selectivity and sensitivity of MS/MS. In addition these added resolution elements increase the range and complexity of samples which can be analyzed.

CHAPTER 3
ADDED RESOLUTION ELEMENTS IN THE COLLISIONALLY-ACTIVATED DISSOCIATION PROCESS

The CAD process offers several effective resolution elements which increase the informing power of MS/MS. The ion kinetic energy can be varied from 0 to 30 volts on this instrument with a practical resolution of 2 volts. The use of energy resolution (control of ion kinetic energy), therefore, increases the informing power of MS/MS by a factor of 15 (Table 1) with respect to MS/MS alone. Energy resolution can provide an added dimension of information in the determination of fragmentation pathways and in the structure elucidation of gas-phase ions.

The control of the pressure of the collision gas in the center quadrupole also provides an effective resolution element. Varying the pressure over the range from 0 to 10 millitorr, with a practical resolution of 0.5 millitorr, increases the informing power 20 fold over MS/MS alone. In addition to providing kinetic data, pressure resolution aids in the optimization of the CAD process. The effect of pressure on the efficiency of the CAD process has also been investigated.

Another useful resolution element in MS/MS is the choice of a reactive collision gas. These associative ion/molecule reactions are particularly valuable in the elucidation of ion structure because of their selectivity. Each of these resolution elements is discussed in detail following a discussion of ion excitation.

Ion Activation

Following ionization and mass selection of the parent ions by the first analyzer, daughter ions (of different m/z) can be obtained by a variety of ion-activation processes. Table 2 lists several ion activation methods which produce positive ions. These choices themselves offer an added dimension of information which increases the informing power of MS/MS.

"Metastable ions" are ions which are stable enough to leave the ion source but have adequate internal energy to decompose unimolecularly before reaching the detector. These transitions are observed in normal geometry sector mass spectrometers as broad peaks at apparent mass $m^* = m_2^2/m_1$. Pioneering studies of metastables were performed by kinetic energy spectroscopy (IKES). This technique has been discussed in detail by Graham Cooks and coauthors (8). IKES permits measurement of peak shapes for these transitions due to the kinetic energy release upon fragmentation. This information is valuable for elucidation of reaction pathways and for structural elucidation of isomers. The energetics and mechanisms of

Table 2. Ion Activation Processes in MS/MS

Unimolecular (metastable)	$m_1^+ \rightarrow m_2^+ + m_3$
Collisionally activated dissociation	$m_1^+ \xrightarrow{N} m_2^+ + m_3$
Photodissociation	$m_1^+ \xrightarrow{h\nu} m_2^+ + m_3$
Electron excitation	$m_1^+ \xrightarrow{e^-} m_2^+ + m_3$
Charge stripping	$m_1^+ \xrightarrow{N} M_1^{2+} + e^-$
Charge inversion	$m_1^- \xrightarrow{N} m_1^+ + 2e^-$
Charge exchange	$m_1^+ \xrightarrow{N} m_1 + N^+$
Associative ion/molecule reactions	$m_1^+ + N \rightarrow m_1N^+$

metastable decomposition have also been discussed by Beynon and Gilbert (56). Unfortunately, these metastables are not found in appreciable abundance and are often associated with structural rearrangements (11). In order to increase the number of peaks and their intensity, sufficient energy must be added to the parent ion to cause it to fragment. Ion excitation can be carried out by any of the methods listed in Table 2.

In photodissociation the amount of energy added to the ion is selected by varying the excitation wavelength. This can provide more precise energy control than can varying ion energy in CAD. Griffiths and coworkers have compared the photodissociation spectra of n-butyl and n-pentyl benzene with the high energy CAD spectra (57). The photodissociation of small ions has been studied with triple quadrupole instruments by Vestal and Futrell (28) and by McGilvery and Morrison (27). Ions trapped within an ion cyclotron resonance mass spectrometer (ICR) can be excited by a beam of electrons. By varying the potential difference between the filament and the cell, the excitation energy can be controlled. Comparisons between electron and collisional excitation have been published (58).

The most common method of adding internal energy to an ion in MS/MS, however, is collisional excitation with a neutral gas N:

$$AB^{+} \xrightarrow{N} (AB^{+})^{*} \quad A^{+} + B$$

This collisional excitation is generally carried out in one of two different energy regimes because of the kinetic energy requirements of different mass analyzers. Collisions at high energy (>1 KeV) in sector MS/MS instruments involve a two step process, excitation followed by unimolecular decay. These glancing high energy collisions lead to a direct Franck-Condon type electronic excitation (59) and are characterized by minimal momentum transfer and small scattering angles. The scattering angle of a given product ion is a function of the energy transferred and can be investigated by angle-resolved mass spectrometry (60,61). Energy-resolved breakdown curves are compared with angle-resolved spectra. Several other processes are observed with high energy collisions. Charge stripping and charge inversion are normally limited to sector instruments because of the high kinetic energy requirements of these reactions. Charge inversion has proven to be useful in the MS/MS analysis of polyaromatic hydrocarbons in solvent refined coal (38).

In contrast to these high energy collisions, collisional excitation in quadrupole and ICR instruments (62) is generally performed at low collision energies (0-100 eV). These low energy "billiard ball" collisions involve vibrational excitation by momentum transfer (56,30) and are characterized by significant momentum transfer and large scattering angles. The function of the center quadrupole in triple quadrupole MS/MS instruments is to focus the daughter ions scattered through large angles. It has been proposed that the low energy CAD mechanism involves a two step process, vibrational excitation followed by unimolecular decay (63). It will be shown, however, at least in the case of associative ion/molecule reactions at very low energies, that a one step mechanism involving the formation of a collision complex predominates.

Daughter ions arising from charge exchange and associative ion/molecule reactions can only be observed in MS/MS instruments with a quadrupole or ICR as the second mass analyzer, because these ions are formed with low (and indeterminate) kinetic energy. They cannot, therefore, be mass analyzed with energy dependent analyzers such as sector or time-of-flight analyzers. The associative ion/molecule reactions are particularly valuable because of their selectivity (see Chapter 4). Hybrid instruments which combine both high and low energy analyzers (such as a magnetic sector and a quadrupole (64)) permit a wider range of kinetic energy to be accessed.

In order to control the energy transferred in the collision process, two experimental variables can be adjusted. The ion kinetic energy (in center-of-mass coordinates) can be varied either by changing the collision cell potential relative to the source, or by changing the collision gas pressure. The latter method involves controlling the average number of collisions in the collision cell (65).

A variety of collision cells are used for CAD in MS/MS instruments, depending on the kinetic energy and the mass analyzers. The majority of sector instruments use a 1-3 cm long collision chamber with entrance and exit slits for the ion beam, pressurized with helium. The main disadvantage of this type of cell is the effusion of target gas through the slits, resulting in a significant number of collisions occurring outside the optimum focal region. This leads to an overall CAD efficiency of <1% (11,66,67). McLafferty and coworkers have recently described a nozzle/skimmer collision system located at the focal point between two double focussing analyzers (17). With the skimmer at the entrance to a 7000 L/sec diffusion pump, a CAD efficiency for methane of 11% at 25 keV was obtained. Recently, Todd and Glish have designed a simpler "molecular beam" collision region which uses a hypodermic needle as a means of introducing collision gas (68). These "beams" designs have led to a ten fold improvement in the efficiency of the high energy CAD process.

In the case of tandem quadrupole MS/MS systems, three different approaches to cell design have been taken. The most common collision region consists of an RF-only quadrupole (30) (such as the one in our instrument), enclosed within a gas-tight cylinder which can be pressurized with the collision gas. An alternate design (69,70) uses a "leaky dielectric" tube, extending into the two mass filters, as a collision cell which simulates an RF-only quadrupole. This cell can also be pressurized with a collision gas. A third design (71) consists of a "90% gas-transparent" quadrupole with a collision gas jet. The area surrounding this collision region is cryogenically pumped. The overall CAD efficiency for quadrupole systems with an RF-only collision cell ranges from 10% to 65% (29). A fourth design, using a short field-free collision chamber (33), is less efficient for CAD.

Energy Resolution

In collisional excitation the control of ion energy is achieved by selecting the ion kinetic energy. In the triple quadrupole this is achieved by applying a DC potential of 0 to 30 V to the center quadrupole collision region, referenced to the grounded ion source. Energy resolution increases the informing power of MS/MS (Table 1) and provides an added dimension of information in the determination of fragmentation pathways and in the structure elucidation of ions.

Because mass separation by quadrupoles is independent of ion kinetic energy, the accelerating voltage can be readily varied with little or no effect on resolution or transmission. The use of energy resolution in sector MS/MS instruments has received little attention due to the energy dependence of the mass analyzers. The effects of ion energy on the CAD spectra of the molecular ion of n-propanol and on the $C_7H_7^+$ ion from toluene are compared at high energies (KeV) in sector MS/MS instruments and at low energy in the triple quadrupole.

Comparison of Kinetic Energy Effects at Low and High Collision Energies

The change in appearance of CAD spectra with changing collision energy is generally more pronounced at low energies (<100 eV) than at high (KeV) energies. For highly endothermic reactions, however, significant effects are observed at both low and high energies. For example, the CAD spectra (recorded at an Ar pressure of 4.0 millitorr) of $C_7H_7^+$ (produced by 70 eV electron impact of toluene) includes four C_6 fragment ions ($C_6H_5^+$ through $C_6H_2^{+\cdot}$) arising from increasing endothermic reactions. The ratio of $C_6H_2^{+\cdot}$ (m/z 74) to $C_6H_5^+$ (m/z 77) (appearance energies 21 eV and 15 eV, respectively (72)) increases considerably with increased kinetic energy of the parent ion. Figure 7 compares the m/z 74/77 ratio as a function of energy observed at low energies with those reported at kilovolt energies (17). The two curves show remarkably similar trends even though the energies are different by three orders of magnitude. Increasing the ion kinetic energy results in an increase in intensity of the ion of higher appearance energy ($C_6H_2^{+\cdot}$) at the expense of the ions ($C_6H_5^+$) with a lower appearance energy.

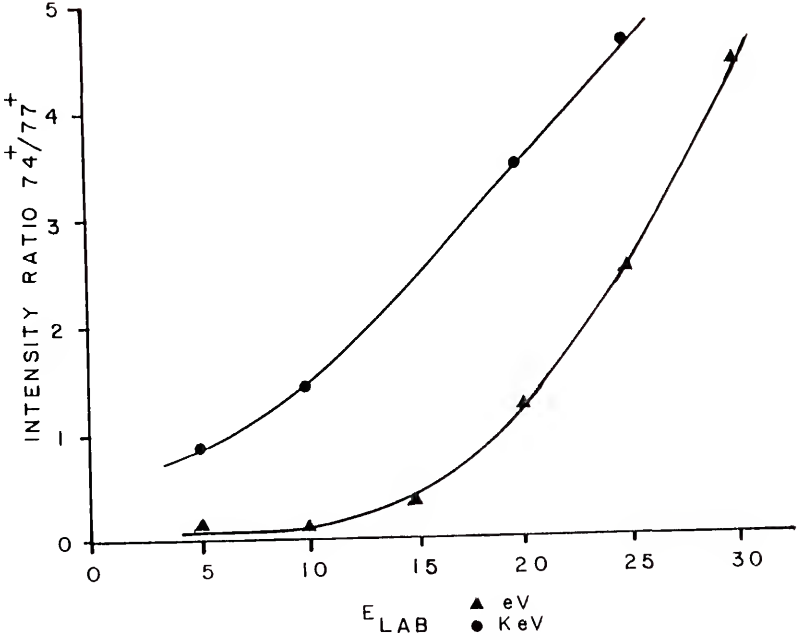

Figure 7. Intensity ratio $74^+/77^+$ for the CAD of $C_7H_7^+$ at (a) low kinetic energies (this study); (b) high kinetic energies (17).

A similar behavior for the ratio of CH_3O^+ to $C_3H_6^{+\cdot}$ (with appearance energies (72) of 11.3 and 10.5 volts, respectively) from the CAD of the n-propanol molecular ion at low and high (73) energies is shown in Table 3. Increasing the ion energy from 2.0 to 8.0 eV in these experiments shows a similar trend to varying the kinetic energy from 0.45 to 9.6 KeV in the high energy experiments. As demonstrated in Table 3, the intensity of ions with higher appearance energies increases at the expense of ions with lower appearance energies as the ion kinetic energy is increased.

It can be seen that small changes in the ion kinetic energy in the triple quadrupole can have a dramatic effect on the appearance of the daughter spectrum. The increase in the number and abundance of daughter ions is an indication that most of the parent ions' kinetic energy can be transferred into internal energy (vibrational excitation). Ions resulting from rearrangement or other low energy processes can best be observed in the triple quadrupole at low kinetic energies, while more structurally significant fragments are best observed at increased ion energies. By varying the ion energy (energy resolution) both types of fragment ions can be observed.

Energy-Resolved Breakdown Curves

The dramatic changes observed in the low energy CAD spectra with increasing ion kinetic energy result from the highly efficient collision process. The effect of ion

Table 3. Ratio Of CH_3O^+ to $C_3H_6^{+\cdot}$ Produced By The CAD Of n-propanol Molecular Ion At Low Kinetic Energies From This Study, And High Kinetic Energies

Low Energy		High Energy[a]	
E_{lab}, eV	$CH_3O^+/C_3H_6^{+\cdot}$	E_{lab}, KeV	$CH_3O^+/C_3H_6^{+\cdot}$
2.0	0.26	0.45	0.23
4.0	0.47	1.25	0.50
6.0	0.96	3.75	0.79
8.0	1.55	9.6	1.6
10.0	2.10		
12.0	2.61		
18.0	3.50		
20.0	4.07		
24.0	4.25		

a. Source: Reference 11.

internal energy on the dissociation process is represented in breakdown curves (plots of the relative intensities of the molecular and all fragment ions as a function of internal energy of the molecular ion.) These theoretical curves, calculated from the quasi-equilibrium theory (QET) (73), may be compared with experimental breakdown curves obtained by plotting relative abundances of the ions vs kinetic energy in CAD experiments or those obtained by angle-resolved mass spectrometry (60,61).

The energy-resolved CAD breakdown curves were obtained by operating the instrument in the daughter spectrum mode, in which molecular ions produced by 70 eV electron impact are mass selected by the first quadrupole and undergo CAD in the center RF-only quadrupole. The daughter or fragment ions are then mass-analyzed by scanning the third quadrupole. The kinetic energy of the ions is readily selected by varying the DC potential applied to the center quadrupole relative to the ion source potential. No significant effects on resolution were observed over the range of kinetic energies available with this instrument. Each data point represents an average of at least 10 scans and is reproducible to within ±2%.

The breakdown curves are plotted as $F/(\Sigma F+P)$ vs E_{cm} where F is the intensity of a specific fragment ion, ΣF is the sum of the intensities of all fragment ions, and P is the intensity of the parent ion. The center-of-mass energy (E_{cm}) is the fraction of the kinetic energy in the laboratory coordinate system (E_{lab}) which is available for ineleastic scattering. Specifically,

$$E_{cm} = E_{lab} \times \frac{m}{m + M}$$

where m is the mass of neutral target gas and M is the mass of the parent ion. Because the low energy CAD process is very efficient, it is possible to transfer most or all of this kinetic energy into internal energy. As a result, small changes in ion kinetic energy can have dramatic effects upon the appearance of the daughter spectrum as shown in Figure 7 and Table 3.

Plots of the relative abundance of the parent and daughter ion vs energy yield energy-resolved CAD breakdown curves have been compared with the data from the QET theory and angle-resolved mass spectrometry by Fetterolf and Yost (74). The energy-resolved CAD breakdown curves for various molecular ions have been obtained by varying the ion energy (E_{lab}) from 0 to 30 eV. Breakdown curves for n-propanol and propane are shown in Figures 8-11.

N-propanol. Figure 8 compares the energy-resolved CAD breakdown curves for n-propanol with breakdown curves from QET calculations (73). The energy-resolved CID data are similar to the QET results in several aspects. The fragment ions $42^{+\cdot}$ and 59^{+} exhibit maxima at approximately E_{cm} = 1.0 and 1.5 eV, respectively, as predicted by the QET. The CAD appearance energy for m/z 29 also agrees with

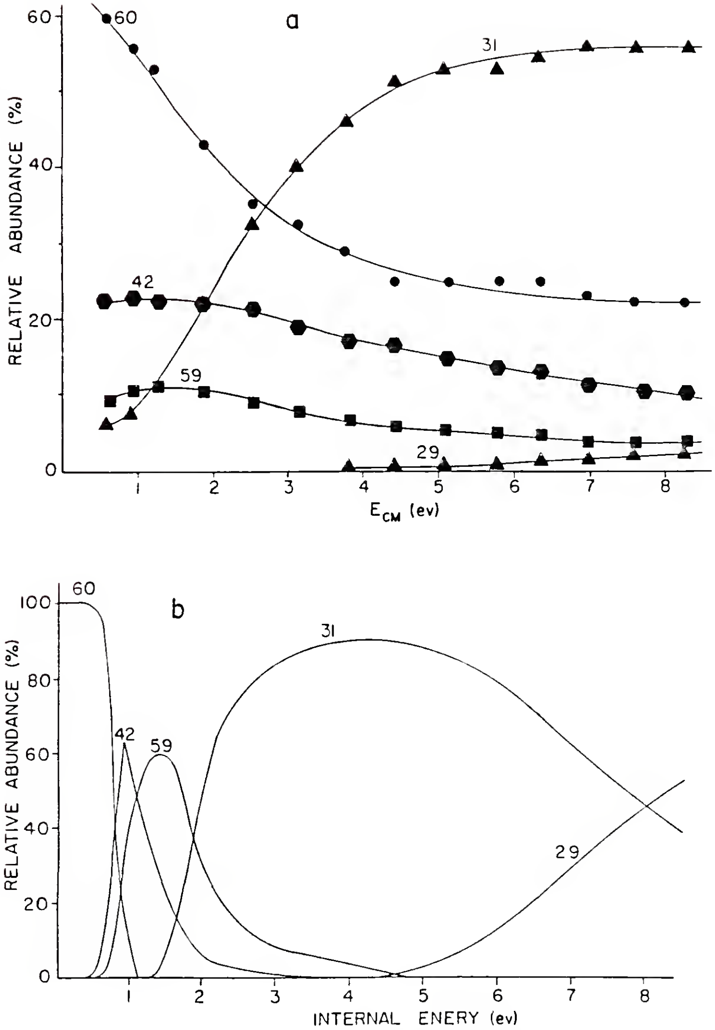

Figure 8. Breakdown curves for n-propanol (a) energy-resolved CAD (1.5 millitorr N_2); (b) QET theory (73).

QET calculations. The abundant 31^+ fragment ion exhibits a broad maximum. The main difference between the energy-resolved CAD and QET results is the limited energy resolution in the experimental data. These broadened curves are due to the approximately 2 eV (E_{cm}) kinetic energy spread of the parent ion which reduces the informing power. Furthermore, fragment ions of high appearance potential (such as 29^+) are generally lower in abundance than predicted by the QET. Since the collisions involving the largest transfer of internal energy lead to large scattering angles (and the loss of most of the ion's forward momentum), the collection of these fragment ions in the quadrupole collision region is less efficient.

In the angle-resolved data (Figure 9), no parent ion (m/z 60) or the fragment ion at m/z 42 (loss of H_2O) was reported. The m/z 27 ion, observed in the angle-resolved experiments, was less than 0.01% relative abundance in our experiments and was not reported in the QET calculations. The angle-resolved curves show trends similar to those in the energy-resolved curves with similar energy resolution. While the energy-resolved technique is currently limited to lower energies than the angle-resolved methods, it permits the investigation of internal energies near zero.

Propane. The energy-resolved CAD breakdown curve and the QET results for propane are shown in Figure 10. Despite the limited energy resolution, the ions at m/z 27 and m/z 29 exhibit broad maxima. The CAD appearance

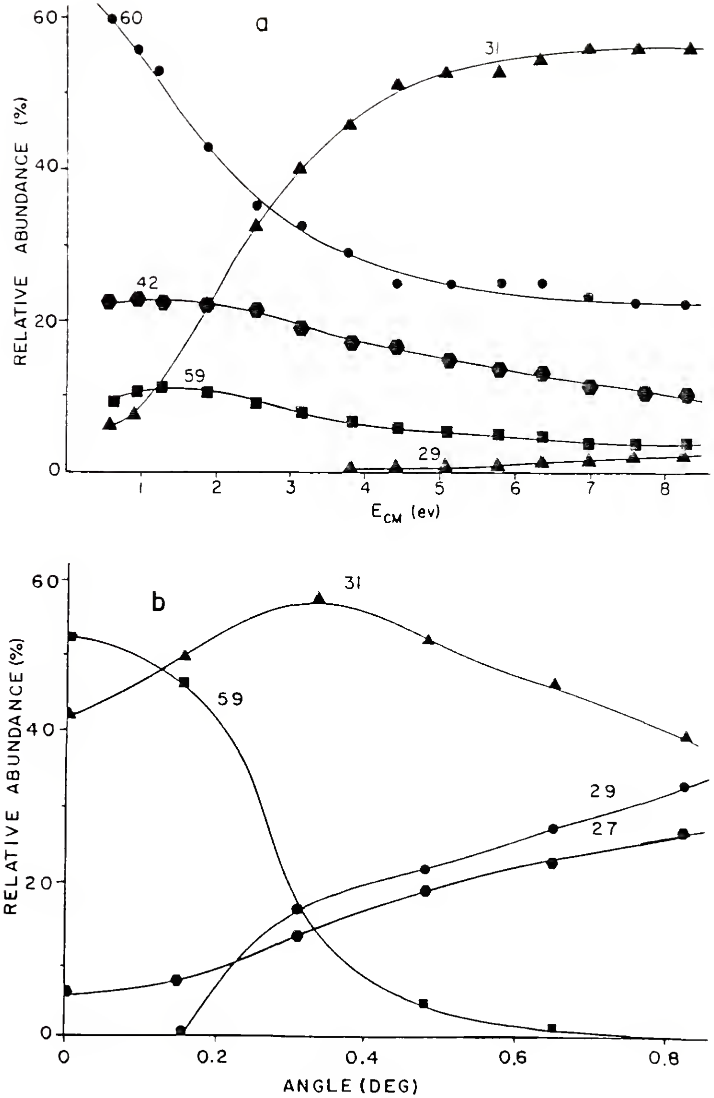

Figure 9. Breakdown curves for n-propanol (a) energy-resolved CAD (1.5 millitorr N_2); (b) angle-resolved (60).

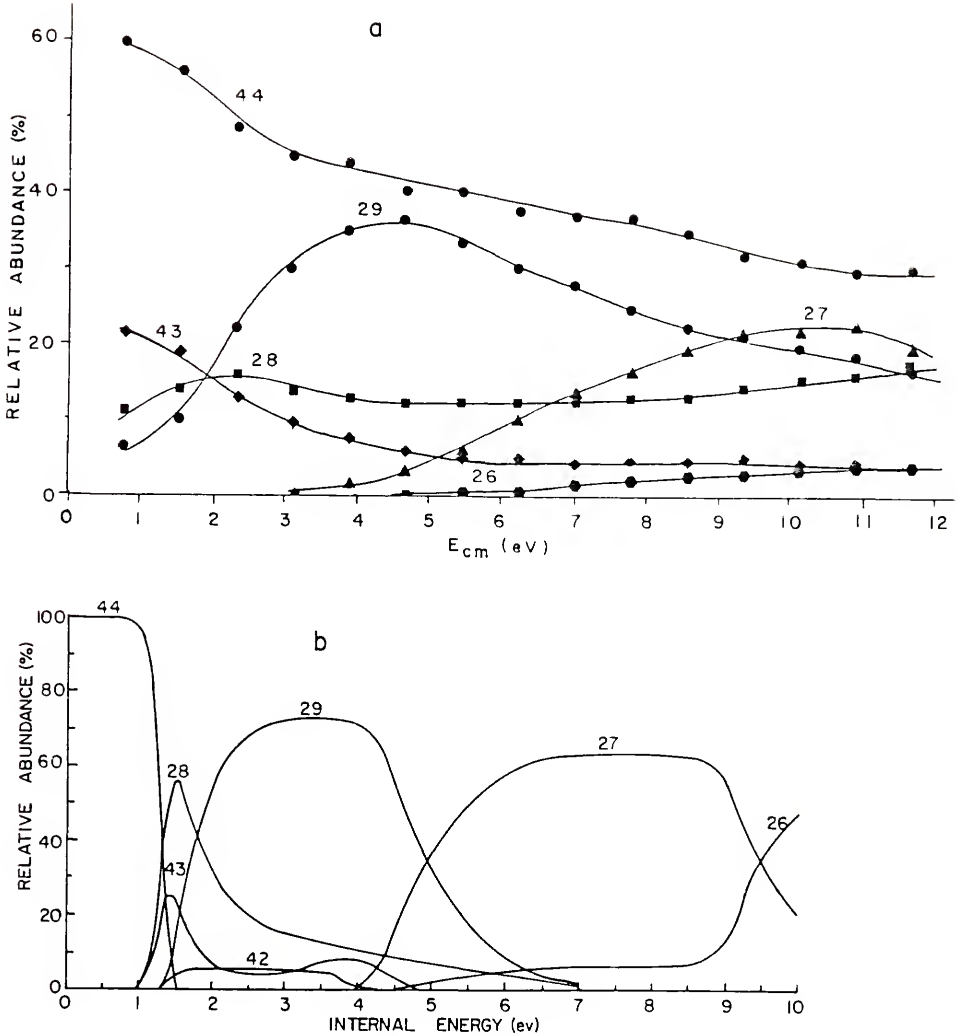

Figure 10. Breakdown curves for propane (a) energy-resolved CAD (3.0 millitorr N_2); (b) QET theory (73).

threshold for m/z 26 at 4.5 eV agrees well with the QET results. The slight increase in the relative abundance of m/z 28 at higher energies is due to the production of $N_2^{+\cdot}$ by charge exchange to the collision gas.

Figure 11 compares the energy-resolved breakdown curves with the angle-resolved breakdown curves (60). The ions at m/z 42 and m/z 43 corresponding to the loss of H_2 and $H^{\cdot}$, respectively, were not reported in the angle-resolved results.

The use of energy resolution not only increases the informing power of MS/MS but also aids in the determination of fragmentation pathways. In addition the use of energy resolution aids in the optimization of the CAD process. Consider, for example, the determination of propane (Figure 10) using single reaction monitoring. For the reaction in which m/z 44 loses a methyl group to form m/z 29, the optimum ion energy would be approximately 4.5 eV (E_{cm}). The loss of CH_5 to form m/z 27, however, reaches a maximum at approximately 10 eV (E_{cm}).

The added dimension of information in the energy-resolved CAD breakdown curves makes it possible to distinguish between isomeric ion structures. As an example of this capability, the differentiation of isomeric $C_3H_6^{+\cdot}$ ions is discussed below. Additional applications of energy-resolved breakdown curves are presented in Chapter 4.

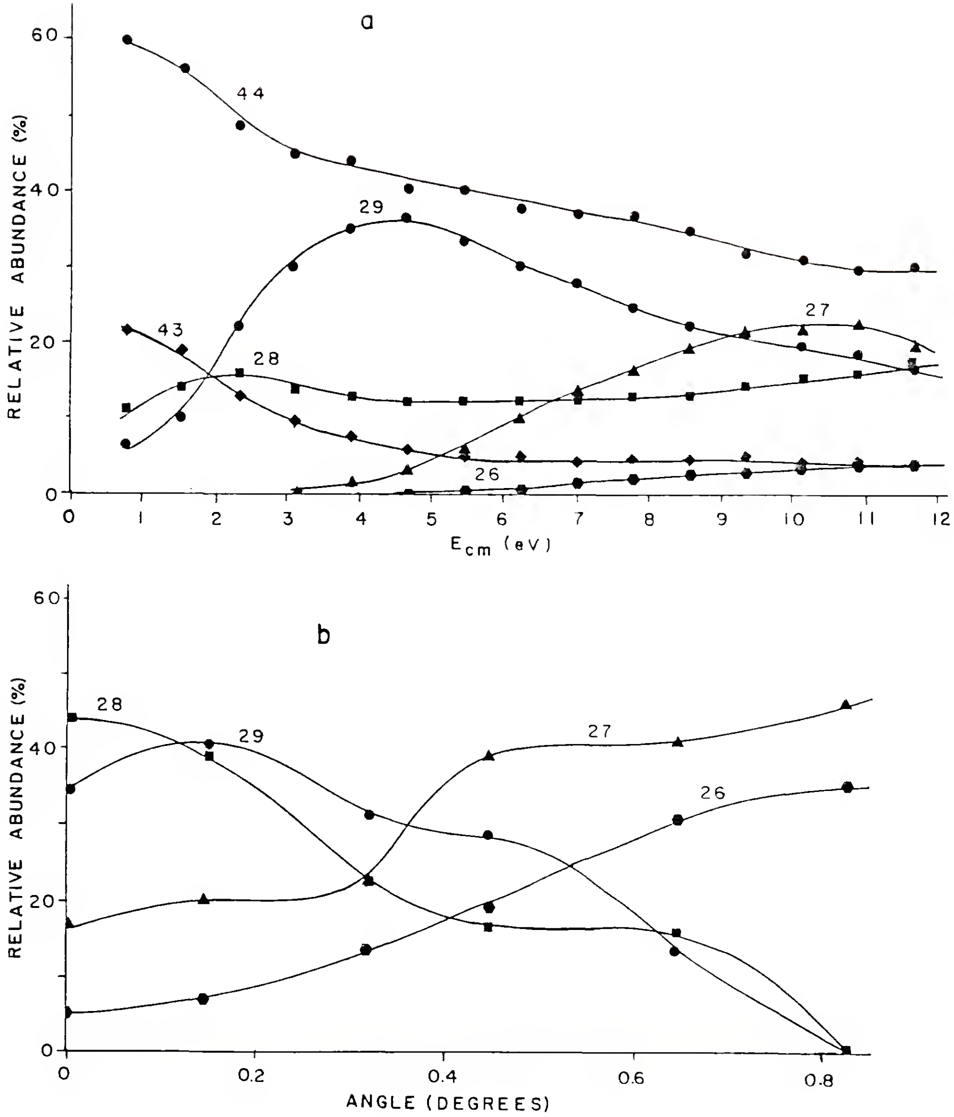

Figure 11. Breakdown curves for propane (a) energy-resolved CAD (3.0 millitorr N_2); (b) angle-resolved (60).

$C_3H_6^{+}$. The isomeric propene ion and cyclopropane ions are difficult to distinguish by low or high energy CAD techniques (17). The addition of energy resolution, however, makes it possible to distinguish these isomeric ions. Figure 12 compares the energy-resolved curves for both the cyclic $C_3H_6^{+\cdot}$ ion (from tetrahydrofuran (75)), and linear $C_3H_6^{+\cdot}$ ion (from propene (75)). The loss of a hydrogen from the cyclic ion to yield m/z 41 is more abundant at low energies and exhibits a maximum near 12 eV. In addition, the loss of a methyl group to form m/z 27 is greater for the strained cyclic structure than for the linear ion. The energy-resolved breakdown curves provide a great deal more information than does a daughter spectrum at a single energy, making it easier to distinguish between the two isomeric structures of $C_3H_6^{+\cdot}$.

Pressure Resolution

Another resolution element in the CAD process which can increase the informing power in MS/MS is the pressure of gas in the collision chamber. In the center quadrupole of this instrument, the pressure can be varied from 0.1 to 10 millitorr with a practical resolution of 0.5 millitorr. Kinetic information as well as breakdown curves can be obtained as the pressure is varied. The relative abundancesof the daughter and parent ions from n-propanol are shown in Figures 13 and 14. For first order kinetics, one would expect that a plot of $\ln(P/P_0)$ vs pressure would be linear. Figure 13 shows a plot of $\ln(P/P_0)$ vs the pressure

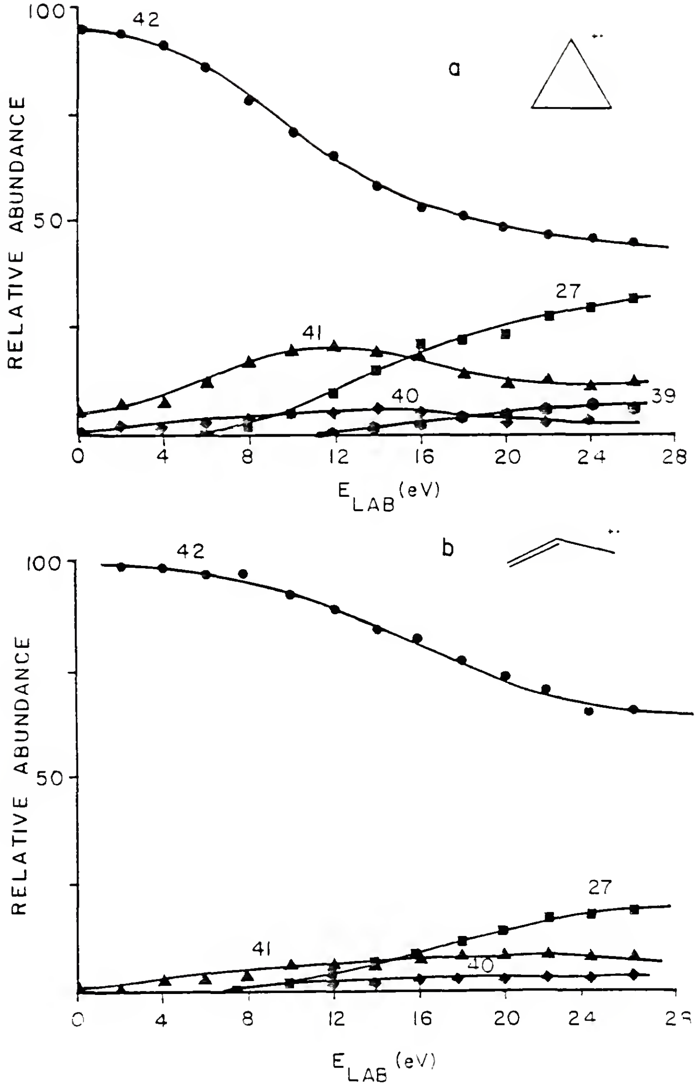

Figure 12. Energy-resolved breakdown curves for the isomeric $C_3H_6^{+\cdot}$ ions (a) cyclopropane (from tetrahydrofuran); (b) propene (from propene).

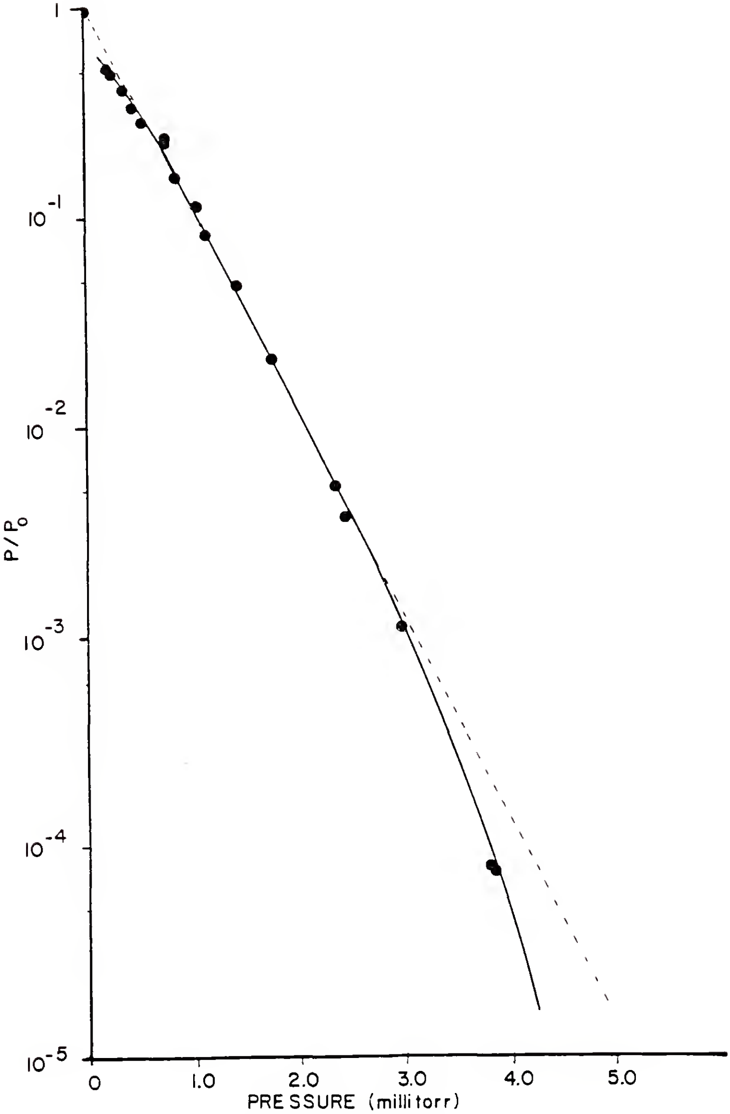

Figure 13. Parent ion transmission (P/P_0) vs CAD pressure for n-propanol.

of N_2 in the collision cell. Indeed, first order kinetics is observed for the attenuation of the parent ion over the range of 0.5 to 3.0 millitorr. The slight deviation at low pressures is undoubtedly due to the difficulty in accurately measuring these pressures with the thermocouple gauge. One possible explanation for the deviation from linearity at high pressures is the loss of most of the parent ions' forward momentum after several collisions. The slow-moving ions experience an increased number of RF-cycles in the center quadrupole and are more likely to be lost.

The effects of varying the pressure on the relative abundance ($F/\Sigma F+P$) for the individual daughter ions of m/z 59, 42, and 31 are shown in Figure 14. Increasing the pressure results in a linear increase in the relative abundance of the daughter ions due to an increase in the average number of collisions.

Varying the pressure also has an important effect upon the efficiency of the CAD process. For instance, at 0.5 millitorr of pressure the sum of the fragment ions for n-propanol (Figure 14) is approximately 17% of the total ion current. Increasing the pressure to 2 millitorr increases the sum of the fragment ions to 46%. The effects of pressure and energy on the efficiency of the CAD process were investigated for CH_4.

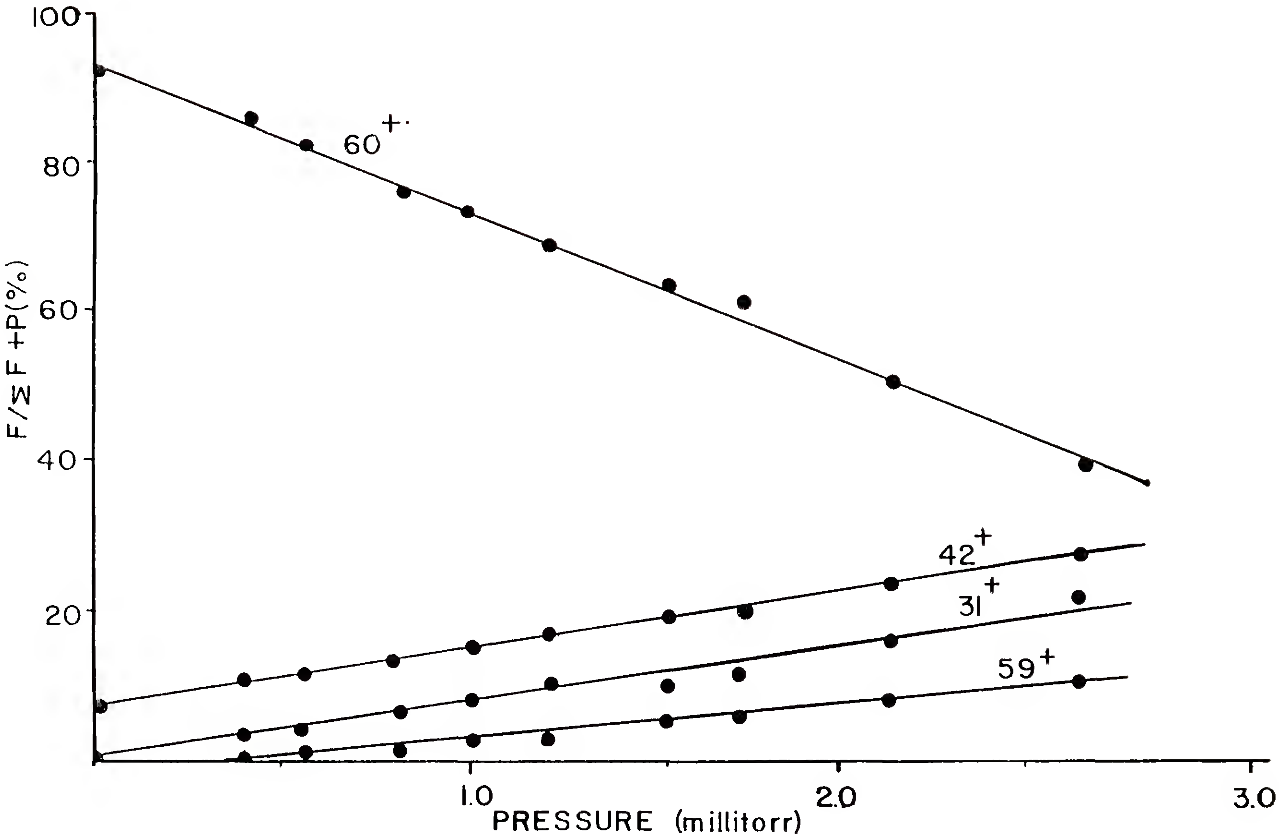

Figure 14. Pressure breakdown curve for n-propanol.

Efficiency of the CAD Process

An important concept in MS/MS is the efficiency of the CAD process. Table 4 shows a series of equations first developed by Yost and Enke (29,30) and extended by Yost and Fetterolf (7) to describe the efficiency in terms of the fragment ion intensity (F), and the parent ion intensity at the entrance (P_o) and exit (P) of the collision cell.

Because of the differences in collision cell design, location and type of pressure gauges, and calibration problems associated with changing collision gases, it has been suggested (17,68) that parent ion transmission (P/P_o) or attenuation ($1-P/P_o$) be reported rather than pressure. In this way, efficiency curves plotted vs P/P_o could be more easily compared for different instruments. Unfortunately, plotting the data in this manner hides the true nature of the collection efficiency, E_c, and therefore the overall efficiency E_o. From Table 4, we see that $E_C = (P/P_o)/(1-E_F)$ and $E_o = E_C \times E_F = (P/P_o)E_F/(1-E_F)$. Plotting either of these vs P/P_o gives curves that are dependent only on the fragmentation efficiency, E_F.

Figures 15-17 display the fragmentation, collection, and overall efficiencies for the CAD of CH_4^+ as a function of collision gas pressure and ion kinetic energy. These curves contain a great deal more information than those

Table 4. Expressions for Efficiency of CAD Process

Fragmentation efficiency:	E_F[a]	$= \frac{\Sigma F}{\Sigma F + P}$	
Collection efficiency:	E_C	$= \frac{\Sigma F + P}{P_o}$	$= \frac{P}{P_o(1-E_F)}$
Overall efficiency:	E_O	$= E_F \times E_C = \frac{\Sigma F}{P_o}$	$= \frac{PE_F}{P_o(1-E_F)}$
Parent ion transmission:	$\frac{P}{P_o}$	$= E_C - E_O$	$= E_C(1-E_F)$
Parent ion attenuation:	$1 - \frac{P}{P_o}$		$= 1 - E_C(1-E_F)$

[a] ΣF = summed intensity of all fragment ions.

P_o = parent ion intensity at entrance of collision cell.

P = parent ion intensity at exit of collision cell.

for a spectrum taken at fixed pressure or energy and provide an insight into the fundamental aspects of the low-energy CAD process.

The fragmentation efficiency ($\Sigma F/\Sigma F+P$), shown in Figure 15, is the fraction of ions leaving the collision cell which are daughter ions. As the collision gas pressure or ion energy is increased, the abundance of the daughter ions increase. The fragmentation efficiency ranges from less than 1% at 2 eV ion energy and 0.1 millitorr to nearly 10% at a pressure of 3 millitorr and an ion kinetic energy of 26 eV. It can also be seen that the same fragmentation efficiency can be obtained at various combinations of energy and pressure.

Although increasing the pressure improves the fragmentation efficiency the collection efficiency ($\Sigma F+P/P_o$) decreases, as shown in Figure 16. The collection efficiency is the ratio of ions leaving the collision cell to those entering. With no collision gas present the collection efficiency is 100%. As the pressure is increased the collection efficiency decreases due to scattering of the ions. At a given pressure, however, increasing the ion energy results in only a slight increase in the collection efficiency. As the ion kinetic energy and collision gas pressure are increased, the fragmentation efficiency increases but the collection efficiency decreases. The product of these curves, the overall

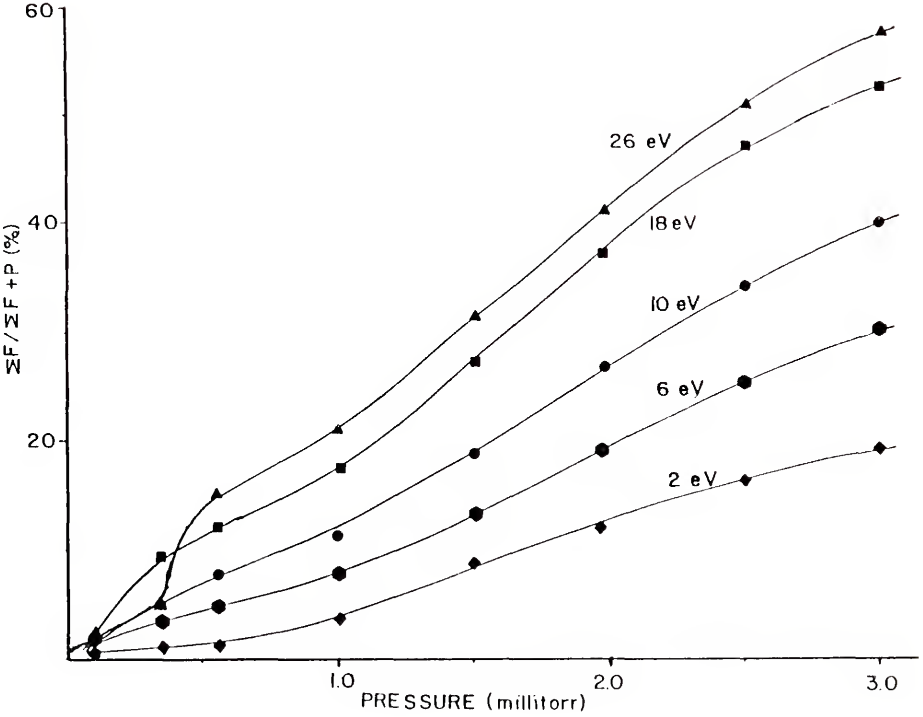

Figure 15. Fragmentation efficiency for the CAD of methane vs pressure (N_2) at various collision energies.

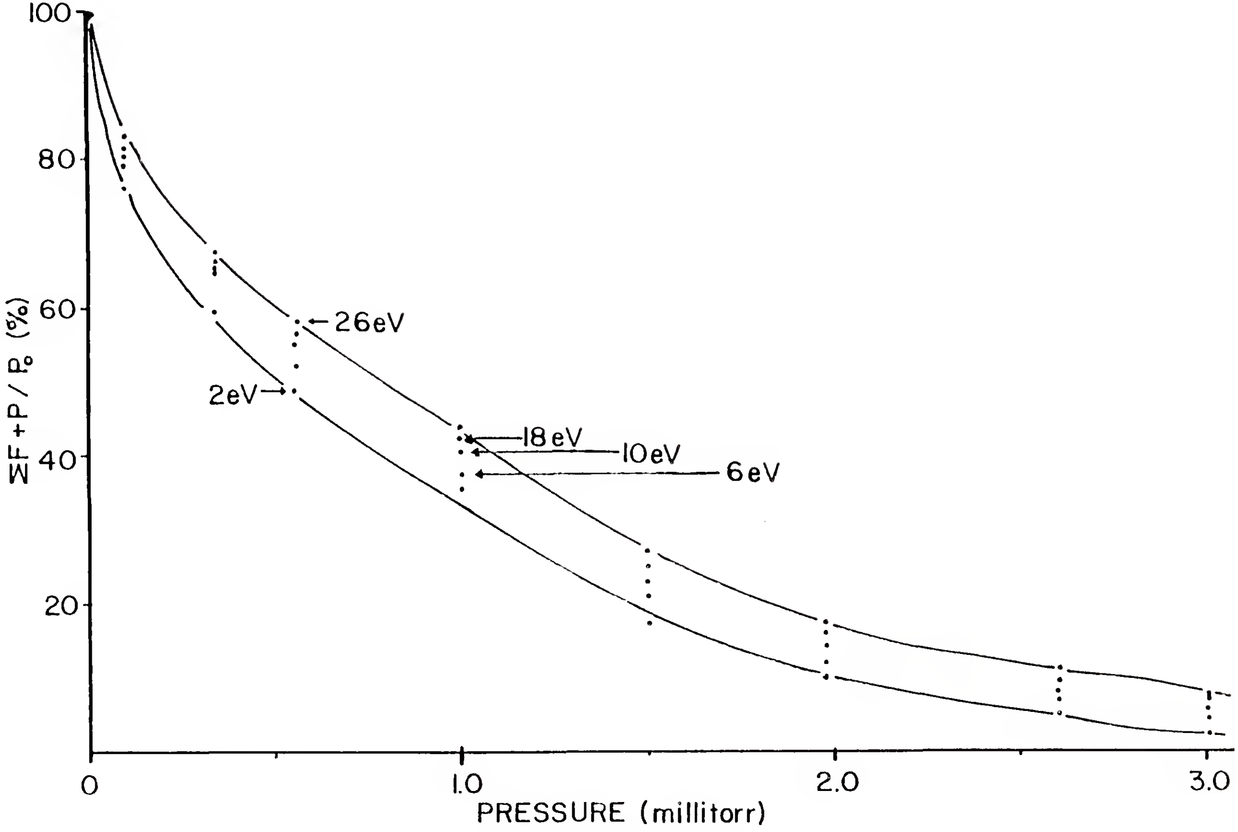

Figure 16. Collection efficiency for the CAD of methane vs pressure (N_2) at various collision energies.

efficiency ($\Sigma F/P_o$), exhibits a maximum at some intermediate value. The overall efficiency for CH_4^+ is shown in Figure 17. It increases as the pressure is increased, until reaching a broad maximum centered at approximately 1 millitorr. The overall efficiency then decreases with further increases in pressure due to scattering losses.

The information contained in these curves is important in terms of the optimization of the collision process. For CH_4^+, a collision pressure of 1 millitorr and 26 eV corresponds to the maximum overall efficiency (9%). Although the efficiency curves are plotted for the sum of all fragments, the ion kinetic energy and pressure also affect the relative abundance of the individual daughter ions. This is shown in Figure 18. A linear plot is found for the relative abundance of the daughter ions at each of the ion energies vs the log of transmittance (P/P_o). Extrapolating to zero pressure ($P/P_o = 100\%$) should give the CAD spectrum resulting from a single collision. At low ion energies the relative abundance of the daughter ions remains fairly constant; however, at higher energies the relative abundance of low mass daughter ions such as CH^+ increasesat the expense of higher mass daughters, such as CH_3^+. This is due to successive collisions of the daughter ions with the collision gas resulting in their further fragmentation.

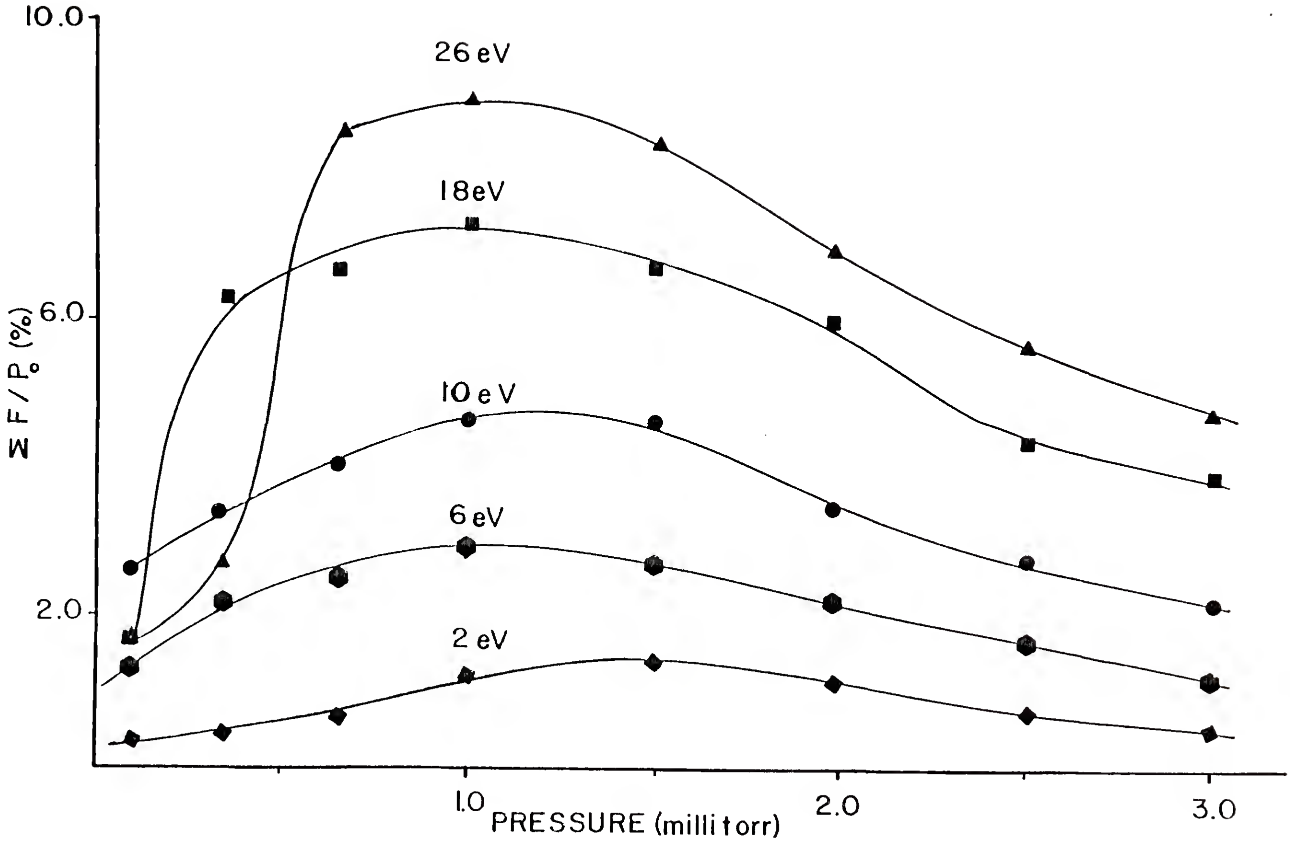

Figure 17. Overall CAD efficiency of methane vs pressure (N_2) at various collision energies.

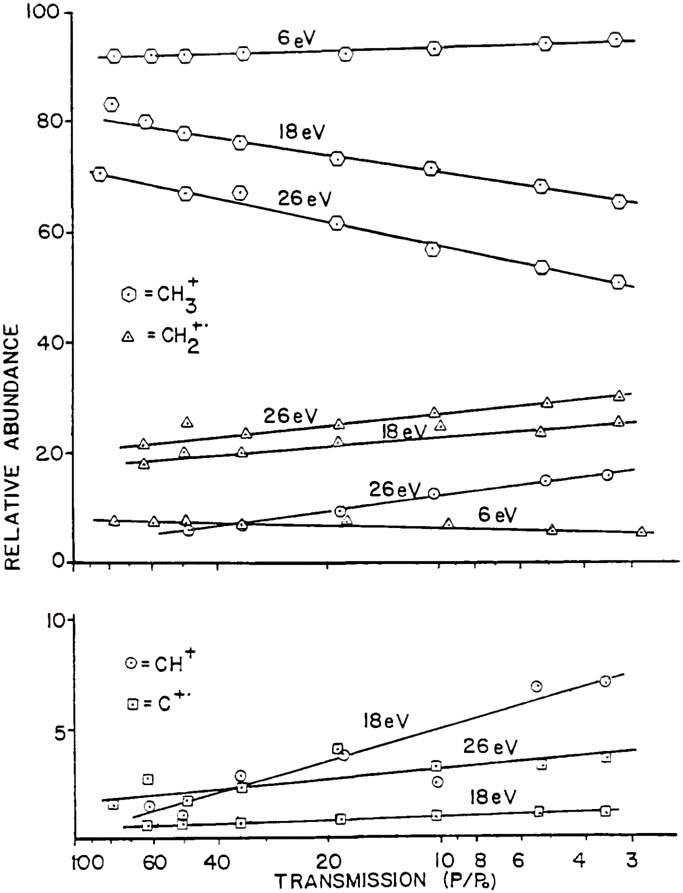

Figure 18. Relative abundances of the daughter ions of methane vs log parent ion transmission at various collision energies.

For most qualitative work (structure elucidation) CAD spectra are obtained under multiple collision conditions and high energy because of the increase in the number and abundance of daughter ions. In quantitative analysis using single reaction monitoring however, it is important to operate at the energy which maximizes the abundance of the particular daughter ion of interest and at a pressure which minimizes scattering losses.

In order for a given ion to be observed in the CAD spectrum the energy transferred in the CAD process (E_{cm}) must exceed the appearance energy for that ion. Since the pressure affects the amount of energy transferred, extrapolating the appearance kinetic energies of the daughter ions to zero pressure makes it possible to determine the CAD threshold energy for the daughter ions. Table 5 compares the CAD threshold energies for the daughter ions of methane with the electron impact appearance energies (72). The agreement is well within the kinetic energy spread of the CH_4^+ parent ion, showing that it is possible to transfer nearly all the kinetic energy into internal energies at these low collision energies.

Reactive Collisions

The informing power of MS/MS when CAD is used is only half that indicated in Table 1 because the daughter ions must have a mass less than the parent ion. The use of reactive collisions (ion/molecule reactions) can result in reaction products with a mass greater than that of the

Table 5. Comparison Of Collisional Energies With Electron Impact Appearance Energies (Minus The Ionization Energy) For the Fragment Ions Of Methane Molecular Ion

Ion	CAD Threshold Energies E_{cm} (eV)	Electron Impact[a] AE-IE (eV)
CH_3^+	1.3	1.5
CH_2^+	2.9	2.5
CH^+	10.6	9.5
C^+	12.9	12.5

[a] *Source*: Reference 72.

parent ion, thereby increasing the informing power. These reactive collisions can be used not only to differentiate isomeric ion structures due to their selectivity but also to investigate the nature of the low energy collision process in the triple quadrupole and the reactions of reagent ions in chemical ionization.

VME and Propene

Recently, vinylmethylether (VME; $H_2CCHOCH_3$) has been used as a CI reagent gas to determine the location of carbon-carbon double bonds in isomeric mono-olefins (76,77). The electron impact mass spectra of such isomers are frequently very similar making it difficult to locate the position of the double bond. The reaction between the $VME^{+\cdot}$ ion and propene (C_3H_6) as well as the reactions between the $C_3H_6^{+\cdot}$ ion and VME were investigated with the triple quadrupole in order to elucidate the mechanism of these reactions under CI conditions and to investigate the effects of ion kinetic energy on reaction collisions.

The principle reaction between $VME^{+\cdot}$ and propene, as shown in Figure 19, involves the formation of a four-centered collision complex which fragments to form either m/z 58 or m/z 72. It has been speculated (77) that this four-centered collision complex may be formed by the reaction of either molecular ion ($VME^{+\cdot}$ or $C_3H_6^{+\cdot}$) with the neutral molecule of the other species. By selecting the parent ion from one species with quadrupole one, and using the other as the collision gas in the center quadrupole,

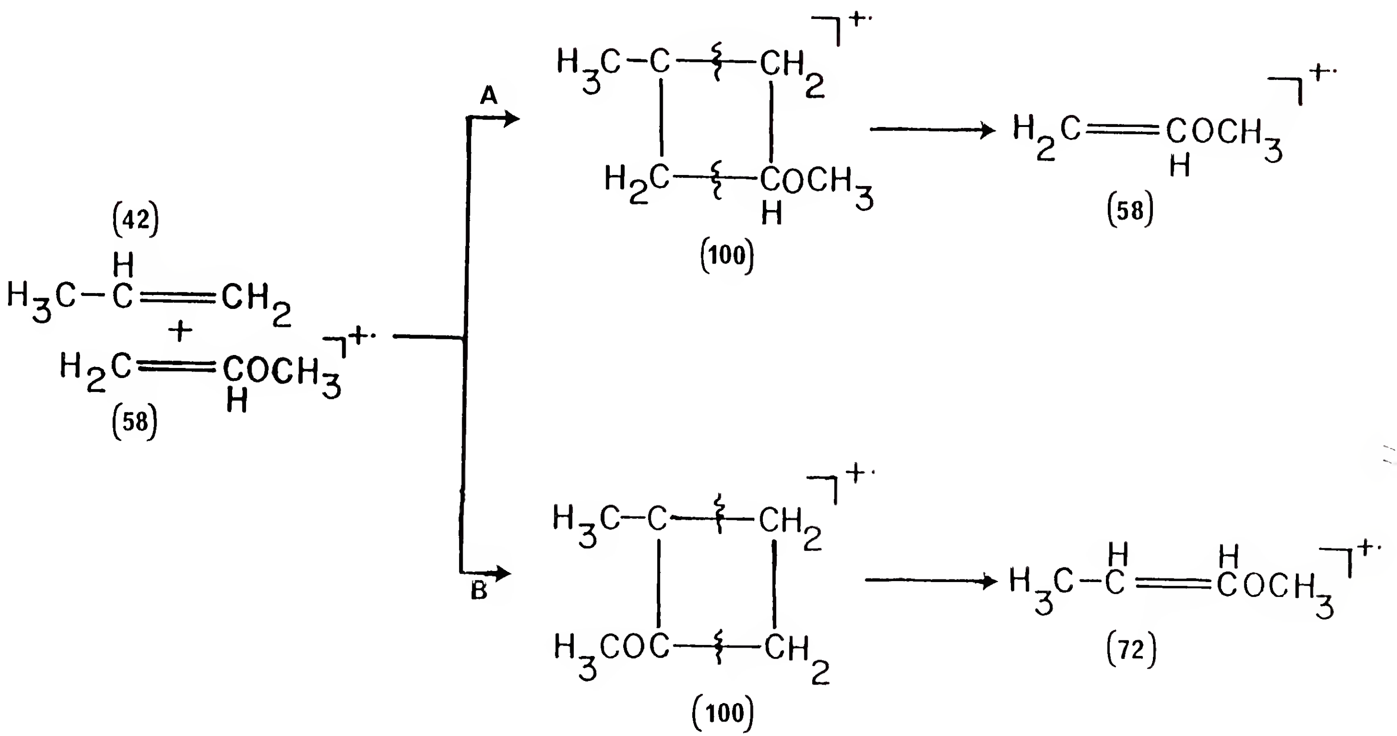

Figure 19. Mechanism for the formation and dissociation of the four-centered collision complex in the reaction of the VME molecular ion with propene.

it should be possible to determine the mechanism of formation of this four-centered collision complex. The spectra obtained for both cases are compared in Figure 20. Although the collision complex at m/z 100 is not observed in either case, the ion at m/z 72 (loss of C_2H_4 from the complex) is only observed when $VME^{+\cdot}$ is used as the parent ion. This also indicates that the four-centered complex has been formed via reaction "B" in Figure 19. The m/z 58 ion is due mainly to unreacted parent ions but may also be due to the dissociation of the collision complex formed via reaction "A". When $C_3H_6^{+\cdot}$ is used as the parent ion charge transfer to form $VME^{+\cdot}$ and proton transfer to form $(VME+H)^+$ are observed. The $VME^{+\cdot}$ ions formed by charge transfer undergo sequential reactions with other VME molecules to form $(VME)_2^{+}$ (m/z 116) which further dissociates. The mechanism for the formation of the various fragment ions in Figure 20 are shown in Table 6 and are discussed in detail below. The structure of each ion was confirmed by CAD of the ions formed when VME and propene were simultaneously introduced into the ion source. When $VME^{+\cdot}$ is reacted with C_3H_6 fragment ions at m/z 69, 72, and 85 are observed. These ions are formed when the collision complex (m/z 100) dissociates. Ions formed by the collision of $C_3H_6^{+\cdot}$ with VME result from the dissociation and rearrangement of the VME dimer.

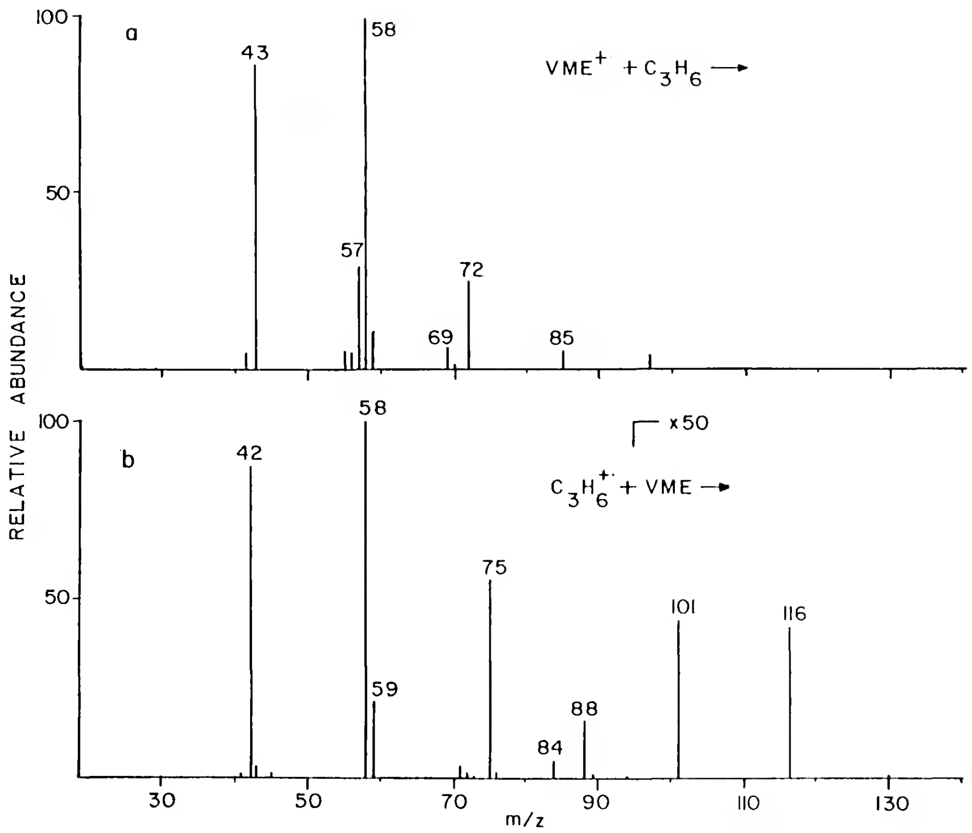

Figure 20. Mass spectra for the reactions of (a) vinylmethyl ether ($VME^{+\cdot}$) with propene ($C_3H_6\cdot$); (b) propene ($C_3H_6^{+}\cdot$) with vinylmethyl ether (VME).

Table 6. Ions Formed In The Reactive Collisions Between Vinylmethyl Ether And Propene

	$VME^+ + C_3H_6$	
m/z	Formula	Mechanism[a]
43	$C_2H_3O^+$	$(100 - C_3H_7O)^+$
57	$C_3H_7O^+$	$(100 - C_2H_3O)^+$
58	$C_3H_6O^{+\cdot}$	$VME^{+\cdot}$
59	$C_3H_7O^+$	$(VME + H)^+$
69	$C_5H_9^+$	$(100 - H_3CO)^+$ [a]
72	$C_4H_8O^{+\cdot}$	$(100 - C_2H_4)^{+\cdot}$
85	$C_5H_9O^+$	$(100 - CH_3)^+$
	$C_3H_6^+ + VME$	
42	$C_3H_6^+$	$C_3H_6^{+\cdot}$
58	$C_3H_6O^{+\cdot}$	$VME^{+\cdot}$
59	$C_3H_7O^+$	$(VME + H)^+$
75	$C_3H_7O_2^+$	$(VME_2 - C_3H_5)^+$
84	$C_5H_8O^{+\cdot}$	$(VME_2 - CH_3OH)^{+\cdot}$
88	$C_4H_8O_2^{+\cdot}$	$(VME_2 - C_2H_4)^{+\cdot}$
101	$C_5H_9O_2^+$	$(VME_2 - CH_3)^+$
116	$C_6H_{12}O_2^{+\cdot}$	$(VME_2)^{+\cdot}$

a. 100 refers to the four centered collision complex of m/z 100.

The energy-resolved curves for these reactions give an insight into the dissociation of the collision complex and the nature of associative reactions in the triple quadrupole. For a particular ion/molecule reaction at a fixed ion energy (E), the cross section σ(E) is given by

$$\sigma(E) = \frac{\Sigma F}{P_0 n \ell}$$

where ΣF is the sum of the ion current for the fragment ions, P_o is the ion current for the parent ion incident on the target gas with number density n (# molecules per unit volume). The length of the collision cell is given by ℓ. As demonstrated in the breakdown curves and in the energy-resolved associative reactions given below the relative abundance of a given ion varies with changes in ion energy. The energy dependence of the cross section for an associative ion/molecule reaction can be computed from the formula (78):

$$\sigma(E) = \sqrt{2}\ \pi e \left(\frac{\alpha m}{\mu}\right)^{\frac{1}{2}}\ E^{-\frac{1}{2}}$$

where α is the polarizability of the neutral, μ is the reduced mass of the colliding particles, m is the mass of the parent ion and E is the energy of the parent ion in the laboratory coordinate system. It can be seen that, for an associative ion/molecule reaction, the cross section is inversely proportional to the square root of the ion energy. As E_{LAB} is increased, the collision complex will contain excess internal energy and is likely to dissociate.

The effects of ion kinetic energy can be observed in the energy-resolved curves for the reaction between $VME^{+\cdot}$ and propene, as shown in Figure 21.

The ion at m/z 72 (arising from reaction "B" in Figure 19) decreases rapidly with an increase in ion energy, indicative of the formation and dissociation of the four-centered collision complex. The hydrogen abstraction from propene to form m/z 59 and the charge transfer to form m/z 58 also decrease with an increase in ion kinetic energy. The ions at m/z 57, 69, 85, and 97, all of which are dissociation products of the four-centered collision complex, increase, as expected, with an increase in ion kinetic energy. The ion at m/z 43 results from the loss of C_3H_7O from the collision complex.

The energy-resolved curves for the reaction between $C_3H_6^{+\cdot}$ and VME are shown in Figure 22. The ion at m/z 58 is due to charge transfer to the VME collision gas. This ion undergoes subsequent reactions with VME molecules producing the dimer $(VME_2)^{+\cdot}$ which dissociates to form ions at m/z 75, 84, 88, and 101 through the loss of C_3H_5, CH_3OH, C_2H_4, and CH_3, respectively.

The ions at m/z 59 and 88, which are formed by rearrangement reactions of the dissociating VME dimer, are independent of the ion kinetic energy.

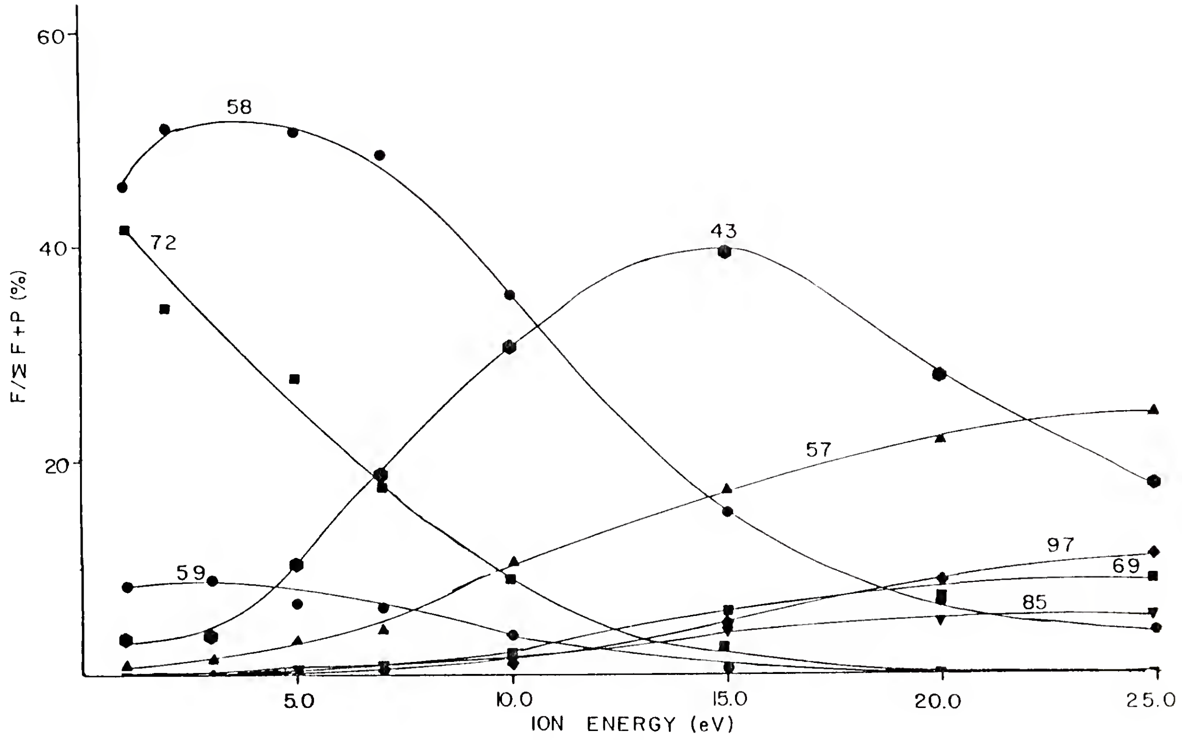

Figure 21. Energy-resolved reactive collisions of VME$^{+\cdot}$ with propene (C_3H_6).

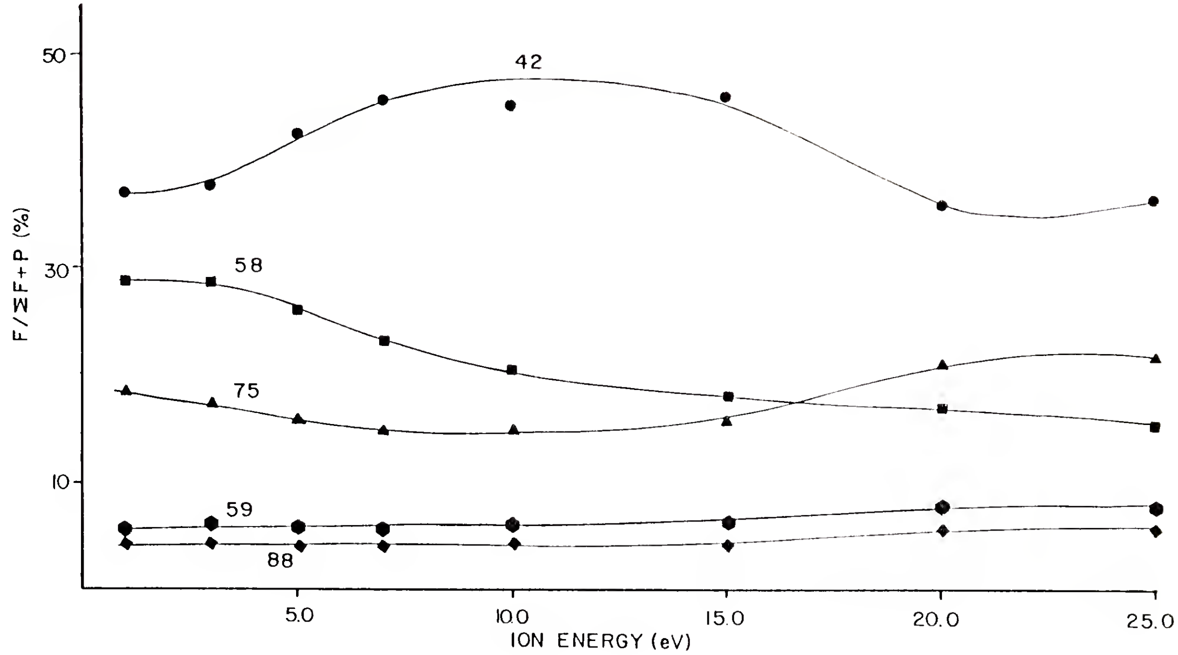

Figure 22. Energy-resolved reactive collisions of $C_3H_6^{+\cdot}$ with VME.

The application of energy resolution to reactive collisions aids in the elucidation of the structure and mechanisms for the formation of collision complexes. In addition it provides an insight into the low energy collision process. It has been suggested that the low energy collision process in MS/MS involves vibrational excitation by momentum transfer followed by unimolecular decomposition (63). It appears, however, at least in the case of associative ion/molecule reactions, a one step mechanism, involving the formation of a collision complex predominates. Reactive collisions are also discussed in Chapter 4, as they may be applied to the differentiation of isomeric structures and in the investigation of reactions of hydrocarbon ions with acetylene.

CHAPTER 4
APPLICATION TO STRUCTURE ELUCIDATION

The application of MS/MS to elucidate the structure of gas phase ions (11) and therefore that of the original molecule (36) is widely appreciated. It permits the analyst to separate a portion of a molecule and fragment it, enabling him to build up the structure piece by piece. If this process is carried out systematically, all pathways for the formation or fragmentation of every ion in the mass spectrum can be determined. As an example, consider the structure analysis of nonan-4-one, in which the 47 peaks in the EI mass spectrum produced over 400 CAD peaks (31). This enormous amount of information forms a promising data base for computerized structure elucidation.

It is not uncommon for two ions of different structures to give CAD spectra which are too similar to enable their differentiation. The use of the added resolution elements, as discussed in Chapters 2 and 3, can help discriminate between isomeric ion structures. Examples of the use of energy resolution and reactive collisions for the differentiation of ion structures are presented below. In addition, reactive collisions are used to investigate the reactions of hydrocarbon ions with acetylene. The use of daughter spectra for the structure elucidation of adduct ions formed under chemical ionization is also discussed. Finally, computer-aided interpretation of MS/MS data is discussed.

Isomer Differentiation

Varying the ion kinetic energy in the triple quadrupole provides an effective resolution element. The energy-resolved breakdown curves (discussed in Chapter 3) provide a great deal more information than does a daughter spectrum at a single energy. The isomeric linear and cyclic $C_3H_6^{+\cdot}$ ions can be distinguished by the use of energy-resolved breakdown curves as illustrated in Figure 12. As further examples of this capability, several other chemical systems have been investigated.

Bromobenzoic Acid (o-,m-,p-)

Table 7 shows the effect of ion kinetic energy on the ion abundances (F/ΣF+P) for the CAD of the ^{81}Br molecular ion form o-, m-, and p-bromobenzoic acid. The molecular ion (m/z 202) was produced by 70 eV EI and mass selected by quadrupole 1. The CAD spectra (recorded at a collision gas pressure of 1.5 millitorr N_2) are quite similar at 10 eV, while significant differences can be observed at 20 and 30 eV. For each isomer, it can be seen that increasing the collision energy results in an increase in the intensity of all daughter ions, particularly those resulting from the loss of the carboxylic acid group to form m/z 157 and the loss of CO_2 and ^{81}Br to form the m/z 77. For

Table 7. Effect Of Ion Energy On The Relative Abundance Of Molecular And Fragment Ions From The CAD Of o-, m-, And p-Bromobenzoic Acid Molecular Ions (With ^{18}Br, m/z 202)

m/z	Neutral Loss	Ion Energy (E_{LAB})								
		10 eV			20 eV			30 eV		
		o	m	p	o	m	p	o	m	p
202	--	78.8	78.9	78.1	45.4	47.6	44.7	28.5	30.3	24.8
185	OH	20.7	20.3	21.6	52.5	47.2	52.6	59.7	50.7	62.8
174	CO	0.52	0.3	0.3	0.9	0.8	0.6	0.9	1.0	0.6
157	COOH	0.02	0.1	0.01	1.0	2.4	0.6	10.2	13.8	8.7
121	Br	0.02	0.3	0.01	0.2	1.9	0.4	0.5	3.4	0.5
77	CO_2, Br	0.01	0.02	0.01	0.05	0.1	1.1	0.3	0.8	2.6

example, the loss of COOH from m-bromobenzoic acid increases from 0.1% at 10 eV to 13.8% at 30 eV. Similarly, the ion at m/z 77 increases from 0.02% to 0.8%. Varying the ion kinetic energy increases the selectivity in MS/MS which aids in the differentiation of the isomeric bromobenzoic acids.

Aminophenol (o-,m-,p-)

Table 8 shows the effect of ion kinetic energy on the relative abundances (F/ΣF+P) of the daughter ions for the CAD of o-, m-, and p-aminophenol. The daughter spectra show losses of H_2O, CHO, and C_2H_5O. The loss of H_2O to form m/z 91 is characteristic of the "ortho effect". At 30 eV this loss is 2.05% for the ortho isomer while the corresponding loss is only 1.20% and 0.45% for the meta and para isomers, respectively. It can also be seen, that as the ion kinetic energy is increased, the intensity of the peak due to structural rearrangement of the ring and loss of CHO increases dramatically. The use of energy resolution aids in the differentiation of the isomeric aminophenols.

$C_3H_6^{+\cdot}$

Reactive collisions can also aid in the differentiation of isomeric structures. As was illustrated in Figure 12 the linear and cyclic $C_3H_6^{+\cdot}$ ions can be distinguished by energy resolution. They can also be differentiated by reactive collisions using NH_3 as the collision gas. The

Table 8. Effect Of Ion Energy On The Relative Abundance Of Molecular And Fragment Ions From The CAD of o-, m-, and p-Aminophenol

m/z	Neutral Loss	Ion Energy (E_{LAB})								
		10 eV			20 eV			30 eV		
		o	m	p	o	m	p	o	m	p
109		91.50	96.00	93.00	60.62	73.94	79.04	25.27	34.65	31.46
108	$H^{\cdot}$	2.84	0.83	2.46	6.64	3.11	5.65	7.08	5.33	12.22
91	H_2O	0.22	0.18	0.05	1.12	0.55	0.24	2.05	1.20	0.45
80	CHO	5.34	2.94	4.49	30.66	22.11	14.97	61.10	57.25	55.05
64	C_2H_5O	0.10	0.05	0.01	0.96	0.29	0.10	4.50	1.57	.82

differentiation of $C_3H_6^{+\cdot}$ ions by reaction with NH_3 has also been carried out using low-energy ion/molecule reactions in an ICR (79,80).

Figure 23 compares the reaction of reactions of the cyclic $C_3H_6^{+\cdot}$ (cyclopropane) and linear propene ions with 1.2 millitorr of NH_3 at an ion energy of 5.5 eV. The reaction of the cyclopropane structure with NH_3 produces a reaction complex $[C_3H_6NH_3^+]^*$, which is not observed, but which rapidly dissociates to form m/z 31 (CH_5N) and m/z 30 (CH_4N). No reaction is observed, however, in the case of the linear isomer. The ion at m/z 17 is due to charge exchange to the NH_3 collision gas. Table 9 summarizes the reactions of $C_3H_6^{+\cdot}$ from a number of parent molecules. The differences in the relative abundances (with respect to the parent ion at m/z 42) of m/z 30 and 31 are also observed in the energy-resolved studies of this reaction, in which m/z 30 increases with increasing ion energy, indicating that these differences are probably due to differences in the internal energy of the collision complex prior to dissociation. The assignment of these ion structures by reactive collisions are in agreement with metastable studies by Gross and Lin (81).

$C_5H_6^{+\cdot}$

The CAD spectra of cyclopentadiene (c-$C_5H_6^{+\cdot}$) and 1-pentene-3-yne ($C_5H_6^{+\cdot}$) are compared in Figure 24. It can be seen that both isomers produce very similar daughter

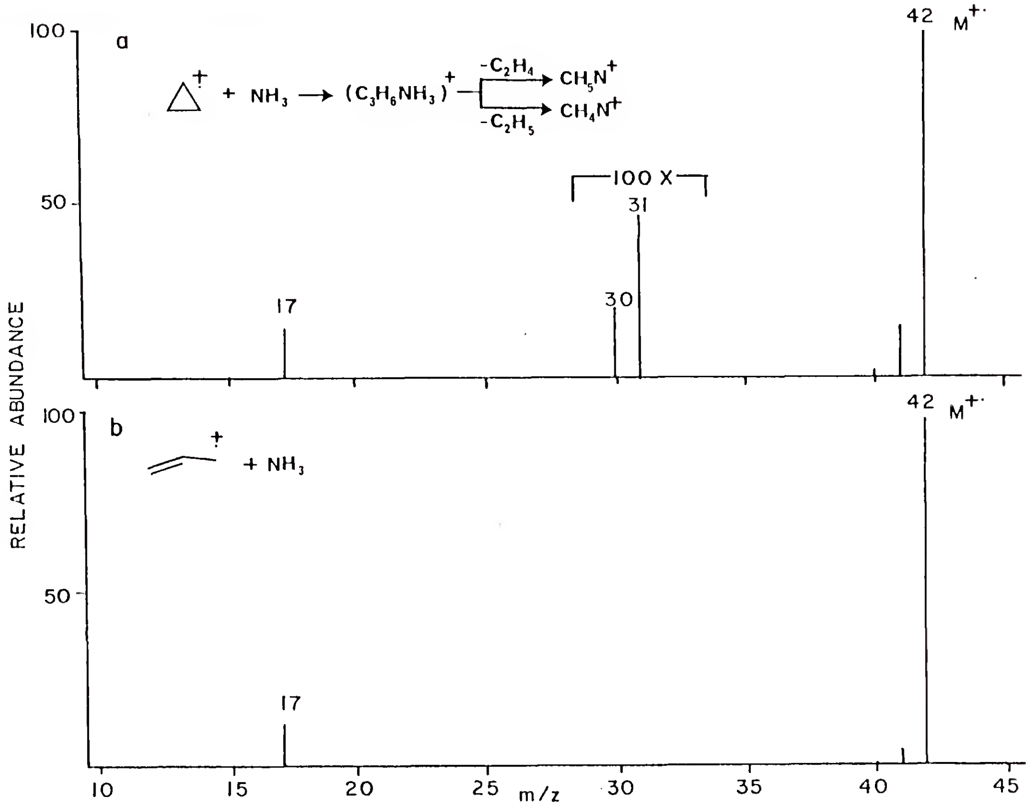

Figure 23. Differentiation of isomeric $C_3H_6^{+\cdot}$ ions by reactive collisions with NH_3 (1.2 millitorr, 5.5 eV): (a) cyclopropane; (b) propene.

Table 9. Differentiation of Isomeric $C_3H_6^{+\cdot}$ Structures By Reactive Collisions with NH_3

	Relative Abundance (X100)	
Origin	m/z 30	31
Cyclopropane-type Structure		
Tetrahydrofuran	21	48
Cyclohexanone	11	1
Propene-type Structure		
Propene	--	--
n-Pentyl Alcohol	--	--
Hexane	--	--

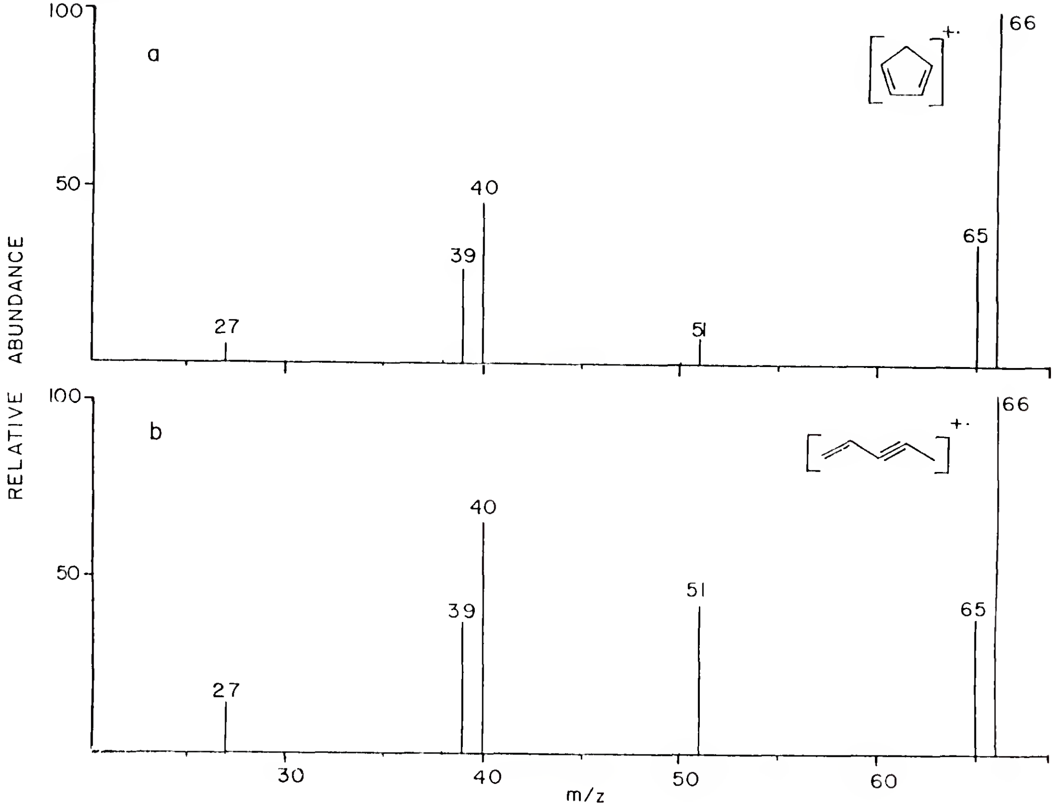

Figure 24. Daughter spectra of m/z 66 from (a) cyclopentadiene; (b) 1-pentene-3-yne.

spectra. The two isomers can readily be distinguished by reactive collisions using isobutane (i-C_4H_{10}), a common CI reagent gas, as the collision gas. Figure 25 compares the reactions with isobutane of the cyclopentadiene ion (from dicyclopentadiene) and the linear 1-propene-3-yne molecular ion. In the case of the linear isomer, several intense addition products are observed, while no addition products are observed for the cyclic ion. The m/z 57 ion is due to hydride abstraction from the collision gas.

$C_3H_3^+$

Ausloos and Lias have recently described a procedure for the differentiation of the cyclic and linear $C_3H_3^+$ ions based upon their chemical reactivity in an ICR (82). $C_3H_3^+$ is of particular interest because it is the dominant positive ion found in fuel rich and sooting flames (83,84). Studies by Holmes and Lossing have shown that ionization at the thermochemical threshold of propargyl chloride (C_3H_3Cl) and propargyl bromide produces exclusively the cyclopropenium ion (85). Propargyl iodide, in contrast, produces exclusively the linear propargyl ion. At energies, above threshold, however, a mixture of $C_3H_3^+$ ion structures may be produced due to higher internal energy imparted to the ions in the ionization process.

For these experiments $C_3H_3^+$ ions were produced from the propargyl halides by electron impact or by dissociative charge exchange:

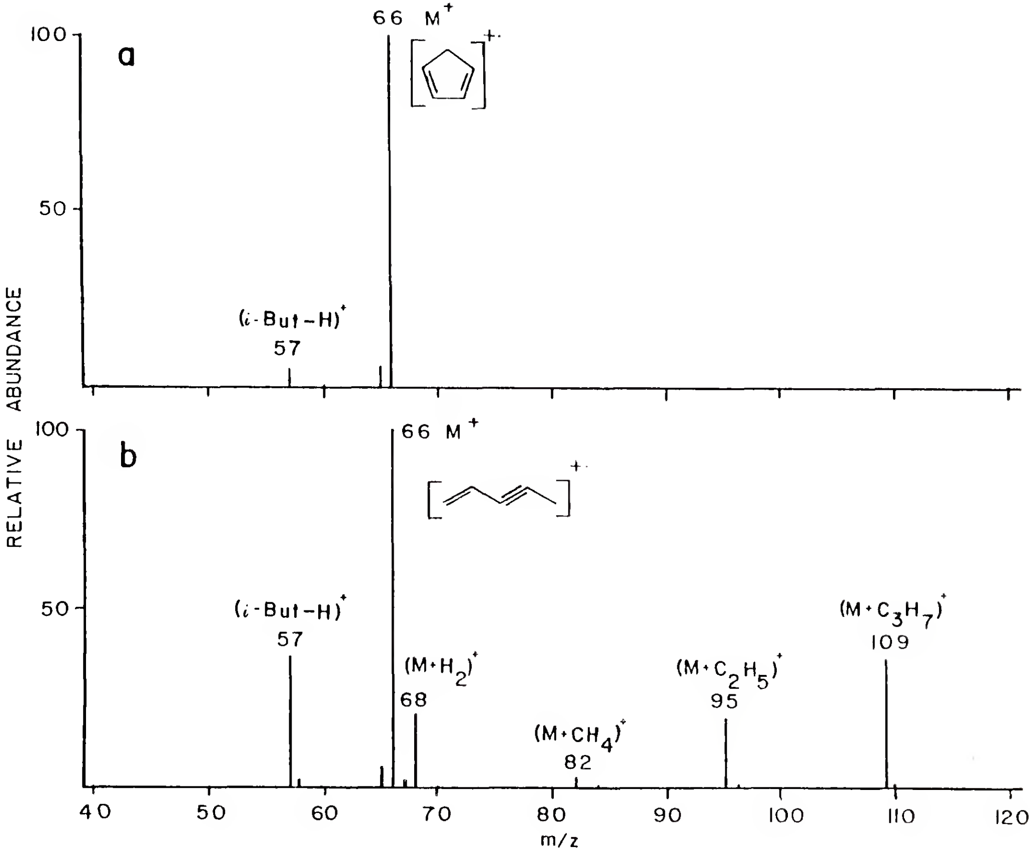

Figure 25. Differentiation of isomeric $C_5H_6^{+\cdot}$ ions by reactive collioions with isobutane (6.0 millitorr, 2.6 ev): (a) cyclopentadiene; (b) 1-pentene-3-yne.

$$C_3H_3X + M^+ \rightarrow C_3H_3^+ + M + X$$

where X = Cl, Br, or I and M^+ is the charge exchange species produced by 30 eV electron impact of various gases (M + Xe, CO_2, CO, N_2, Ar, Ne, He) at 2×10^{-6} torr. The propargyl halides were introduced from a heated batch inlet at a pressure twenty times less than that of the charge exchange reagent. The $C_3H_3^+$ ions produced in the ion source were mass selected by quadrupole one and reacted with acetylene (C_2H_2) in the center quadrupole. Acetylene pressure was adjusted for 75% attenuation of the $C_3H_3^+$ ion (approximately 4 millitorr). The reaction products were then mass analyzed by scanning quadrupole three. The following reactions were observed:

$$C_3H_3^+ + C_2H_2 \rightarrow C_5H_5^+$$

$$\rightarrow C_5H_3^+ + H_2$$

The effect of collision energy on these reactions was investigated by varying the ion kinetic energy in the center quadrupole. Figure 26 indicates that, for all three precursors, the production of $C_5H_5^+$ increases, as expected, with a decrease in ion energy. At higher energies, an increase in the production of $C_5H_3^+$ arises from the dissociation of the $C_5H_5^+$ collision complex due to increased internal energy. Based upon the obvious differences in the ratio of $C_5H_5^+$ to the original amount of

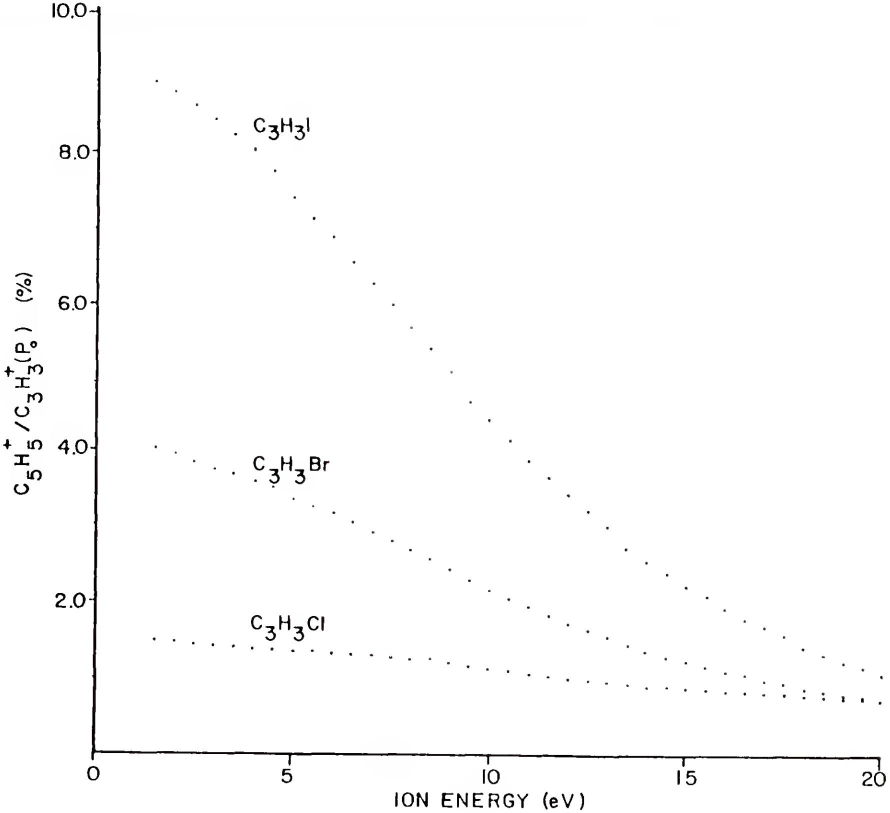

Figure 26. Intensity ratio of $C_5H_5^+/C_3H_3^+$ for $C_3H_3^+$ produced by electron impact from the propargyl halides vs ion energy for the reactive collisions with C_2H_2.

C_3H_3 without collision gas present (P_0) in Figure 26 and upon earlier studies (82,86), where the linear $C_3H_3^+$ is seen to be more reactive, it appears that the propargyl iodide produces more of the reactive linear isomer than does the bromide or chloride under electron impact ionization.

The effects of varying the charge exchange reagent ion were also investigated. For a charge transfer reaction, it can be assumed that the internal energy of the parent is given by the recombination energy of the charge donor. This is particularly true when rare gas atomic ions are used. It is conceivable that, for di- and tri-atomic ions, some of the internal energy may be carried away as vibronic energy in the neutral. The effect of this change in internal energy of the parent molecule can lead to changes in the relative population of the cyclic and linear ions.

Figure 27 shows the effects of varying the charge exchange species on the $C_5H_5^+/C_3H_3^+$ ratio for $C_3H_3^+$ from the various propargyl halides. The data for the monoatomic species produce smooth curves, while di- and tri-atomic data (open symbols) all lie above the curves. The differences observed between the results when $CO_2^{+\cdot}$ (recombination energy, 13.8 eV) is replaced by CO^+ (recombination energy, 14.0 eV) or when N_2 (recombination energy, 15.6 eV) is replaced by Ar^+ (recombination energy, 15.8 eV) indicates that some of the energy is carried away as vibronic energy

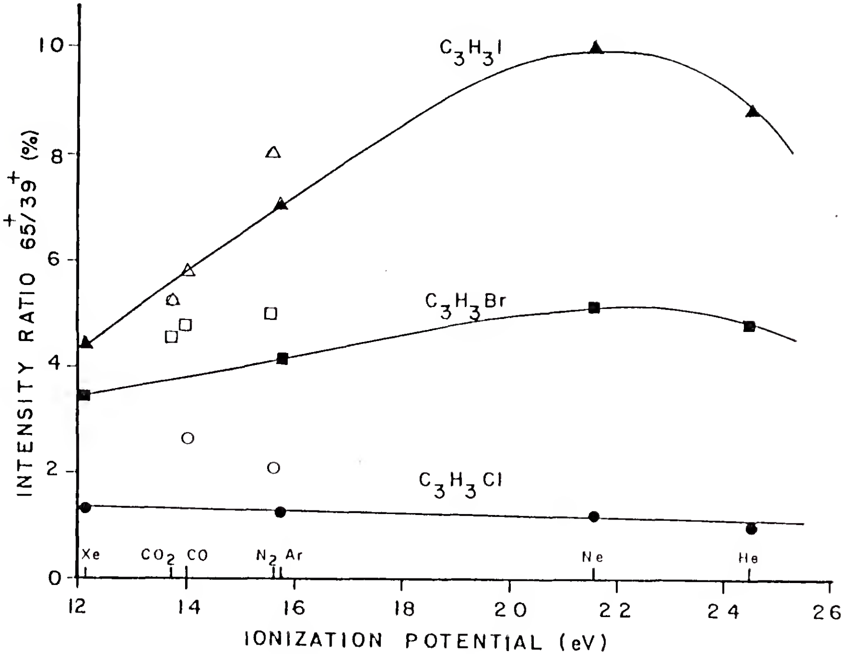

Figure 27. Intensity ratio of $C_5H_5^+/C_3H_3^+$ for $C_3H_3^+$ produced by dissociative charge exchange (with various gases) of the propargyl halides as a function of ionization potential (monoatomics - solid symbols; di- and tri-atomics - open symbols). Collision energy 2eV.

which results in a change in the relative population of the cyclic and linear ions formed in the ionization process. The differences in the ratio of linear to cyclic $C_3H_3^+$ with changes in the charge exchange species has also been observed in the ICR studies (82).

The use of reactive collisions aids in the differentiation of isomeric structures, as demonstrated in the cases of $C_3H_6^{+\cdot}$, $C_5H_6^{+\cdot}$, and $C_3H_3^+$. These reactive collisions provide a very selective method for differentiating isomeric ion structures when the CAD spectra are too similar and provide a convenient means of studying the reactions of hydrocarbon ions with acetylene.

Reactions of Hydrocarbon Ions with Acetylene

Ion/molecule reactions occurring in the center quadrupole can be used, as just shown, to differentiate isomer structures. They can also be used to investigate "synthesis" of new species, as in the sequential ion/molecule reactions of hydrocarbon ions with acetylene. The MS/MS can also be used to investigate the structure of new chemical species formed in the ion source. An active area of research in chemistry is the investigation of the role of ion/molecule reactions in combustion and soot formation (87,88). The high concentration of ions in flames has been recognized for some time. Mass spectrometric sampling of fuel rich flames has indicated that $C_3H_3^+$ (84,85) is the dominant positive ion. In addition to the many other ionic species present, relatively large aromatic molecules have also been observed (89). The condensation reactions (polymerization) of acetylenic species have been investigated by high pressure mass spectrometry (90) and by ion cyclotron resonance mass spectrometry (91).

The triple quadrupole was used to investigate the sequential ion/molecule reactions of $C_3H_3^+$, $C_5H_5^+$, and $C_7H_7^+$ with acetylene. In addition, daughter spectra were recorded for the ions formed under high pressure chemical ionization conditions when acetylene was used as the reagent gas.

Sequential Ion/Molecule Reactions

The sequential ion/molecule reactions of $C_3H_3^+$ are of interest due to the abundance of $C_3H_3^+$ in fuel rich flames and its possible role in the formation of soot. An abrupt shift from $C_3H_3^+$ as the major charged species to larger ions is the main feature that changes in going from nonsooting to sooting flames (86). Two species, one reactive and one nonreactive, of $C_3H_3^+$ have been observed in the triple quadrupole (as described earlier) and in an ICR (82,87). The electron impact of toluene provides a convenient source for $C_3H_3^+$, $C_5H_5^+$, and $C_7H_7^+$ ions. Each ion, selected by quadrupole one, can undergo ion/molecule reactions with acetylene in the center quadrupole. Table 10 shows the efficiency ($\frac{F}{P_o}$) for these reactions which are of the general form:

Table 10. Efficiencies For The Reactions Of $C_nH_n^+$ Hydrocarbon Ions From Toluene With Acetylene

Parent Ions		Product Ions			
Formula	m/z	Formula	m/z	$(\frac{F}{P_o})$	$(\frac{C_nH_n^+}{C_5H_5^+})$
$C_3H_3^+$	39	$C_5H_3^+$	63	6.64×10^{-3}	2.00×10^{-2}
		$C_5H_5^+$	65	9.24×10^{-3}	2.77×10^{-2}
		$C_7H_7^+$	91	1.46×10^{-3}	4.38×10^{-2}
$C_5H_5^+$	65	$C_7H_7^+$	91	3.33×10^{-1}	1.00
$C_7H_7^+$	91	$C_9H_7^+$	115	8.77×10^{-4}	2.63×10^{-3}

$$C_nH_n^+ + C_2H_2 \rightarrow C_{n+2}\,H_{n+2}^+ \qquad (1)$$

$$\rightarrow C_{n+2}\,H_n^+ + H_2 \qquad (2)$$

The value of P_o was measured when no acetylene was present in the center quad. The reaction of $C_3H_3^+$ (m/z 39) with acetylene (C_2H_2, MW 26) proceeds via reactions 1 and 2 to produce $C_5H_5^+$, (m/z 65) and C_5H_3 (m/z 63), respectively. The $C_5H_5^+$ ion undergoes further collisions with acetylene to form $C_7H_7^+$ (m/z 91). The reaction of $C_5H_5^+$ with C_2H_2 to form C_7H_7 (m/z 91) proceeds via reaction 1 and is approximately 33% coefficient. This is due to the formation of the very stable tropylium ion. This stability is further demonstrated by the fact that the reaction of $C_7H_7^+$ from toluene is less than 0.01% efficient. These sequential ion/molecule reactions offer a possible explanation for the formation of m/z 65, 91, and 115 all of which have been observed in sooting acetylene-oxygen flames (87).

If these sequential ion/molecule reactions are carried out in the ion source rather than in the center quadrupole, the resulting ions can be mass selected by quadrupole one and fragmented by CAD. The polymerization of C_2H_2 in the ion source has been investigated.

Polymerization of Acetylene

Historically, the mechanisms proposed for the nucleation step (the transformation from a molecular to a particulate system) in soot formation have involved the polymerization of acetylene and the formation of polynuclear or aromatic structures (87).

Figure 28 shows the mass spectrum of acetylene at an ion source pressure of 0.12 torr. The major ions ranging from $C_2H_2^{+\cdot}$ (m/z 26) to $C_{14}H_8^{+\cdot}$ (m/z 176) were observed. Table 11 classifies each ion according to reaction type for its formation. For each class, M^+ reacts with acetylene to form $(M+C_2H_2)^+$ which, if not stabilized by collisions, dissociates via the loss of H_2 to form $(M+C_2)^+$. In addition hydrogen abstraction to form $(M+C_2H)^{+\cdot}$ can occur. Each ion is then mass selected by quadrupole one and dissociated in the center quadrupole. The daughter spectrum for each ion is also given in Table 11. The CAD spectra were recorded at an ion energy of 20 eV and at a pressure of 1.5 millitorr of N_2. The daughter spectra show simple fragmentation involving the loss of H, H_2, or C_2H_2. This fragmentation is consistant with the formation of polyacetylenic species and polyaromatic hydrocarbons. The CAD of polyaromatic hydrocarbons has been studied by MS/MS (92). Approximately half of the ions observed in the high pressure mass spectrum of acetylene have been observed as either ionic or molecular species in flames (87). Possible structures for these ions based upon their daughter spectra and previous results (87) are given in Table 12. It is of interest to note

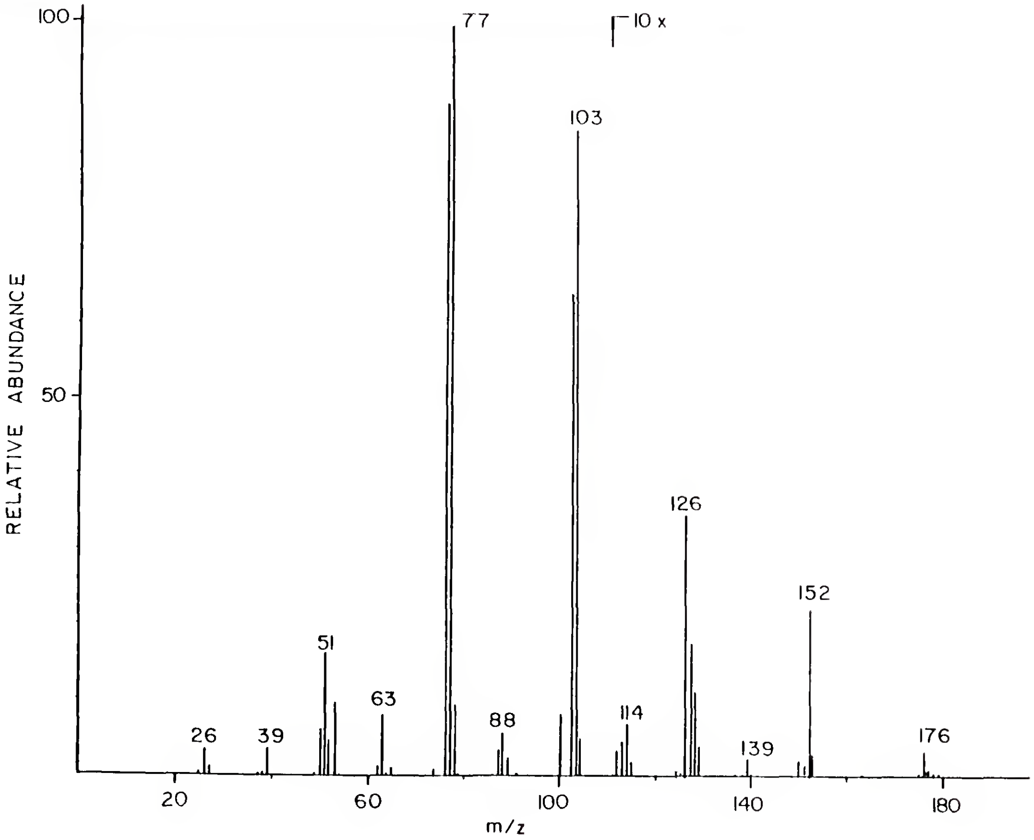

Figure 28. Mass spectrum of acetylene at a source pressure of 0.12 torr.

Table 11. Polymerization Of Acetylene

$$C_{2n}H_{2n}^{+\cdot} + C_2H_2 \xrightarrow{CI} C_{2n+2}H_{2n+2}^{+\cdot} \xrightarrow{CAD^a} C_{2n}H_{2n}^{+\cdot} + C_2H_2$$

$$\rightarrow C_{2n+2}H_{2n}^{+\cdot} + H_2 \rightarrow C_{2n}H_{2n-n}^{+\cdot} + C_2H_2$$

Parent Ion		Daughter Spectra
m/z	Formula	m/z (relative abundance %)
50[b]	$C_4H_2^{+\cdot}$	50(100)
76	$C_6H_4^{+\cdot}$	76(100);50(26)
78	$C_6H_6^{+\cdot}$	78(100);77(9);52(16);51(6)
100	$C_8H_4^{+\cdot}$	100(100);74(80)
102	$C_8H_6^{+\cdot}$	102(100);76(23)
104	$C_8H_8^{+\cdot}$	104(100);103(6);78(19);77(8)
126	$C_{10}H_6^{+\cdot}$	126(100);125(4);100(1);76(3)
128[b]	$C_{10}H_8^{+\cdot}$	128(100);127(8);102(21)

$$C_{2n+1}H_{2n+1}^{+} + C_2H_2 \xrightarrow{CI} C_{2n+3}H_{2n+3}^{+} \xrightarrow{CAD} C_{2n+1}H_{2n+1} + C_2H_2$$

$$\rightarrow C_{2n+3}H_{2n+1}^{+} + H_2 \rightarrow C_{2n+1}H_{2n-1} + C_2H_2$$

39[b]	$C_3H_3^{+}$	39(100);38(18);37(9)
63[b]	$C_5H_3^{+}$	63(100);62(15);61(3)
87	$C_7H_3^{+}$	87(100);86(12)
89	$C_7H_5^{+}$	89(100);88(9);63(34)
91[b]	$C_7H_7^{+}$	91(100);90(7);65(11)

Table 11 - continued.

$$C_{2n}H_{2n-1} + C_2H_2 \xrightarrow{CI} C_{2n+2}H_{2n+1} \xrightarrow{CAD} C_{2n}H_{2n-1} + C_2H_2$$

$$\rightarrow C_{2n+2}H_{2n-1} + H_2 \rightarrow C_{2n}H_{2n-2} + C_2H_2$$

Parent Ion		Daughter Spectra
m/z	Formula	m/z (relative abundance %)
51[b]	$C_4H_3^+$	51(100);50(24)
53[b]	$C_4H_5^+$	53(100);52(11);27(11)
77[b]	$C_6H_5^+$	77(100);51(27)
101	$C_8H_5^+$	101(100);75(52);74(9);51(6)
103[b]	$C_8H_7^+$	103(100);77(24)
127	$C_{10}H_7^+$	127(100);126(14);101(5);77(17)
129[b]	$C_{10}H_9^+$	129(100);128(28);127(11);103(7)
153$_b$	$C_{12}H_9^+$	153(100);152(20)
	Other Hydrocarbon Ions	
139[b]	$C_{11}H_7^+$	139(100)
150	$C_{12}H_6^{+\cdot}$	150(100)
152[b]	$C_{12}H_8^{+\cdot}$	152(100);151(9);150(1);126(1)
176[b]	$C_{14}H_8^{+\cdot}$	176(100)
177	$C_{14}H_9^+$	177(100);151(28)

a. CAD: 20 eV; 1.5 millitorr N_2

b. Ions or molecules of this molecular weight have been observed in flames (85).

Table 12. Structures Of Ions Formed In The Mass Spectrum Of Acetylene At 0.12 Torr

m/z	Formula	Proposed Structure[a]
39	$C_3H_3^+$	$HC{\equiv}C{-}\dot{C}H_2$
51	$C_4H_3^+$	$H_2C{=}\dot{C}{-}C{\equiv}CH$
53	$C_4H_5^+$	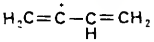 $H_2C{=}\dot{C}{-}\underset{H}{C}{=}CH_2$
63	$C_5H_3^+$	$HC{\equiv}C{-}C{\equiv}C{-}\dot{C}H_2$
77	$C_6H_5^+$	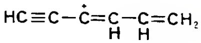 $HC{\equiv}C{-}\dot{C}{=}\underset{H}{C}{-}\underset{H}{C}{=}CH_2$
89	$C_7H_5^+$	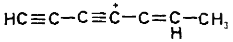 $HC{\equiv}C{-}C{\equiv}\dot{C}{-}C{=}\underset{H}{C}{-}CH_3$
91	$C_7H_7^+$	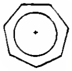
103	$C_8H_7^+$	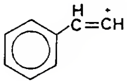
128	$C_{10}H_8^{+\cdot}$	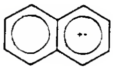
129	$C_{10}H_9^+$	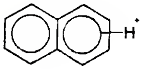
139	$C_{11}H_7^+$	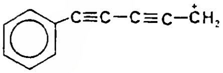

Table 12 - continued.

m/z	Formula	Proposed Structure[a]
141	$C_{11}H_9^+$	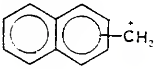
152	$C_{12}H_8^{+\cdot}$	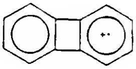
152	$C_{12}H_8^{+\cdot}$	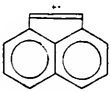
153	$C_{12}H_9^+$	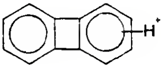
153	$C_{12}H_9^+$	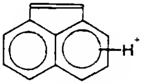
176	$C_{14}H_8^{+\cdot}$	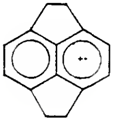

[a] Based upon daughter spectra in Table 11 and previous work (87).

that the ion at m/z 176 ($C_{14}H_8^{+\cdot}$, cyclopent(f,g)acenaphthylene) which is the heaviest major ion observed in Figure 27 is one of the major molecular polyaromatic hydrocarbons in sooting flames (87).

The use of ion/molecule reactions in the center quadrupole and in the ion source provides a method of synthesizing and mass analyzing new chemical species. The ion/molecule reactions in the center quadrupole can be quite selective as shown in the cases of $C_3H_6^{+\cdot}$ and $C_5H_6^{+\cdot}$. New species generated in the ion source can also be analyzed by MS/MS.

Ions Formed in Chemical Ionization

The most common use of ion/molecule reactions in analytical mass spectrometry is in chemical ionization. For mixture analysis by MS/MS it is desirable to form only one ion for each component, characteristic of its molecular weight. Chemical ionization is the method of choice. The added resolution elements offered by chemical ionization are discussed in Chapter 2.

The most commonly used reagent gases in CI are methane, isobutane, and ammonia. In the case of methane, for example, in addition to converting the sample molecules to the protonated molecular ion $(M+M)^+$, adduct ions at $(M+C_2H_5)^+$ and $(M+C_3H_5)^+$ are observed. In cases in which identification of the $(M+H)^+$ peak is in doubt, observation of peaks at 28 and 40 mass units higher can help confirm this identification. Determining the site of protonation and alkylation is important in structure elucidation by MS/MS. As discussed in Chapter 2 the CI mass spectra of ethylbenzene and m-xylene can be distinguished based upon the daughter spectra of their $(M+H)^+$ ions. In the case of ethylbenzene protonation takes place on the ring, whereas protonation of m-xylene occurs on one of the methyl groups. In direct mixture analysis by MS/MS, the adduct ions at $(M+C_2H_5)^+$ or $(M+C_3H_5)^+$ of one compound may correspond to the protonated molecular ion of another member of a homologous series. As an example of this, the CI mass spectrum of toluene and n-propylbenzene were investigated.

Toluene and n-Propylbenzene

The normal methane CI mass spectra of toluene (MW = 92) and propylbenzene (MW = 120) are shown in Figure 29. The spectrum of toluene shows a protonated molecular ion at m/z 93 and $(M+29)^+$ and $(M+41)^+$ adduct ions at m/z 121 and 133, respectively. The $(M+29)^+$ ion of toluene and the $(M+H)^+$ ion of n-propylbenzene are isomers at m/z 121. The corresponding $(M+29)^+$ and $(M+41)^+$ peaks are also observed for n-propylbenzene at m/z 149 and 161, respectively. The daughter spectra of m/z 121 from toluene and n-propylbenzene are shown in Figure 30.

From a comparison of the two daughter spectra it is obvious that these ions are of different structure. The daughter spectrum of the $(M+C_2H_5)^+$ ion from toluene shows a major loss of ethylene (C_2H_4) and rearrangement to form the

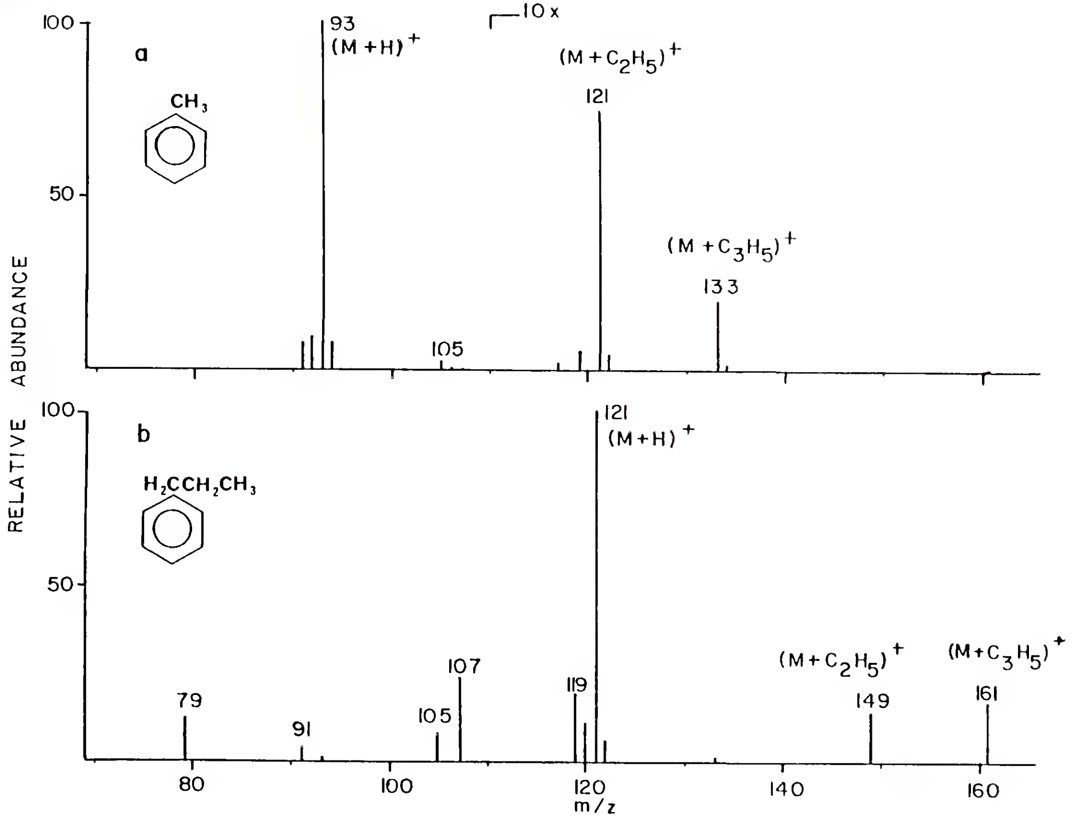

Figure 29. Methane CI mass spectra of (a) toluene; (b) n-propylbenzene.

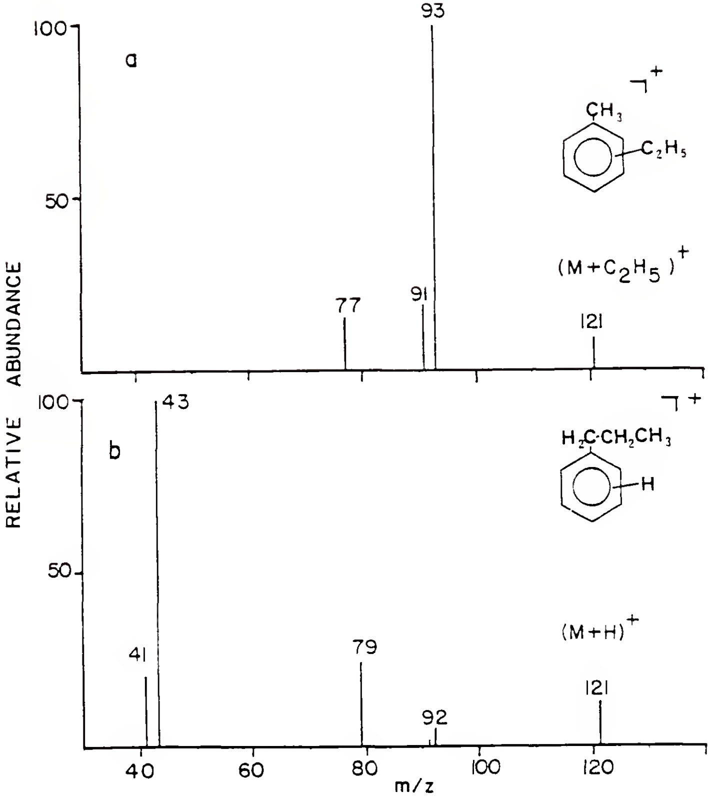

Figure 30. Daughter spectra of m/z 121 for (a) toluene $(M+C_2H_5)^+$; (b) n-propylbenzene $(M+H)^+$.

protonated toluene ion at m/z 93. In addition the loss of the ethane (C_2H_6) to form m/z 91 is observed. The ion at m/z 77 arises from the loss of both the CH_3 and C_2H_5 alkyl groups. In the case of ethylbenzene protonation occurs on the aromatic ring and fragmentation occurs via the loss of C_3H_6 to form the protonated benzene structure at m/a 79 and the loss of benzene to form m/z 43. The ions at m/z 41 and 92 are due to the $C_3H_5^+$ and $C_7H_8^+$ ions, respectively. The daughter spectra for the $(M+29)^+$ and $(M+41)^+$ adduct ions from n-propylbenzene are shown in Figure 31. In both cases fragmentation occurs the losses of ethylene (C_2H_4), C_3H_6, and cyclopentane (C_5H_{10}). The loss of cyclopentane (MW = 70) via rearrangement is an indication that alkylation also coccurs on the aromatic ring as does protonation. In addition both ions exhibit fragments at m/z 41 and 43, corresponding to $C_3H_5^+$ and $C_3H_6^+$, respectively. In all cases (at least for this example) alkylation and protonation occurs on the aromatic ring rather than the side chain. These added functional groups are then easily lost in the daughter spectra through rearrangement reactions.

In the MS/MS analysis of complex mixtures in which several members of a homologous series (such as the alkyl benzenes) are present the identity of an ion as an $(M+29)^+$ or $(M+41)^+$ adduct ion can be confirmed by the loss of ethylene (C_2H_4) in the daughter spectrum, even if the ion is also due to another member of the series.

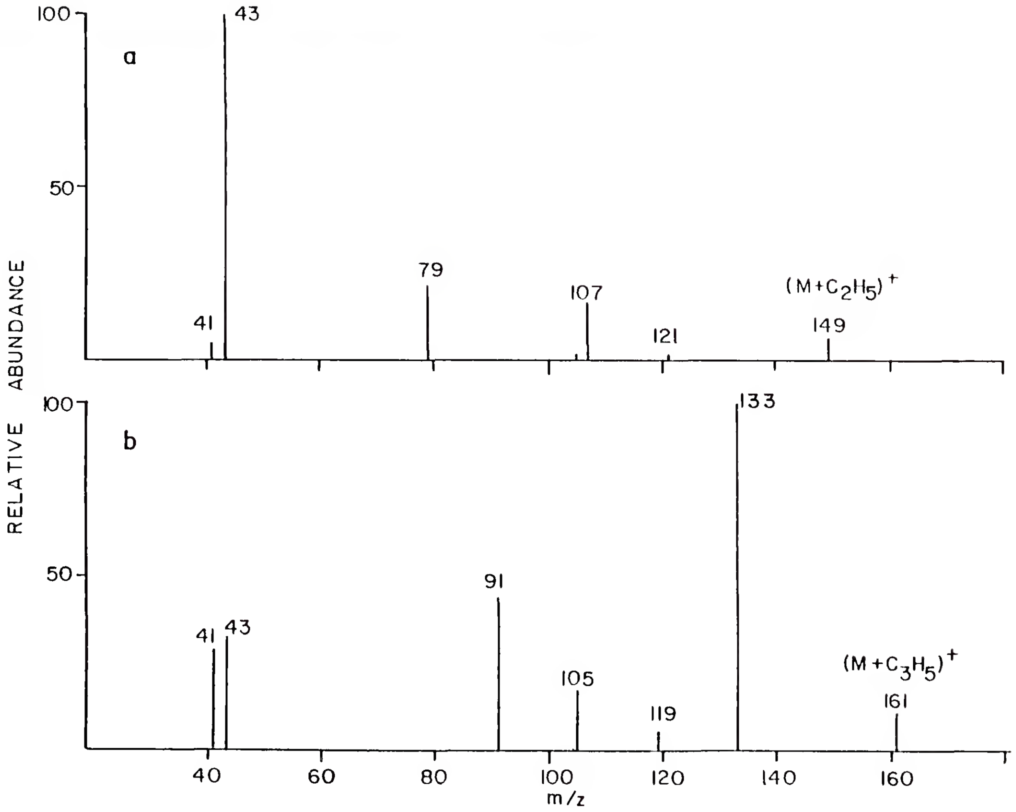

Figure 31. Daughter spectra for (a) ethylbenzene $(M+C_2H_5)^+$; (b) ethylbenzene $(M+C_3H_5)^+$.

Anisole and Benzyl Alcohol

The choice of the chemical ionization reagent gas as described in Chapter 2 can be an effective resolution element which increases the selectivity of MS/MS. For example, the isomers anisole and benzyl alcohol can be differentiated using NH_3 as the CI reagent gas. The adduct ions at $(M+NH_4)^+$ and $(M+N_2H_7)^+$ were also investigated.

The use of NH_3 CI has recently emerged as a useful technique for the analysis of acid-labile compounds. The factors affecting the reactivity in ammonia CI have been investigated (93). Figure 32 illustrates the difference in the Townsend Discharge NH_3 CI spectra of anisole and benzyl alcohol in the region of the molecular ion at m/z 108. Anisole only shows a molecular ion at m/z 108. The spectrum of benzyl alcohol (Figure 32b) exhibits an intense $(M+NH_4)^+$ and $(M+N_2H_7)^+$ adduct ions, as well as an $(M+NH_4 - H_2O)^+$ ion at m/z 108 (see below). The observed difference suggests that the hydroxyl oxygen is more basic than the ether oxygen in anisole. The daughter spectra for the ions at m/z 108 are compared in Figure 33. The daughter spectrum of m/z 108 from anisole (Figure 33a) indicates that this peak is due to the molecular ion. The daughter spectrum of m/z 108 from benzyl alcohol (Figure 33b) is different. This ion has been assigned the structure $(N+NH_4 - H_2O)^+$ by high resolution mass spectrometry (94). Based upon this assignment the loss of 17 to form m/z 91 corresponds to the loss of NH_3.

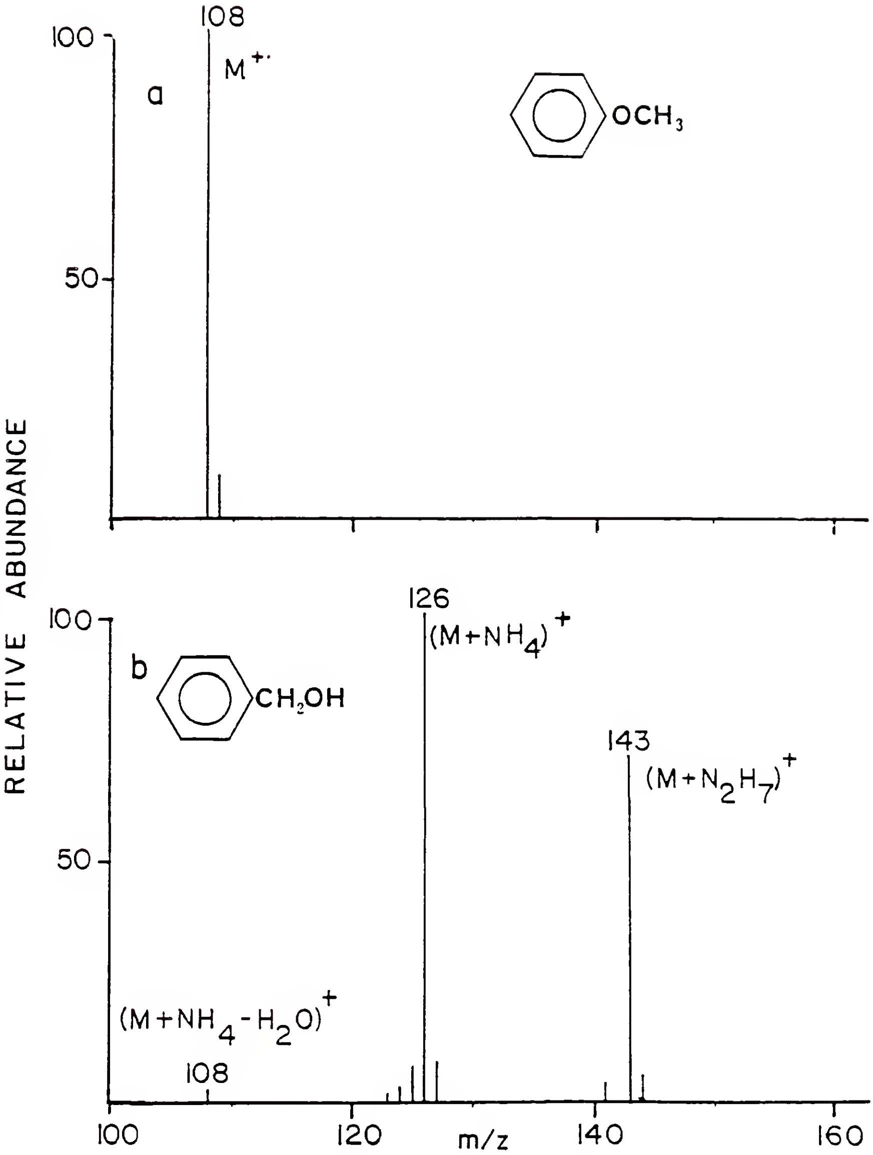

Figure 32. Ammonia CI mass spectra for (a) benzyl alcohol; (b) anisole.

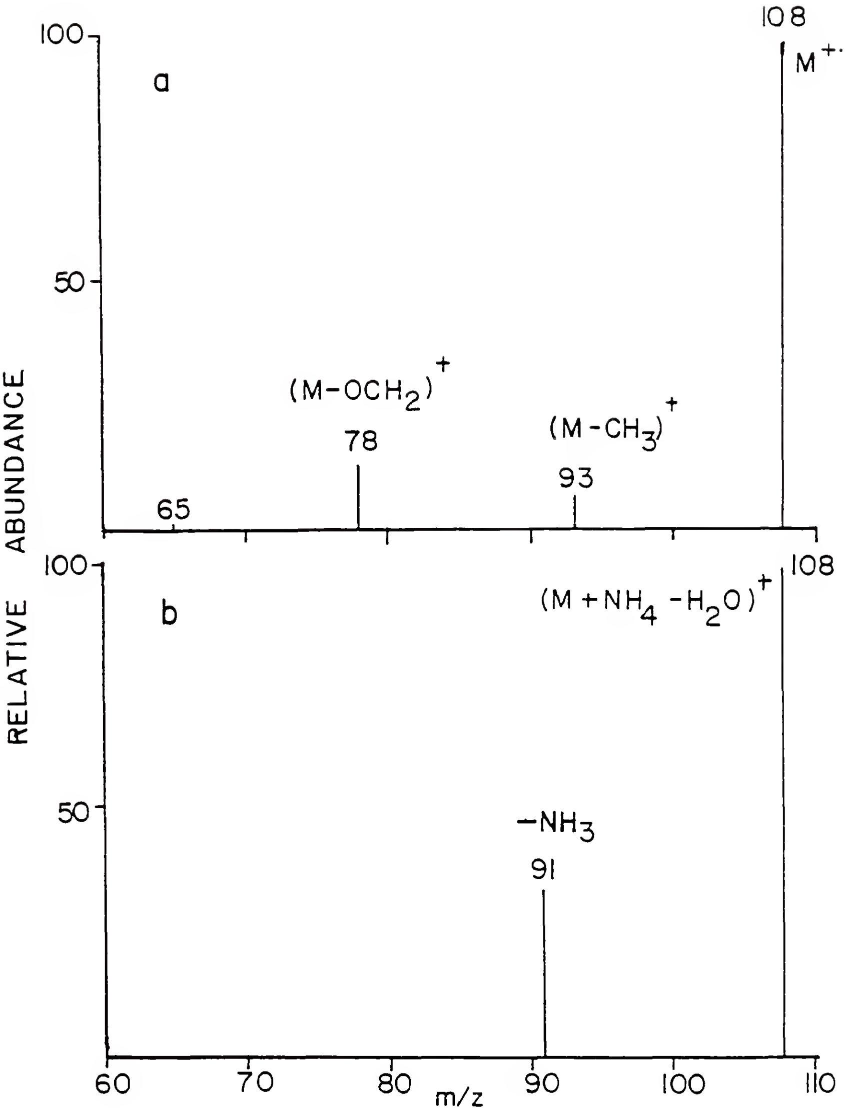

Figure 33. Daughter spectra of m/z 108 for (a) anisole $M^{+\cdot}$; (b) benzyl alcohol $(M+NH_4-H_2O)^+$.

The structural assignment for the ions at m/z 126 and 143 in the CI mass spectrum of benzyl alcohol were confirmed by daughter spectra. The very stable ion at m/z 126 corresponding to the $(M+NH_4)^+$ ion yielded no daughter ions. This stability is further indicated in the daughter spectrum of the $(M+N_2H_7)^+$ ion at m/z 143 which shows a major ion at m/z 123 due to the loss of NH_3 and fragment ion at m/z 35 corresponding to $N_2H_7^+$.

The added dimension of information in daughter spectra aids in the elucidation of the structure of ions formed in chemical ionization. These adduct ions are useful in the confirmation of the molecular ion as well as in the differentiation of the isomeric ion structures.

Computer-Aided Interpretation

In order to realize the tremendous potential of MS/MS, computerized control of the instrument and computerized handling of the data is necessary. Often, the analyst will want to define a set of predetermined operating modes and instrument configurations through which to be cycled during data acquisition. Table 13 shows an example of one such experiment (originally supplied by Finnigan, but with modifications) used in tuning the instrument with the calibration compound FC43 (perflurotributylamine).

The sequence involves acquiring both positive and negative ion CI mass spectra with quadrupole 1 and quadrupole 3 at a preamp gain of 10^{-6} V/A. Collision gas is then turned on, and a sequence of daughter, parent, and

Table 13. Example of an Operator Defined MS/MS Experiment.

```
EXPERIMENT EDITOR              INPUT FILE:FT

                               QUAD ONE         QUAD THREE
CALIBRATION TABLES:            CAL111201        CAL111203
SYSTEM DESCRIPTORS:            01               Q3

  18 MASSES BETWEEN    50.00 AND  800.00
  18    MID DESCRIPTORS: FS,CG,DG,PA,NL
  18 CONFIG DESCRIPTORS: 1+MS,1-MS,3+MS,3-MS,CGIN,D283,D219,D633,D634,
                         P214,P131,P183,P219,N069,N150,N170,N050,CGOT

ENTRY   MASS  MID      TIME      MASS    CONFIG.
 NO.     SET  DESC.   (SEC)    WINDOWS   DESC.

   1  500.00  FS (Q1) 1.04    80- 701   1+MS:Q1 MASS SPEC/+/GAIN:6
   2  500.00  FS (Q1) 1.04    80- 701   1-MS:Q1 MASS SPEC/-/GAIN:6
   3  500.00  FS (Q3) 1.03    80- 701   3+MS:Q3 MASS SPEC/+/GAIN:6
   4  500.00  FS (Q3) 1.03    80- 701   3-MS:Q3 MASS SPEC/-/GAIN:6
   5  800.00  CG (Q3) 1.99   200- 501   CGIN:DAUGHTERS/-/GAIN:7/CE:25.0
   6  283.00  DG (Q3) 0.50    40- 641   D283:DAUGHTERS/-/GAIN:7/CE:25.0
   7  219.00  DG (Q3) 0.50    40- 641   D219:DAUGHTERS/+/GAIN:7/CE:-24.8
   8  633.00  DG (Q3) 0.50    40- 641   D633:DAUGHTERS/-/GAIN:7/CE:20.0
   9  634.00  DG (Q3) 0.50    40- 641   D634:DAUGHTERS/+/GAIN:7/CE:-24.8
  10  214.00  PA (Q1) 0.50   100- 701   P214:PARENTS/-/GAIN:7/CE:30.0
  11  131.00  PA (Q1) 0.50   100- 701   P131:PARENTS/+/GAIN:7/CE:-30.0
  12  433.00  PA (Q1) 0.50   100- 701   P183:PARENTS/-/GAIN:7/CE:30.0
  13  219.00  PA (Q1) 0.50   100- 701   P219:PARENTS/+/GAIN:7/CE:-30.0
  14   69.00  NL (Q3) 0.51     5- 621   N069:NEUTRAL LOSS/-/GAIN:7/CE:20.0
  15  150.00  NL (Q3) 0.51     5- 621   N150:NEUTRAL LOSS/+/GAIN:7/CE:-30.0
  16  170.00  NL (Q3) 0.51     5- 621   N170:NEUTRAL LOSS/-/GAIN:7/CE:30.0
  17   50.00  NL (Q3) 0.51     5- 621   N050:NEUTRAL LOSS/+/GAIN:7/CE:-24.8
  18  800.00  CG (Q1) 2.01   200- 501   CGOT:Q1 MASS SPEC/+/GAIN:6
```

neutral loss scans are acquired with various collision energies (-30 to +30 V), mass ranges, ion polarities, and preamplifier gains.

For many applications, rather than use a predetermined sequence of scans, it would be preferable to use continuous feedback from the data in order for the data system to intelligently select the best instrument configuration for acquiring the next set of data. An example of this would involve the screening of complex mixtures for several targeted compounds using single reaction monitoring (SRM). If one or more of the compounds is found in the SRM screening step, the data system could immediately acquire a full daughter spectra of the suspect parent ions. It could then compare these with a library to confirm the presence of these compounds.

A portion of the data handling for MS/MS data can be performed with familiar GC/MS data processing programs, including background subtraction, quantitation, and plotting. In addition to the standard data handling programs, special programs are necessary to process the multi-dimensional data that are produced by MS/MS instrumentation. These include graphic display of various two- and three-dimensional slices of data out of the multi-dimensional space. Particularly useful are programs which display the interconnections of "genetic relationships" between ions for elucidation of fragmentation pathways and molecular structure. The isomeric nitroanisoles were investigated using the "TREE" software program provided by Finnigan which acquires a daughter spectrum of every ion in the normal mass spectrum and then determines the relationships between each of the various ions. The fragmentation tree for the major ions in o-nitroanisole is shown in Figure 34. The parent ion at m/z 153, for example, produces several daughter ions, including m/z 123. The m/z 123 ion further fragments to form ions at m/z 106, 93, etc. From this fragmentation tree, and a similar one for p-nitroanisole, the different fragmentation pathways for the molecular ions can be contrasted. Figure 35 compares the fragmentation pathways based upon the fragmentation trees for ortho- and para-nitroanisole. It can be seen that both ions exhibit an isobaric loss of 30 amu. However, daughter ions from m/z 123 indicate that these two ions are of different structure. Those daughter spectra suggest that ions of 30 amu from the ortho isomer corresponds to the loss of CH_2O. The proposed fragmentation mechanism based upon the daughter spectra for the ortho isomer is in agreement with that proposed by Benoit and Holmes from the electron impact mass spectrum (95). The loss of 30 amu from the para isomer, however, is due to the loss of NO. This assignment is in agreement with metastable peak shape studies by McDonald and Lacey (96). Such fragmentation trees can be generated automatically in less than two minutes with the triple quadrupole.

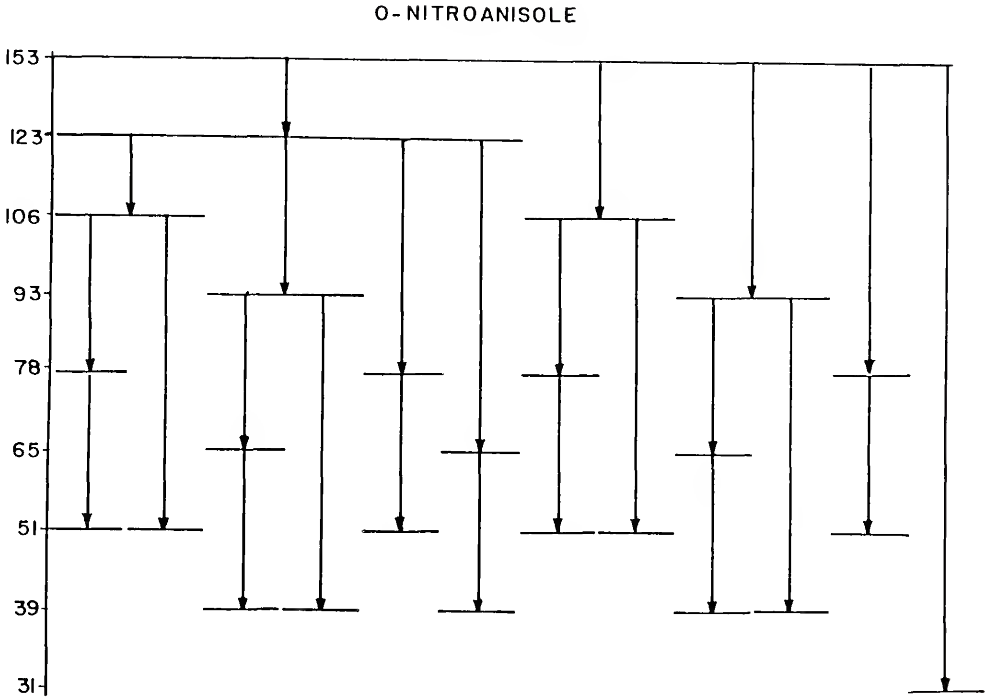

Figure 34. Fragmentation tree for o-nitroanisole ($(M+H)^+ = 153$).

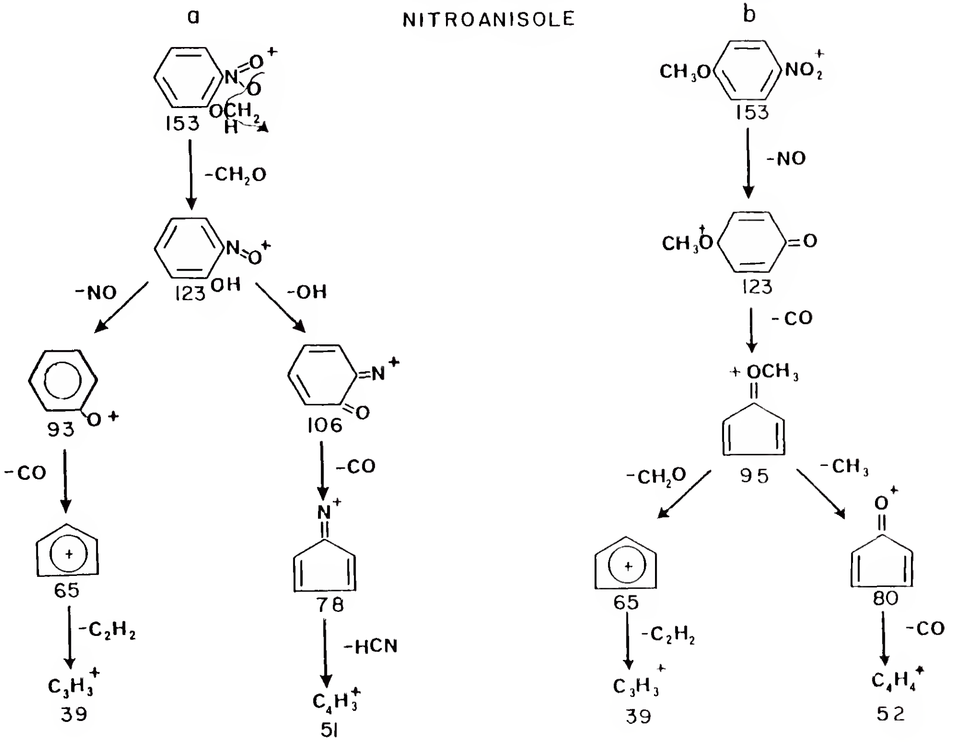

Figure 35. Fragmentation pathways for (a) o-nitroanisole; (b) p-nitroanisole.

The enormous amount of information available in MS/MS is a promising data base for computerized structure elucidation as shown by the computer-generated fragmentation tree in Figure 34. The use of computer control of the instrument and computer-aided structure elucidation will help in attaining the full potential of MS/MS. Rather than using all of the informing power available, techniques which employ data-dependent decisions for instrument control use only selected portions of the 3-dimensional data space, thereby reducing the analysis time.

CHAPTER 5
APPLICATION TO MIXTURE ANALYSIS

One of the most common applications of MS/MS is in the analysis of targeted compounds in complex mixtures. In mixture analysis the sample can either be introduced directly into the instrument, as was illustrated in Figures 2 and 3 for the identification of camphor in the tree bark, or separated first as were the isomers ethyl benzene and m-xylene (Figure 4). In terms of informing power (Table 1), an extremely powerful resolution element in mass spectrometry is the use of a chromatographic step for the separation of mixture components.

In addition to providing a daughter spectrum for each chromatographic peak, the MS/MS can provide a molecular weight profile for all compounds with a specific functional group through the use of neutral loss and parent scans. The direct analysis of priority pollutants by MS/MS has been discussed by Yost (97) and by Hunt (40). The use of the MS/MS as a versatile "selective" GC detector has been demonstrated by Fetterolf and Yost for the analysis of base/neutral extractable priority pollutants (98).

GC/MS/MS Analysis of Priority Pollutants

The separation of the 47 base-neutral extractable priority pollutants (Supelco, Inc.) at the concentrations of 50 ng/μl (except polyaromatic hydrocarbons; 25 ng/μl) was carried out using a 20 m SE-54 capillary column temperature programmed from 50 to 250 C at 10 C/min. Positive chemical ionization with methane was employed. The normal GC/MS chromatogram for a 1 μL injection is shown in Figure 36. The characteristic CI ions observed for each of the 47 compounds are given in Table 14. These ions include the protonated molecular ion $(M+H)^+$ as well as the $(M+C_2H_5)^+$ and $(M+C_3H_5)^+$ adduct ions when formed. In the case of polychlorinated compounds, the major ions in the isotopic cluster are given.

If the MS/MS is operated in the parent spectrum mode classes of compounds which produce a common daughter ion in the center quadrupole can be detected. One such class of priority pollutants is phthalates which fragment to produce the protonated phthalic anhydride ion at m/z 149. The only exception to this is dimethyl phthalate (scan 519) which loses CH_3OH to form m/z 163 instead. Figure 37 compares the chromatograms for the normal CI mass spectrum and the GC/MS/MS parent spectrum of m/z 149. The first three peaks are not due to phthalates, but rather are the ^{37}Cl parent ions from the isomeric dichlorobenzenes.

Figure 36. Chromatogram for the analysis of a mixture of 47 base-neutral extractable priority pollutants by GC/MS with a 20m SE-54 capillary column, 50-250 C at 10 C/min and positive CI. Peaks are identified in Table 14.

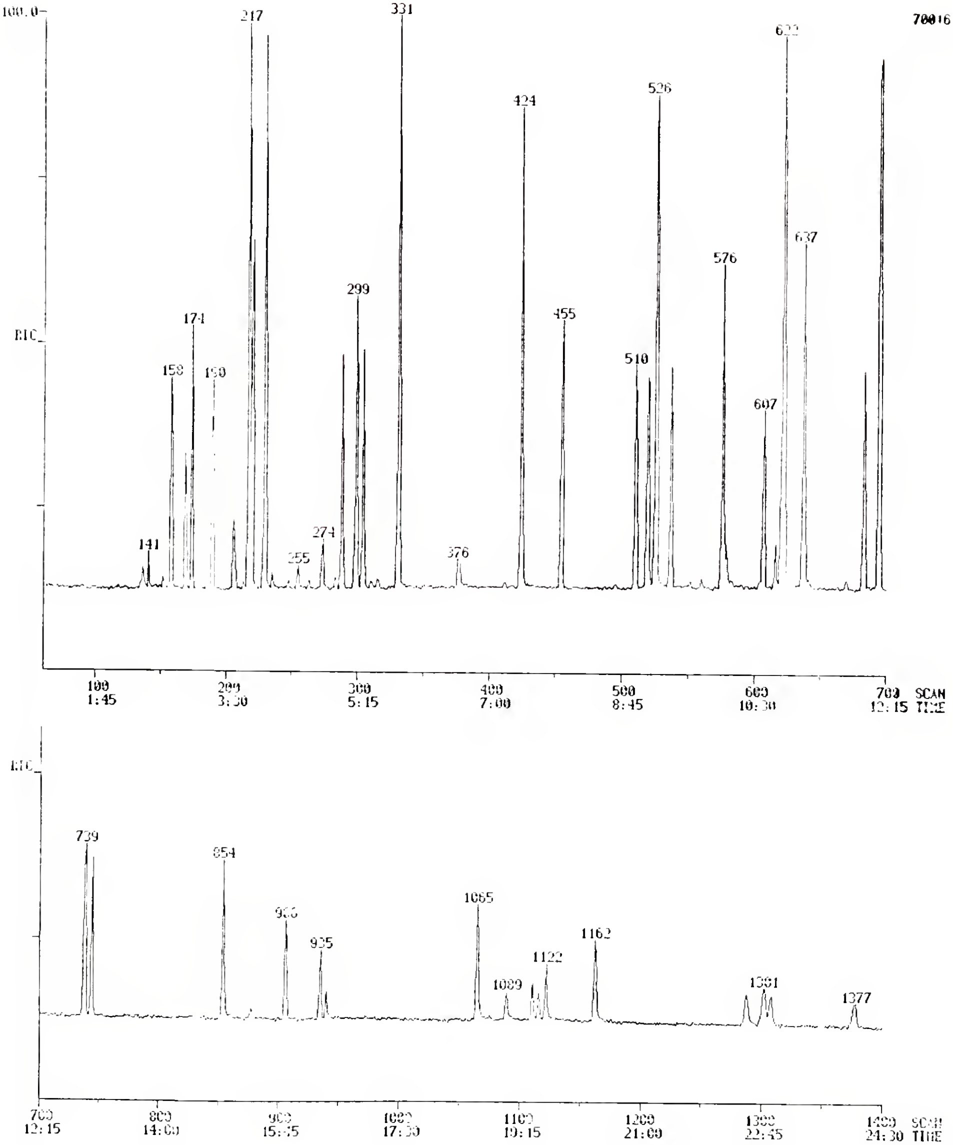
100.0
RIC
70016.
141
158
174
190
217
255
274
299
331
376
424
455
510
526
576
607
622
637
100 1:45
200 3:30
300 5:15
400 7:00
500 8:45
600 10:30
700 12:15 SCAN TIME
RIC
739
854
906
935
1065
1089
1122
1162
1301
1377
700 12:15
800 14:00
900 15:45
1000 17:30
1100 19:15
1200 21:00
1300 22:45
1400 24:30 SCAN TIME

Table 14. Characteristic Ions Of Base/Neutral Extractable Priority Pollutants

Scan #	Compound	Characteristic Ions[a]
57	N-Nitrosodimethylamine[b]	75,103,115
158	bis(2-Chloroethyl)ether	107,109
169	1,3-Dichlorobenzene	147,149,151
174	1,4-Dichlorobenzene	174,149,151
190	1,2-Dichlorobenzene	147,149,151
206	2-Chloroethylvinyl ether	121,123
206	bis-(2-Chloroisopropyl) ether	135,137
217	Hexachloroethane	199,201,202,203,205
220	N-Nitroso-di-n-propylamine	131,159,171
229	Nitrobenzene	124
255	Isophorone	139,167,179
288	bis(2-Chloroethoxy)-methane	93,95,107,109
299	1,2,4-Trichlorobenzene	181,183,185,209,211,213
304	Napthalene	129,157,169
331	Hexachlorobutadiene	223,225,227
424	Hexachlorocyclopentadiene	235,237,239,241
455	2-Chloronaphthalene	163,165,191,193
510	Acenaphthylene	153,181,193
519	Dimethylphthalate	163,195
526	2,6-Dinitrotoluene	183,211

Table 14 - continued.

Scan #	Compound	Characteristic Ions[a]
537	Acenapthene	155,183,195
576	2,4-Dinitrotoluene	183,211
607	Fluorene	167,195,207
616	4-Chlorophenylphenyl ether	205,207,233,235
622	Diethylphthalate	149,177,223
637	1,2-Diphenylhydiazine[c]	183,211
637	N-Nitrosodiphenylamine[d]	170,198
683	4-Bromophenyl phenyl ether	249,251,277,279,289,291
695	Hexachlorobenzene	283,285,287,289
739	Phenanthrene	179,207,219
745	Anthracene	179,207,219
845	Di-n-Butylphthalate	149,205,279,307,319
906	Fluoranthene[e]	203,231,243
935	Pyrene	203,231,243
940	Benzidine	185,213
1065	Butylbenzyl phthalate	149,205
1111	Chrysene[e]	229,257
1116	Benzo(a)anthracene[e]	229,257,269
1122	3,3'-Dichlorobenzidine	253,255,281,283
1162	Di-n-octyl phthalate	149,279,391
1287	bis-(2-ethylhexyl) phthalate	149,261,391

Table 14 - continued.

Scan #	Compound	Characteristic Ions[a]
1302	Benzo(k)fluoranthene[e]	253,281,293
1307	Benzo(b)fluoranthene[e]	253,281,293
1377	Benzo(a)pyrene[e]	253,281
--[f]	Dibenzo(a,h)anthracene[e]	(279)
--[f]	Indeno(1,2,3-cd)pyrene[e]	(279)
--[f]	Benzo(ghi)perylene[e]	(277)

a. $(M+H)^+$ ions are underlined.

b. Detected just after solvent peak (not shown).

c. Detected as Azobenzene (183).

d. Detected as Diphenylamine (170).

e. 25 ng/µl, all others 50 ng/µl.

f. Eluted after acquisition was stopped.

Figure 37. Chromatograms for the analysis of a mixture of 47 base- neutral extractable priority pollutants: (a) GC/MS analysis, conditions as in Figure 36; (b) GC/MS/MS analysis, parent spectrum m/z 149. Compounds identified:
1. 1,3-Dichlorobenzene; 2. 1,4-Dichlorobenzene; 3. 1,2-Dichlorobenzene;
4. Diethyl phthalate; 5. Di-n-butyl phthalate; 6. Butylbenzyl phthalate;
7. Di-n-octyl phthalate; 8. bis-(2-ethylhexyl) phthalate.

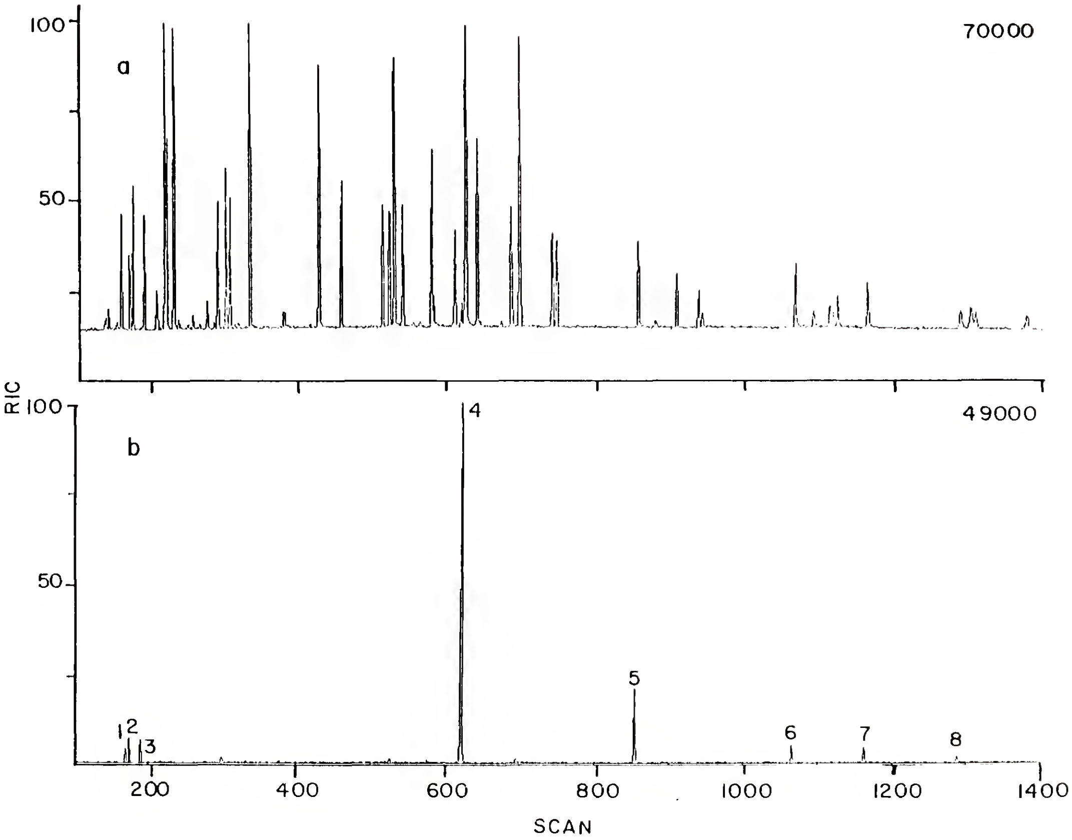
a
70000
b
49000
100
50
RIC
100
50
1
2
3
4
5
6
7
8
200
400
600
800
1000
1200
1400
SCAN

Two important features in MS/MS are observed in the parent spectrum. First, can be seen that the sensitivity from each compound varies greatly, thus requiring a large linear dynamic range in the detection system. The most important feature, however, is the reduction in chemical noise in the GC/MS/MS chromatogram. In the GC/MS chromatogram the elevated baseline accounts for approximately 13% of the total ion current for the largest GC peak. This is due to column and septum bleed as well as background contaminants within the mass spectrometer. This background is often the major limitation on GC/MS detection limits (41). Because of the two stages of mass filtering in MS/MS this chemical noise is greatly reduced. In the GC/MS/MS chromatogram, the background noise is only 0.3% of the total ion current. This background is due in part to the ubiquitous phthalates present in the mass spectrometer.

Parent spectra can also be used to differentiate isomers. Figure 38 compares the spectra for Di-n-octyl phthalate and bis-(2-ethylhexyl)phthalate ($(M+H)^+=391$). In the case of the di-n-octylphthalate, fragment ions corresponding to the loss of one and two of the alkyl groups are observed at m/z 279 and 167, respectively. However, in the case of the bis-(2-ethylhexyl)phthalate a molecule of H_2O is lost rather than the second alkyl group, to form the ion at m/z 261.

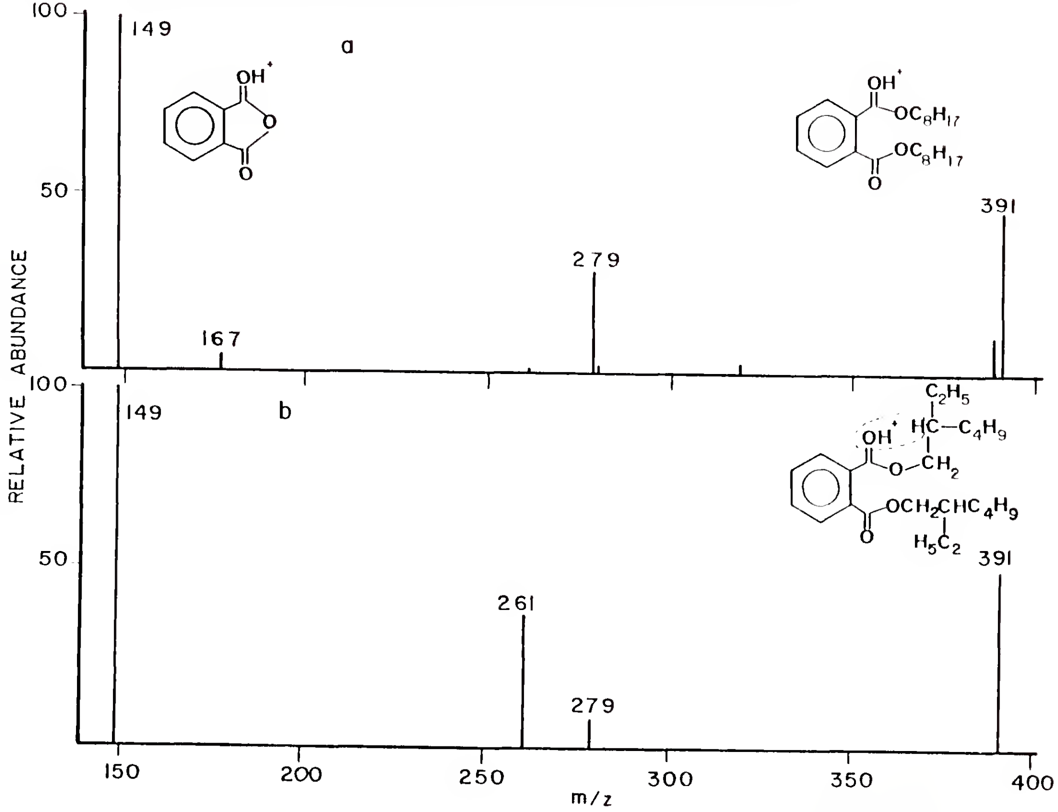

Figure 38. Parent spectra of m/z 149 for (a) Di-n-octyl phthalate; (b) bis-(2-ehtylhexyl) phthalate.

If a class of compounds loses a specific functional group upon CAD, members of this class can be detected by the appropriate neutral loss scan. The mixture of 47 priority pollutants contains 15 chlorinated compounds. Chlorinated compounds can be detected by the loss of Cl (m/z 35 or 37) or HCl (m/z 36 or 38). Figure 39 compares the GC/MS and GC/MS/MS (neutral loss of 35) analyses. Twelve of the fifteen compounds were detected by neutral loss of ^{35}Cl. Not found were the chlorinated ethers which lose HCl rather than Cl. As shown in the parent spectra, there is also a significant difference in sensitivity for each compound. Here again, a dramatic decrease in chemical noise is observed. The baseline in the GC/MS/MS chromatogram is reduced by a factor of 1000 compared to the GC/MS chromatogram. This increase in selectivity and decrease in noise often results in an overall improvement in the limits of detection.

The presence of multi-isotopic elements such as chlorine in a compound can be recognized by the isotopic cluster in the normal mass spectrum. The CAD and neutral loss spectra also show characteristic isotopic cluster patterns. This effect has not been reported until recently (99) because most earlier MS/MS work has been performed with reversed geometry sector instruments which do not provide unit mass resolution in both stages of mass analysis.

Figure 39. Chromatograms for the analysis of a mixture of 47 base-neutral extractable priority pollutants: (a) GC/MS analysis, conditions as in Figure 36; (b) GC/MS/MS analysis, neutral loss for ^{35}Cl. Compounds identified: 1. 1,3-Dichlorobenzene; 2. 1,4-Dichlorobenzene; 3. 1,2-Dichlorobenzene; 4. 2-Chloroethyl vinyl ether; 5. Hexachloroethane; 6. 1,2,4-Trichlorobenzene; 7. Hexachlorobutadiene; 8. Hexachlorocyclbutadiene; 9. 2-Chloronaphthalene; 10. 4-chlorophenyl phenyl ether; 11. Hexachlorobenzene; 12. 3,3'-Dichlorobenzidine. Not found were: bis(2-Chloroisopropyl)ether, bis(2-Chloroethyl)ether, and bis(2-Chloroethoxy)methane.

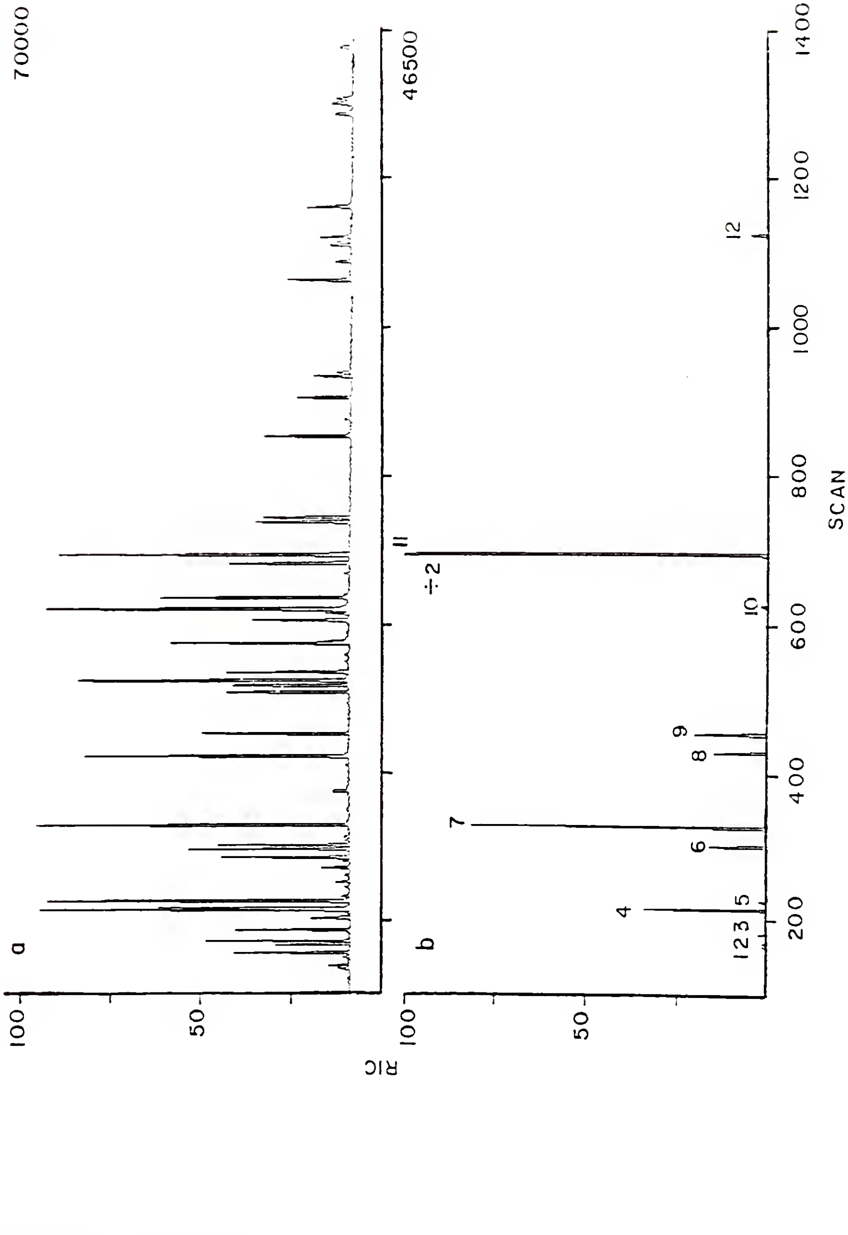
a
70000
b
46500
RIC
100
50
100
50
SCAN
200
400
600
800
1000
1200
1400
1 2 3
4
5
6
7
8
9
10
11
÷2
12

New instruments such as the triple quadrupole or tandem double-focusing MS/MS (17) provide sufficient mass resolution in both stages to observe these isotopic clusters.

Consider, for example, the case of 1,2,4-trichlorobenzene illustrated in Figure 40 (from scan 299 of Figure 39). The characteristic 3-chlorine pattern (100:98:33) is observed in the CI mass spectrum for the molecular ions at m/z 181, 183, and 185. However, in the ^{35}Cl neutral loss spectrum, only a two chlorine pattern (100:33) is observed. A similar behavior is observed in the neutral loss spectra of the other chlorinated compounds in this mixture. For example, the neutral loss spectra of the four hexa-substituted compounds all show a five chlorine pattern.

Rapid screening of samples for a specific class of compounds can be carried out with the direct insertion probe. However, if isomer-specific analysis is required, or if the possibility exists for interference from fragment ions from higher molecular weight compounds, combined GC/MS/MS can provide chromatographic separation and eliminate this interference, often with an increase in sensitivity and with improved confidence in the results.

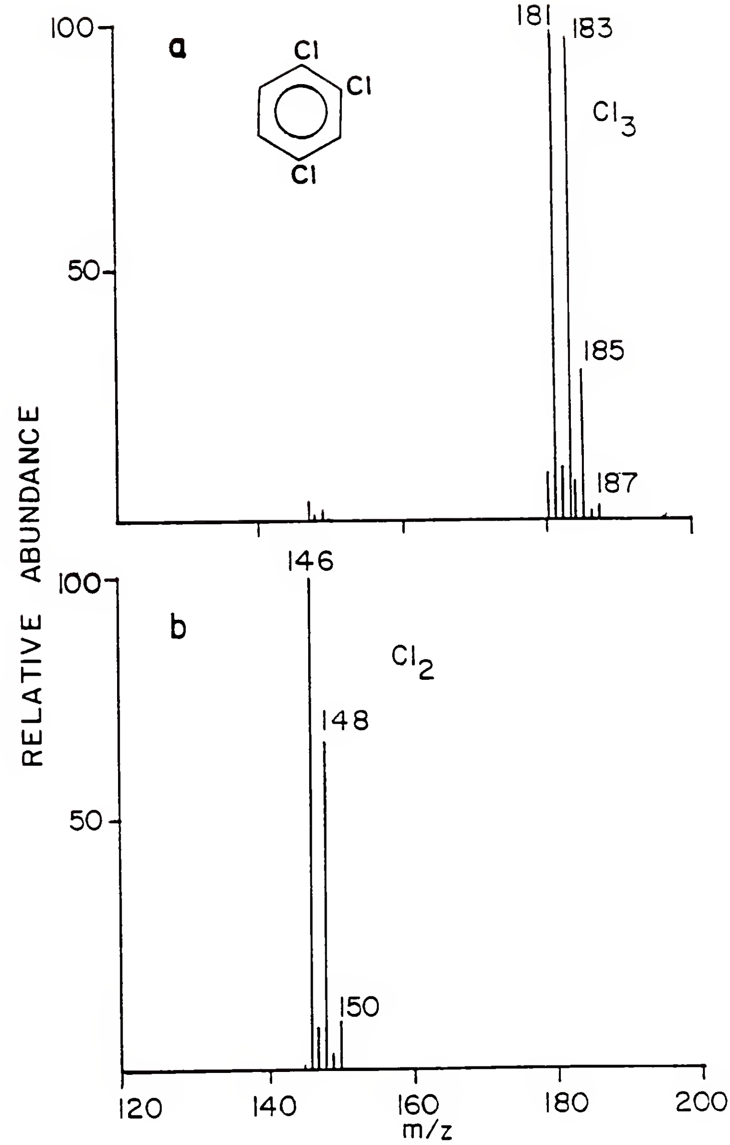

Figure 40. Isotopic pattern for (a) CI mass spectrum of 1,2,4-Trichlorobenzene; (b) ^{35}Cl neutral loss.

Determination of Chlorinated Hydrocarbons in Serum and Urine

The purpose of this study was to investigate the feasibility of triple quadrupole mass spectrometry for the rapid screening of hexachlorobenzene (HCB) and 2,4,5-trichlorophenol at ultra-trace levels (sub-ppb) in serum and urine. These experiments were part of a round-robin investigation with Dr. Peggy Skotnicki (Hooker Research Center, Grand Island, N.Y.) and Dr. J. Ron Hass (National Institute of Environmental Health Sciences (NIEHS), Research Triangle Park, N.C.). The techniques investigated at the Hooker Research Center included capillary-GC with electron capture detection (GC/ECD) and selected ion monitoring (SIM) capillary-GC/MS. The combination of packed column-GC with both high resolution single ion monitoring mass spectrometry (GC/HRMS) and with MS/MS using a MIKES instrument (GC/MIKES) were investigated at NIEHS. The triple quadrupole analysis involved the use of a short (50 cm) packed-GC column and single reaction monitoring. The targeted limits of detection for screening at the onset of this investigation were 0.10 ng/mL (0.10 ppb) for HCB and 10 ng/mL (10.0 ppb) for TCP. A complete report of this round-robin investigation is in preparation (100).

Reagents and Samples

Hexachlorobenzene and 2,4,5-trichlorophenol (Aldrich) were used as received. The hexane and diethylether used in the extraction procedure were ACS reagent grade. The purity of the standards and solvents was confirmed by mass spectrometry. All serum and urine samples were prepared at the Hooker Research Center by spiking pooled serum and urine with methanol solutions of HCB and TCP. Samples were shipped in dry ice and kept frozen until the time of analysis. Samples of serum (Fisher Scientific) were also prepared at UF and analyzed immediately.

Optimization of the Procedure

The added resolution elements in MS/MS such as the choice of the sample introduction technique, ionization method, ion polarity, ion energy, and collision gas pressure needed to be optimized in order to attain the sub-ppb detection limits. The operating conditions for the chromatographic inlet system and the triple quadrupole are shown in Table 15.

The use of the direct insertion probe for the sample introduction was found unsuitable because of the volatility of TCP and HCB. These compounds were readily lost during evacuation of the sample probe vacuum lock. In addition sample turnaround time was approximately 3-5 minutes. Instead a short GC column (1 mm ID x 50 cm) was chosen. This column was interfaced directly to the MS/MS through a glass-lined stainless steel tube without the use of a

Table 15. Operating Conditions for the Determination of HCB and TCP Triple Quadrupole

	HCB	TCP
Column size	1 mm ID x 50 cm[a]	1 mm ID x 50 cm[a]
Column packing	3% OV101 on 80/100 Chromosorb 750	0.5% OV101 on 100/120 glass beads (silanized)
Flow rate (CH_4)	15 ml/min	10 ml/min
Column temperature	150 C	150 C
Injector Temp.	220 C	220 C
Interface	Direct line	Direct line
Single reaction monitoring	$284^- \rightarrow 35^-$	$196^- \rightarrow 160^-$
Scan time	0.10 s	0.10 s
Ion kinetic energy	20 eV	20 eV
CAD pressure (N_2)	2.5 mtorr	1.2 mtorr
Sensitivity	10^{-8} A/V	10^{-8} A/V
Multiplier	2.0 Kv	2.0 Kv
Discharge ionization	3.5 Kv, 350 μA	3.5 Kv, 350 μA
Reagent gas CH_4	0.9 torr	0.9 torr
Source temperature	150 C	150 C

a. Empty columns were silanized with 10% DMCS in toluene.

jet-separator. The chemical ionization gas, methane (CH_4), was used as the carrier gas, with additional reagent gas admitted into the ion source through the normal reagent gas lines to obtain a total pressure of 0.9 torr. For maximum sensitivity and selectivity for these chlorinated compounds, negative ion chemical ionization and single reaction monitoring was chosen. The experimental variables such as CH_4 pressure, discharge energy, and emission current, as well as the potentials on the lenses after the ion source and between the quadrupoles were optimized for maximum transmission of the 283^- ion from the mass calibration compound FC43 (perfluorotributylamine). The reactions monitored by single reaction monitoring were based upon the daughter spectra shown in Figure 41. For TCP, the loss of HCl from the ^{35}Cl molecular ion at m/z 196 to form m/z 160 was monitored. In the case of HCB the only daughter ion observed from the ^{35}Cl molecular ion at 284^- was $^{35}Cl^-$.

The ion energy and pressure can rapidly be optimized by varying these parameters with HCB or TCP in a batch inlet or by repeated injections on the short column. The effect of ion energy on the sensitivity for HCB is shown in Figure 42, in which equal amounts of HCB were injected on the short GC column at several different ion energies. This method of optimization requires less than 10 minutes.

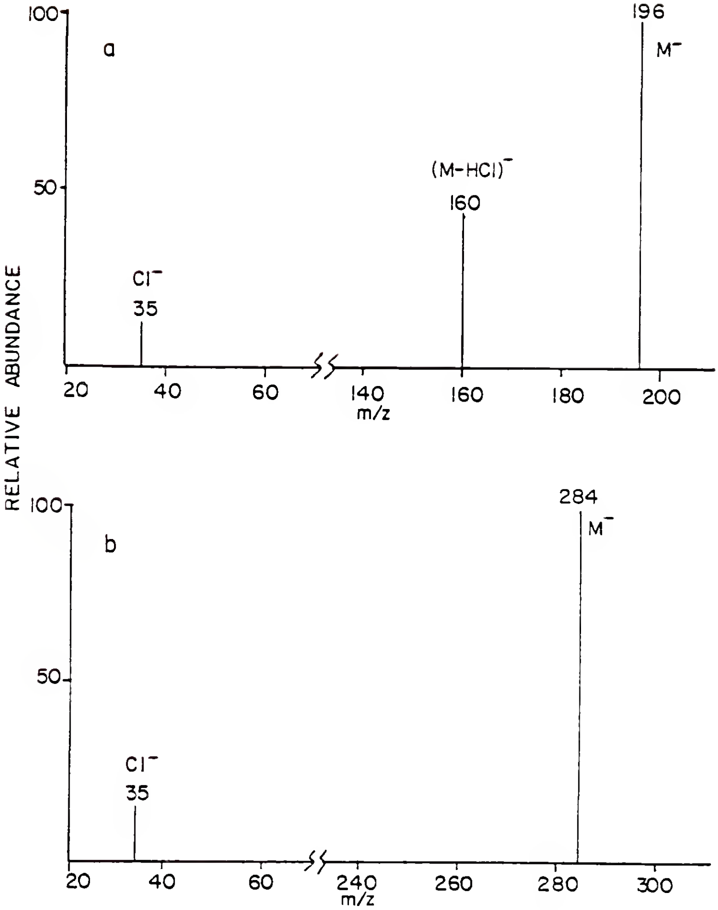

Figure 41. Negative ion daughter spectra of (a) Trichlorophenol; (b) Hexachlorobenzene.

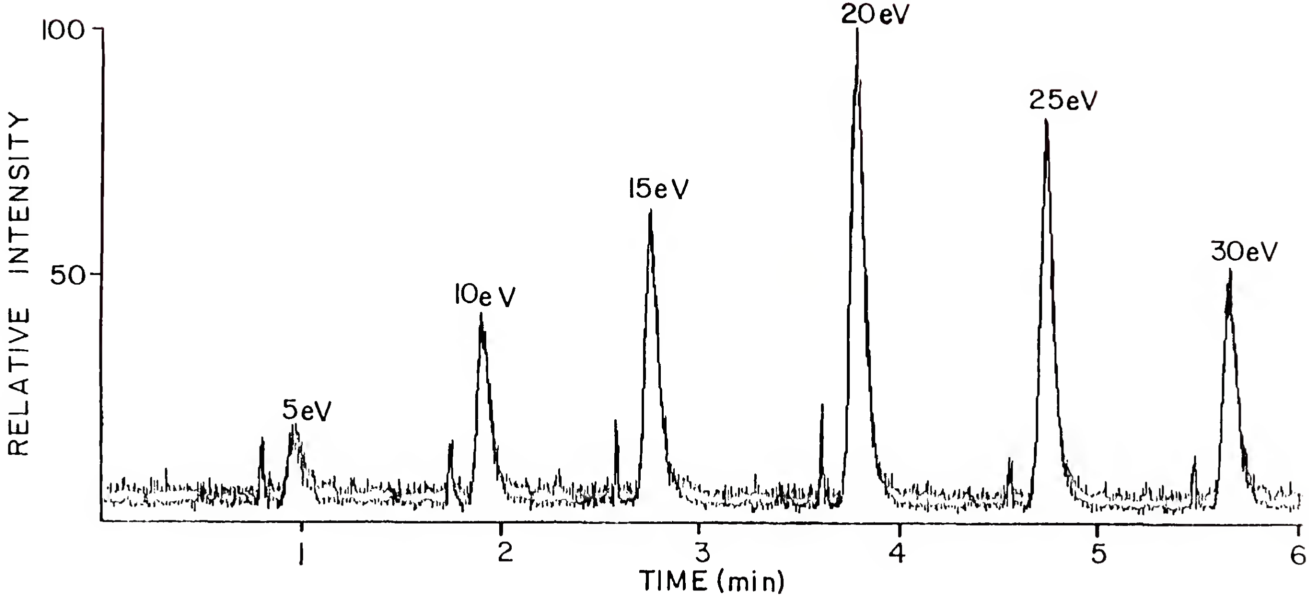

Figure 42. Collision energy optimization for single reaction monitoring of HCB $284^{-} — 35^{-}$.

Sample Preparation

A major concern in trace analysis is the possibility of contamination of solutions (samples, reagents, and blanks) and apparatus (glassware, syringes, and the instrument itself). If samples can be analyzed with little or no sample preparation, as is often the case in MS/MS, the possibility of contamination or sample loss is minimized.

Because of the unknown binding properties of these compounds with serum and urine, and due to the rapid degradation of the GC column with the introduction of serum or urine, a simple extraction procedure was developed. One ml of serum or urine was mixed for 30 min in silanized glassware with 1 ml of hexane to extract HCB or with 1 ml of diethyl ether to extract TCP. One μl samples of the organic layer were then injected into the GC column. Freshly prepared and spiked serum samples showed approximately 85% recovery of TCP and HCB in the range of 10.0 to 100 ppb. Serum and urine samples which had been frozen for several months showed a decrease in recovery (extraction efficiencies as low as 35%).

Calibration

Calibration curves for HCB and TCP were prepared for 1 μl injections of the standards. For example, 1 μl of a 0.10 ppb HCB standard contains 100 femtograms, or 350 attomoles, or 2 x 10^8 molecules of HCB. Calibration curves for HCB and TCP over the range of 0.1 to 100 ppb are shown in Figure 43. The slope of the log/log plot for TCP shows

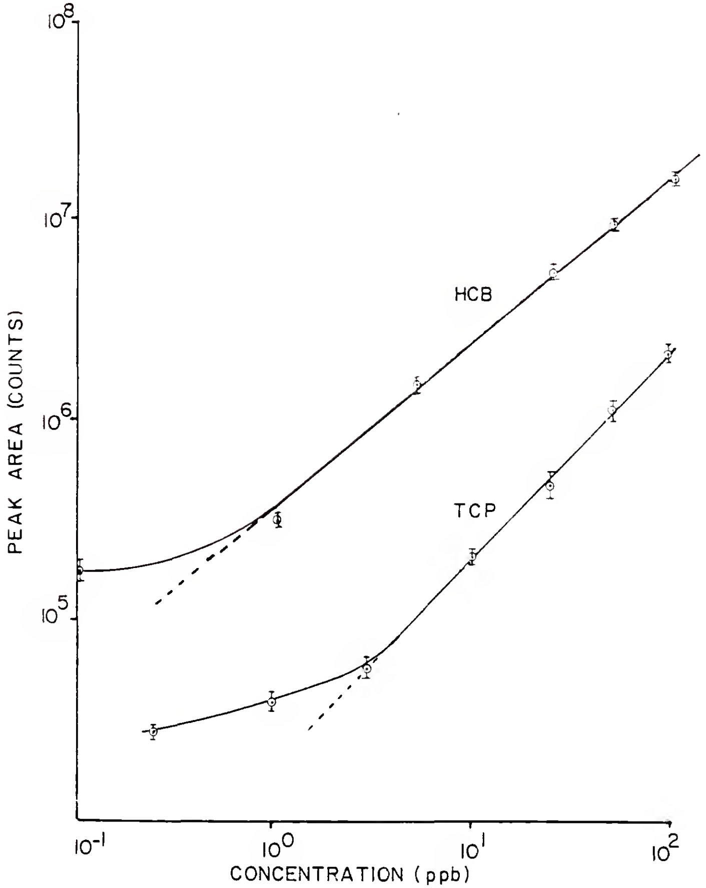

Figure 43. Calibration curves for hexachlorobenzene (HCB) and trichlorophenol (TCP). HCB blank = 14,000; TCP blank = 5,600.

excellent linearity with a slope of 1.02 from 3 to 100 ppb. The sensitivity of the linear plot is approximately 2×10^4 counts/ppb. For HCB, the slope of the log/log plot is 0.85, with a sensitivity of approximately 2×10^5 counts/ppb. In both cases a rapid decrease in sensitivity (slope) is observed below approximately 1 ppb. This decrease in sensitivity may in part be due to the loss of the sample on the column, but is most likely due to contamination of the standards at this low level during preparation. However, these signals are still significantly above the blank level and at an adequate signal-to-noise ratio to permit quantitation.

For both compounds, the peak area was obtained using the GC/MS peak quantitation procedures in the INCOS software. Figure 44a shows the signal from two injections of a blank and three injections of a 0.10 ppb standard. Figure 44b shows the signal for the three injections of an extract of serum spiked with 0.10 ppb HCB. The error bars on the calibration curve indicate the reproducibility (±1 standard deviation) for triplicate analyses of each standard. For HCB the precision over the concentration range of 0.10 to 100 ppb averaged ±9.3%. Limits of detection based on the calibration curves and analysis of the unknowns are given in Table 16.

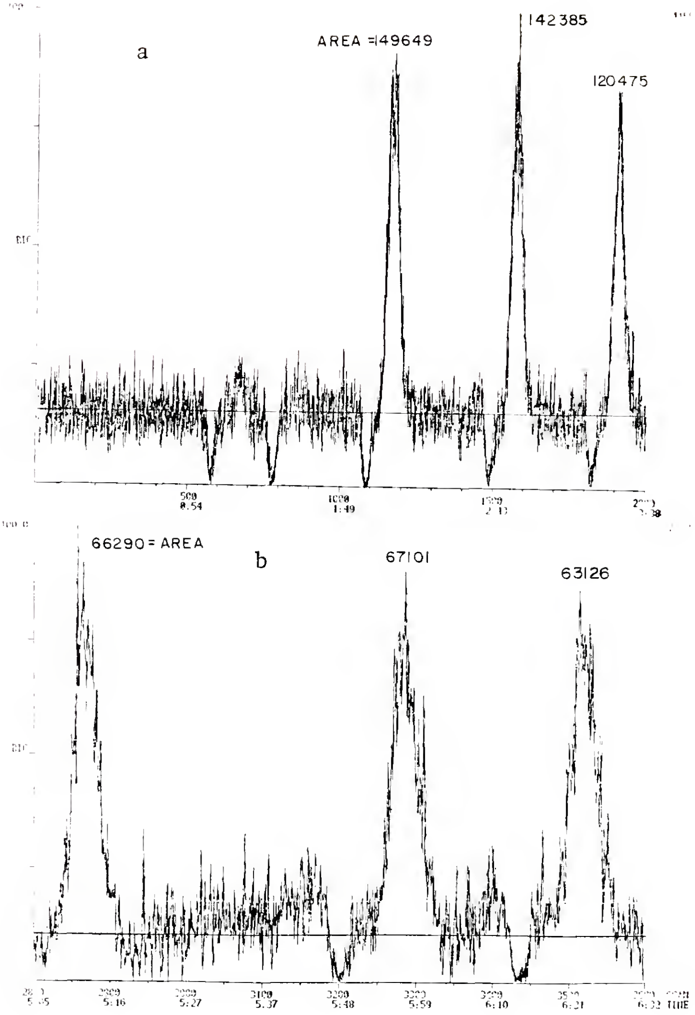

Figure 44. Peak profiles for 1μl injections of (a) two blanks and three 0.10 ppb HCB standards; (b) three plasma extracts containing 0.10 ppb HCB.

Table 16. Limits of Detection (S/N=5/1)

	Concentration (ppb)	Moles	Molecules
HCB	0.050	1.8×10^{-16}	1.1×10^{8}
TCP	0.250	1.3×10^{-15}	7.7×10^{8}

Because of the use of the short GC column, the analyses can be carried out quite rapidly. Consider for example, Figure 45, which illustrates the triplicate analysis of six each of serum extracts, standards, and urine extracts, as well as two sets of 3 blanks (after sample "F" and before sample "G"), all within 36 minutes. This corresponds to an introduction rate of 100 samples/hr. The reproducibility in peak area for the triplicate analyses shown in Figure 45 averaged ±10.3%.

It is also possible to simultaneously determine HCB and TCP by rapidly switching between the two different fragmentation reactions the sensitivity is decreased not only by splitting the analysis time between the two monitored reactions but also by the need to compromise the experimental conditions. The simultaneous analysis is illustrated in Figure 46 for the analysis of the extract of serum spiked with 50 ppb HCB and 100 ppb TCP.

Analysis of Unknowns

The results of the spiked serum and urine samples, extracted by our simple procedure or by the NIEHS procedure, are shown in Table 17. The agreement between the spiked concentrations and the measured concentration is primarily a reflection of the extraction efficiency. In general, it can be seen that the extraction efficiency increases with an increase in concentration. In addition, no signal was observed in for the blanks in our simple extract. High

Figure 45. Triplicate analysis of six extracts from serum and urine and six standards for trichlorophenol (TCP) at the rate of 100 injections per hour.

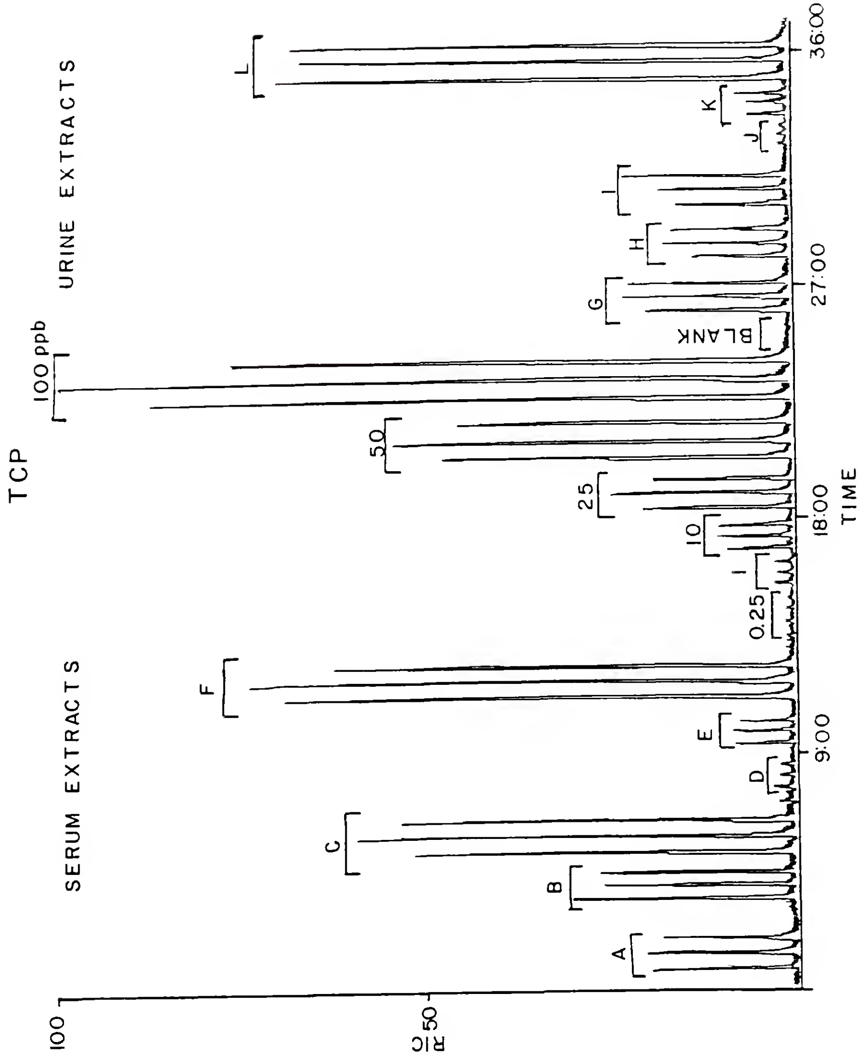
TCP
SERUM EXTRACTS
URINE EXTRACTS
A
B
C
D
E
F
0.25
1
10
25
50
100 ppb
BLANK
G
H
I
J
K
L
100
50
RIC
9:00
18:00
27:00
36:00
TIME

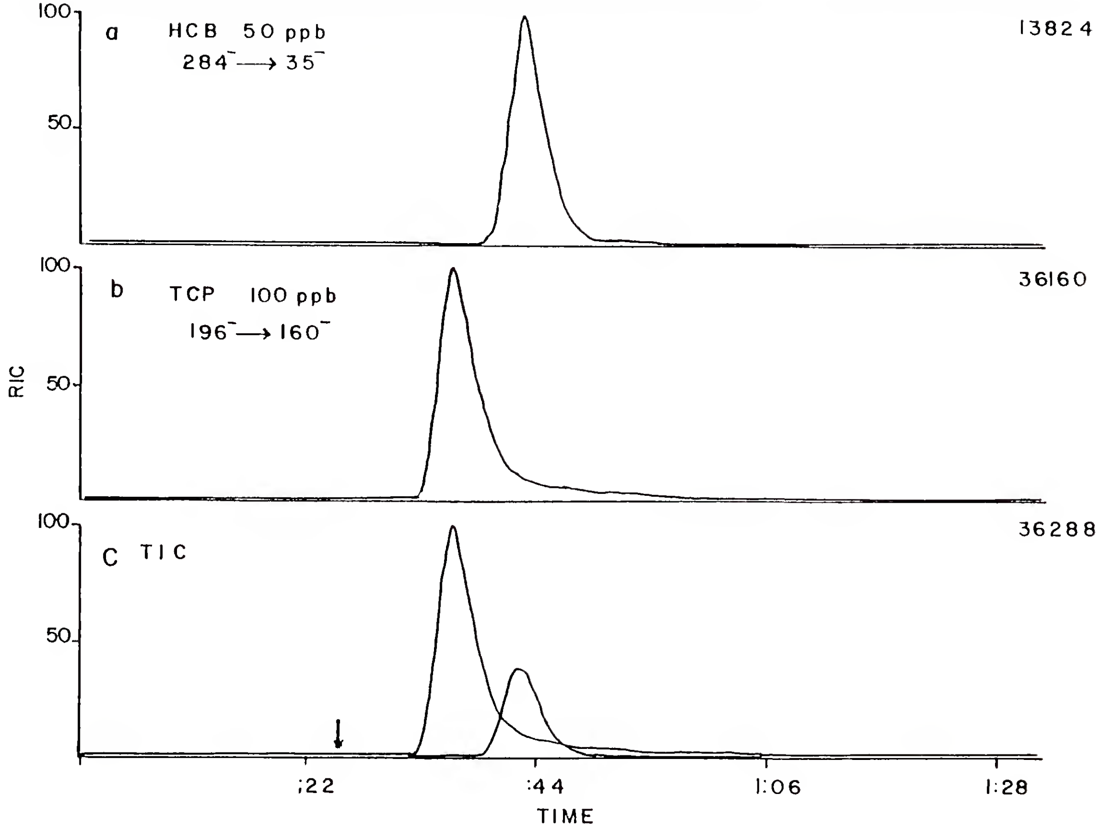

Figure 46. Simultaneous determination of HCB and TCP in an extract of serum using single reaction monitoring. CAD pressure 2.0 millitorr.

Table 17. Determination Of TCP And HCB In Serum And Urine

	TCP			
	Extracted at UF[a]		Extracted at NIEHS[b]	
Actual (ppb)	Serum	Urine	Serum	Urine
0 (Blank)	ND[c]	ND	1.7	ND
10	6.0	3.5	8.0	6.5
25[d]	16.1	19.0	30.6	17.6
30	17.2	18.8	35.9	19.5
50[d]	31.6	34.0	52.9	25.5
100	83.0	75.0	67.6	72.3
		HCB		
0(Blank)	ND	ND	<0.1	<0.1
0.1	0.05	0.04	<0.1	<0.1
5	3.1	2.5	5.9	3.5
12.5[d]	6.0	10.2	13.5	7.0
25[d]	15.5	20.0	27.0	15.0
50	46.5	48.8	46.5	46.0

---

a. 1 ml serum or urine extracted with 1 ml ether or hexane.

b. Received as blind sample.

c. ND = not detected.

d. Received as unknowns.

blanks and extraction efficiencies of greater than 100% observed in the samples extracted at NIEHS, however, point to contamination problems in their more involved extraction procedure.

Conclusion

The optimization of the added resolution elements in MS/MS permits the rapid screening of HCB and TCP in serum and urine at the sub-ppb level at the rate of 100 samples per hr. Limit of detection for HCB of 0.05 ppb and 0.25 ppb for TCP were obtained at a signal-to-noise ratio of 5:1 without preconcentration. In addition the limited sample pretreatment reduces the risk of sample contamination and loss.

CHAPTER 6
CONCLUSIONS AND FUTURE WORK

The concepts of information theory have been applied to tandem mass spectrometry. It has been demonstrated that the added resolution elements (which increase the informing power) in sample introduction and ionization, as well as in the CAD process, lead to increased sensitivity and selectivity in structure elucidation and mixture analysis.

The effects of collision energy on the appearance of the daughter spectra can be represented in the form of breakdown curves, which show good agreement with theoretical curves predicted by the quasi-equilibrium theory and those obtained by angle-resolved mass spectrometry. The effects of collision energy and pressure on the efficiency of the CAD process have also been demonstrated. The use of energy and pressure resolution not only increases our understanding of the low-energy CAD process but also aids in the differentiation of isomeric ion structures. Through the use of reactive collisions, the investigation of the reactions of chemical ionization reagent ions and the development of new selective methods of structure elucidation are possible.

The optimization of these added resolution elements makes possible the development of methods for the rapid screening (100 samples/hr) for trace constituents in samples as complex as serum and urine at the sub-ppb level. In addition, combined chromatography and tandem mass spectrometry has been demonstrated for the separation and identification of isomers as well as the sensitive and selective analysis of classes of compounds in complex environmental mixtures through the use of the various operating modes.

Several studies relating to these added resolution elements are suggested for further work. One such area would be improvements in the sensitivity and selectivity of the CAD process. These might include an investigation of the effects of varying the collision gas size (i.e., the use of He, Ne, Ar, or Xe instead of N_2) on the efficiency of the CAD process. Preliminary studies have shown that the collision efficiency can be dramatically increased by trapping the ions within the center quadrupole. This phenomenon also requires further attention. In addition, new reactive collision gases should be investigated for increased selectivity in analysis.

Currently available computer programs should be investigated and new computer algorithims developed for structure elucidation. These include the use of parent and neutral loss "trees" and substructure searching.

In addition, the use of data-dependent decisions for control of the operating modes should be applied to structure elucidation and mixture analysis.

In the area of mixture analysis, the range of applications should be extended to include the determination of other xenobiotic as well as naturally occurring substances in physiological fluids. Applications should also be extended to the analysis of thermally labile and nonvolatile compounds using desorption ionization techniques for sample introduction and ionization.

REFERENCES

1. Kaiser, H., Anal. Chim. Acta 1978, 33B, 551-576.

2. Fitzgerald, J.J.; Winefordner, J.D., Rev. Anal. Chem. 1975, 2, 299-316.

3. McLafferty, F.W., ed., "Tandem Mass Spectrometry (MS/MS)"; John Wiley and Sons: New York, 1982.

4. McLafferty, F.W., Science 1981, 214, 280-287.

5. Cooks, R.G.; Glish, G.L., Chem. Eng. News 1981 (Nov. 30), 40-52.

6. Burlingame, A.L.; Dell, A.; Russell, D.H., Anal. Chem. 1982, 54, 363R-409R.

7. Yost, R.A.; Fetterolf, D.D., Mass Spectrom. Rev. 1983, 2(1).

8. Cooks, R.G.; Beynon, J.H.; Caprioli, R.M.; Lester, G.R., "Metastable Ions"; Elsevier: Amsterdam, 1973.

9. Barber, M.; Elliott, R.M., ASTM Conference on Mass Spectrometry, June 1964, Montreal.

10. Beynon, J.H.; Caprioli, R.M.: Ast, T., Org. Mass Spectrom. 1971, 5, 229-234.

11. McLafferty, F.W.; Bente, P.F., III; Kornfeld, R.; Tsai, S.-C.; Howe, I.; J. Amer. Chem. Soc. 1973, 95, 2120-2129.

12. Kondrat, R.W.; Cooks, R.G., Anal. Chem. 1978, 50, 81A-92A.

13. Futrell, J.H.; Tiernan, T.L., in "Ion-Molecule Reactions"; Franklin, J.L., ed.; Plenum: New York, 1972, Chapt. 11.

14. Yost, R.A.; Enke, C.G., Anal. Chem. 1979, 51, 1251A-1264A.

15. Slayback, R.F.B.; Story, M.S., Ind. Res. Dev. February 1981, 129-139.

16. Russell, D.H.; Smith, D.H.; Warmack, R.J.; Bertram, L.K., Int. J. Mass Spectrom. Ion Phys. 1980, 35, 381-391.

17. McLafferty, F.W.; Todd, P.J.; McGilvery, D.C.; Baldwin, M.A., J. Amer. Chem. Soc. 1980, 102, 3360-3363.

18. Entranuclear Laboratories, Inc., Pittsburgh, PA.

19. Finnigan MAT, San Jose, CA.

20. Kratos, Ltd., Urmston, Manchester, England.

21. Nicolet Instrument Corp., Madison, WI.

22. Sciex, Inc., Thronhill, Ontario, Canada.

23. VG-Micromass, Altrincham, Cheshire, England.

24. Yu, T.-Y.; Cheng, M.H.; Kempter, V.; Lampe, F.W., J. Phys. Chem. 1972, 76, 3321-3330.

25. Iden, C.R.; Lairdon, R.; Koski, W.S., J. Chem. Phys. 1972, 56, 851-854.

26. Adams, N.G.; Smith, D., Int. J. Mass Spectrom. Ion Phys. 1976, 21, 349-359.

27. McGilvery, D.C.; Morrison, J.D., Int. J. Mass Spectrom. Ion Phys. 1978, 28, 81-92.

28. Vestal, M.L.; Futrell, J.H., Chem. Phys. Lett. 1974, 28, 559-561.

29. Yost, R.A.; Enke, C.G., J. Amer. Chem. Soc. 1978, 100, 2274-2275.

30. Yost, R.A.; Enke, C.G.; McGilvery, D.C.; Smith, D.; Morrison, J.D., Int. J. Mass Spectrom. Ion Phys. 1979, 30, 127-136.

31. Yost, R.A.; Enke, C.G., Org. Mass Spectrom. 1981, 16, 171-175.

32. Hunt, D.F.; Shabanowitz, J.; Giordani, A.B., Anal. Chem. 1980, 52, 386-390.

33. Zakett, D.; Cooks, R.G.; Fies, W.J., Anal. Chim. Acta 1980, 119, 129-135.

34. Porter, C.J.; Beynon, J.H.; Ast, T., Org. Mass Spectrom. 1981, 16, 101-114.

35. Yost, R.A.; Enke, C.G., Amer. Lab. June 1981, 88-95.

36. Bozorgzodeh, M.H.; Morgan, R.P.; Beynon, J.H., Analyst 1978, 103, 613-622.

37. Johnson, J.V.; Yost, R.A., Presented at the International Conference on Computers in Chemical Research and Education, July 1982, Washington, D.C.

38. Zakett, D.; Ciupek, J.D.; Cooks, R.G., Anal. Chem. 1981, 53, 723-726.

39. Brotherton, H.O.; Yost, R.A., Accepted for publication in Anal. Chem.

40. Hunt, D.R., Presented at the National ACS Meeting, May 1982, Las Vegas, NV.

41. Dromey, R.G.; Stefik, M.J.; Rindfleisch, T.C.; Butterfield, A.M., Anal. Chem. 1976, 48, 1368-1375.

42. Voyksner, R.D.; Hass, J.R.; Bursey, M.M., Anal. Lett. 1982, 15, 1-12.

43. Henion, J.D.; Thomson, B.A.; Dawson, P.H., Anal. Chem. 1982, 54, 451-456.

44. Smith, R.D.; Burger, J.E.; Johnson, A.L., Anal. Chem. 1981, 53, 1603-1611.

45. Munson, M.S.B.; Field, F.H., J. Amer. Chem. Soc. 1966, 88, 2621-2630.

46. Jennings, K.R. in "Gas Phase Ion Chemistry"; Bowers, M.T., ed.; Academic Press: New York, 1979, Vol. 2, Chapt. 12.

47. Hunt, D.F.; Shabanowitz, J., Anal. Chem. 1982, 54, 574-578.

48. Reid, N.M.; Buckley, J.A.; French, J.B.; Poon, C.C., Adv. Mass Spectrom. 1979, 8B, 1843-1850.

49. Davidson, W.F.; Fulford, J.; Reid, N.M.; Sakuma, T.; Sushan, B.; Thompson, B.A., Presented at the Conference of Mass Spectrometry and Allied Topics, May 1981, Minneapolis, MN.

50. Cotter, R.J., Anal. Chem. 1980, 52, 1589A-1606A.

51. Weber, R.; Levenson, K., Biomed. Mass Spectrom. 1980, 7, 314.

52. Straub, K.M.; Burlingame, A.L. in "Soft Ionization Biological Mass Spectrometry"; Morris, H.R., ed.; Heyden: London, 1981, pp.39-53.

53. Unger, S.E.; Day, R.J.; Cooks, R.G., Int.. J. Mass Spectrom. Ion Phys. 1981, 39, 231-255.

54. Barber, M.; Bordoli, R.S.; Elliott, G.J.; Sedgwick, R.D.; Tyler, A.N., Anal. Chem. 1982, 54, 645A-657A.

55. Hunt, D.F.; Bone, W.F.; Shabanowitz, J.; Rhodes, J.; Ballard, J.M., Anal. Chem. 1981, 53, 1704-1708.

56. Beynon, J.H.; Gilbert, J.R., in "Gas Phase Ion Chemistry"; Bowers, M.T., ed.; Academic Press: New York, 1979, Vol. 2, Chapt. 13.

57. Griffiths, I.W.; Muckhater, E.S.; March, R.E.; Harris, F.M.; Beynon, J.H., Int. J. Mass Spectrom. Ion Phys. 1981, 39, 125-132.

58. Fodor, D.M.: Cody, R.B.; Burinsky, D.J.; Freiser, B.S.; Cooks, R.G., Int. J. Mass Spectrom. Ion Phys. 1981, 39, 55-64.

59. Yamaoka, H.; Pham. D.; Durup, J., J. Chem. Phys. 1969, 51, 3465.

60. Laramee, J.A.; Carmody, J.J.; Cooks, R.G., Int. J. Mass Spectrom. Ion Phys. 1979, 31, 333-343.

61. Laramee, J.A.; Hemberyer, P.H.; Cooks, R.G., Int. J. Mass Ion Phys. 1980, 33, 231-241.

62. Cody, R.B.; Freiser, B.S., Anal. Chem. 1982, 54, 1433-1435.

63. Douglas, D.J., J. Phys. Chem. 1982, 82, 185-191.

64. Glish, G.L.; McLuckey, S.A.; Ridley, T.Y.; Cooks, R.G., Int. J. Mass Spectrom. Ion Phys. 1982, 41 157-177.

65. Todd, P.J.; McLafferty, F.W., Int. J. Mass Spectrom. Ion Phys. 1981, 38, 371-378.

66. Wachs, T.; Van de Sande, C.C.; Bente, P.F.; Dymerski, P.P.; McLafferty, F.W., Int. J. Mass Spectrom. Ion Phys. 1977, 23, 21-27.

67. Kruger, T.A.; Litton, J.F.; Kondrat, R.W.; Cooks, R.G., Anal. Chem. 1976, 48, 2113-2119.

68. Glish, G.L.; Todd, P.J., Anal. Chem., 1982, 54, 842-843.

69. Fite, W.L., Rev. Sci. Instr. 1976, 47, 326-330.

70. Siegel, M.W., Anal. Chem. 1980, 52, 1790-1792.

71. Dawson, P.H.; French, J.B.; Buckley, J.A.; Douglas, D.J.; Simmons, D., Org. Mass Spectrom. 1982, 17, 205-211.

72. Rosenstock, N.M.; Draxyl, K.; Steinor, B.W.; Herron, J.T., "Energetics of Gaseous Ions"; National Bureau of Standards, Washington, D.C., 1977.

73. Vestal, M.; Lerner, G., "Fundamental Studies Relating to the Radiation Chemistry of Small Organic Molecules", Office of Aerospace Research USAF, ARC 67-01114, 1967.

74. Fetterolf, D.D.; Yost, R.A., Int. J. Mass Spectrom. Ion Phys. 1982, 44, 37-50.

75. Holmes, J.L.; Terlouw, J.K.; Burgers, P.C.; Rye, R.T.B., Org. Mass Spectrom. 1980, 15, 149-151.

76. Ferrer-Correia, A.J.U.; Jennings, K.R.; Sen Sharma, D.K., Org. Mass Spectrom. 1976, 11, 867-872.

77. Chai, R.; Harrison, A.G., Anal. Chem. 1981, 53, 34-37.

78. Gioumousis, G.; Stevenson, D.P., J. Chem. Phys. 1958, 29, 294-299.

79. Gross, M.L.; McLafferty, F.W., J. Amer. Chem. Soc., 1971, 93, 1267-1268.

80. Gross, M.L., J. Amer. Chem. Soc. 1972, 94, 3744-3748.

81. Gross, M.L.; Lin, P.H., Org. Mass Spectrom. 1973, 7, 795-803.

82. Ausloos, P.J.; Lias, S.G., J. Amer. Chem. Soc. 1981, 103, 6505-6507.

83. Hayhurst, A.N.; Kittleson, D.K., Combust. Flame 1978, 31, 37.

84. Goodings, J.M.; Bohme, D.K.; Ng, C.W., Combust. Flame 1979, 36, 27.

85. Holmes, J.L.; Lossing, F.P., Canad. J. Chem. 1979, 57, 249-252.

86. Fetterolf, D.D.; Yost, R.A.; Eyler, J.R., J. Amer. Chem. Soc. submitted.

87. Calcote, H.F., Combust. Flame 1981, 42, 215-242.

88. Olson, D.B.; Calcote, H.F., in "Particulate Carbon Formation During Combustion"; Siegla, D.C., Smith, G.W., ed.; Plenum: New York, 1981, p.177-205.

89. Prado, G.P.; Howard, J.B., "Adv. Chem. Ser., No. 166", ACS: Washington, D.C., 1978, Chapter 10.

90. Futrell, J.H.; Tiernam, T.O., J. Phys. Chem. 1968, 72, 158-164.

91. Brill, F.W.; Eyler, J.R., J. Phys. Chem. 1981, 85, 1091-1094.

92. Shushan, B.; Boyd, R.K., Org. Mass Spectrom. 1980, 15, 445-453.

93. Keough, T.; DeStefano, A.J., Org. Mass Spectrom. 1981, 16, 527-533.

94. Keough, T.; DeStefano, A.J., Finnigan Spectra 1982, 8, 7-11.

95. Benoit, F.; Holmes, J.E., Org. Mass Spectrom. 1970, 3, 993-1007.

96. McDonald, C.G.; Lacey, M.J., Org. Mass Spectrom. 1982, 17, 91-95.

97. Yost, R.A., Presented at the National ACS Meeting, May 1982, Las Vegas, NV.

98. Fetterolf, D.D.; Yost, R.A., Presented at the National ACS Meeting, May 1982, Las Vegas, NV.

99. Todd, P.J.; Barbalos, M.P.; McLafferty, F.W., Org. Mass Spectrom. 1982, 17, 79-80.

100. Skotnicki, P.; Fetterolf, D.D.; Yost, R.A.; Hass, J.R., to be submitted to Anal. Chem.

BIOGRAPHICAL SKETCH

Dean Donald Fetterolf was born on April 24, 1956, and raised in Ashland, Pennsylvania. He graduated from North Schuylkill High School in 1974. He attended Indiana University of Pennsylvania, Indiana, Pennsylvania, from 1974-1978 where he served as President of the ACS Student Affiliate Chapter (1977-1978). He was also a member of Phi Kappa Theta fraternity. He received his B.S. degree in chemistry in May, 1978. He began his graduate studies in analytical chemistry at the University of Florida in September, 1978. This research was performed under the direction of Dr. Richard A. Yost. The author received his Ph.D. degree in April, 1983.

I certify that I have read this study and that in my opinion it conforms to acceptable standards of scholarly presentation and is fully adequate, in scope and quality, as a dissertation for the degree of Doctor of Philosophy.

Richard A. Yost, Chairman
Associate Professor of Chemistry

I certify that I have read this study and that in my opinion it conforms to acceptable standards of scholarly presentation and is fully adequate, in scope and quality, as a dissertation for the degree of Doctor of Philosophy.

John G. Dorsey
Assistant Professor of Chemistry

I certify that I have read this study and that in my opinion it conforms to acceptable standards of scholarly presentation and is fully adequate, in scope and quality, as a dissertation for the degree of Doctor of Philosophy.

James D. Winefordner
Graduate Research Professor of Chemistry

I certify that I have read this study and that in my opinion it conforms to acceptable standards of scholarly presentation and is fully adequate, in scope and quality, as a dissertation for the degree of Doctor of Philosophy.

John R. Eyler

John R. Eyler
Associate Professor of Chemistry

I certify that I have read this study and that in my opinion it conforms to acceptable standards of scholarly presentation and is fully adequate, in scope and quality, as a dissertation for the degree of Doctor of Philosophy.

Hugh A. Moye

Hugh A. Moye
Professor of Food Science and
Human Nutrition

This dissertation was submitted to the Graduate Faculty of the Department of Chemistry in the College of Liberal Arts and Sciences and to the Graduate Council, and was accepted as partial fulfillment of the requirements for the degree of Doctor of Philosophy.

April, 1983

Dean for Graduate Studies and Research

UNIVERSITY OF FLORIDA
3 1262 08553 2173